MA-RNA Interactions in Cells and their Effect on HIV-1 Assembly

by

Dishari Thornhill

A dissertation submitted in partial fulfillment
of the requirements for the degree of
Doctor of Philosophy
(Microbiology and Immunology)
in the University of Michigan
2020

Doctoral Committee:

Professor Akira Ono, Chair
Professor Robert Fuller
Professor Alice Telesnitsky
Professor Billy Tsai

Dishari Thornhill
dishari@umich.edu
ORCID iD: 0000-0002-8164-4531

To my mother

Acknowledgements

I would like to humbly acknowledge the people in the different stages of my life without whose support this massive undertaking would not have been possible. I will be forever in the debt of my mentor, Dr. Akira Ono, for taking me on as his student. His relentless pursuit of perfection, careful eye for even the minutest details, and dedication to student mentorship are truly remarkable. Thank you so much, Akira, for these exciting five years of my life, that have helped me mature as a scientist.

My committee members, Drs. Alice Telesnitsky, Robert Fuller, and Billy Tsai have been most generous with their time and invaluable advice. I am cognizant of their support and well-wishes throughout the various turns of my project and would like to thank them wholeheartedly.

A big thank you to the wonderful and unique members of the Ono Lab, both past and present. Thanks to Dr. Tomoyuki Murakami, Dr. Sukhmani Bedi, Dr. Balaji Olety, Christopher Sumner, and Amanda Haag for your support and friendship through the years. I would like to specially mention Sukhmani and Chris for being such great travel companions on this journey that we undertook together, for the celebrations and the commiserations, thank you both!

I would like to thank Heidi Thompson, for being a good friend, and for her unwavering support during my time in the department. I am grateful for the past and present friendly faces, and the ever-helpful denizens of "5th floor, MSII". I would like to add a special thanks to Drs. Eric Martens, Harry Mobley, and Beth Moore, for their support during my transition to the Ono Lab.

I would like to thank my oldest friend (both in age and chronologically), Martin O'Nions, for suffering me through these years. I am deeply grateful for your friendship and for your encouragement

through all these years. I am thankful for the continued friendship and support from my dear friends, Kinnari Sinha Roy, Dr. Kavitha Santosh, and Dr. Rachel Morris.

The unwavering support of my family has been a light I have drawn on during even the darkest turmoil. I owe my life and my values to my parents, Mr. Kanchan Kumar Mukhopadhyay, and Mrs. Sunanda Mukhopadhyay. They have made countless sacrifices on my behalf; and serve as my role models for their honesty, humanity, and devotion to their work. My sister, Jagari Mukherjee, whom I am incredibly proud of for her many talents, and for her courage to persevere in the face of adversity. Thank you for your unconditional love and for being my forever cheerleaders no matter what.

I would like to extend my heartfelt gratitude to my uncle, Mr. Asish Sengupta, who was my guardian when I came to the United States back in 2009. I will never forget coming out of the international airport and seeing your face as a beacon among a sea of strangers in a foreign land.

I would like to thank my loving in-laws, Mr. Darvis Thornhill and Mrs. Joanne Thornhill, for welcoming me into their family. My sister-in-law, Emily, for having the courage to be the unique person that she is. Time spent with you three is truly a soothing balm for the soul.

Finally, I would like to thank, Kyle Thornhill, my inimitable “hubsand”. He is truly the “lucky” one, who has been able to observe “the PhD student in her natural habitat”. Many thanks for taking care of me and for taking care of the house (and the extremely needy cat!) while I studied or worked. Thank you for believing in me, for loving me, and for being my rock during this unpredictable journey.

The work published in this thesis would not have been possible with the help of many people. I would like to acknowledge Akira for his guidance and invaluable input on all the work presented here. I would like to thank Akira for making Figure 1.2. and Figure 1.3.

Part of the literature review for **Chapters 1 and 4** has been previously published:

Rendezvous at plasma membrane: cellular lipids and tRNA set up sites of HIV-1 particle assembly and incorporation of host transmembrane proteins. Viruses. 2020.

Dishari Thornhill, Tomoyuki Murakami, Akira Ono

I would like to thank my co-author, Dr. Tomoyuki Murakami, for his contributions to the article.

Chapter 2 has been previously published:

Relationships between MA-RNA Binding in Cells and Suppression of HIV-1 Gag Mislocalization to Intracellular Membranes. J Virol. 2019.

Dishari Thornhill, Balaji Olety, Akira Ono

I would like to thank my co-author, Dr. Balaji Olety, for his contribution to the article. I am grateful to Drs. Sebla Kutluay, David Turner and Huanqing Zhang for their helpful advice and support. I would like to acknowledge the support of the staff of the BRCF Microscope Core, University of Michigan.

The work presented in **Chapter 3** was done with the support from the University of Michigan Medical School's Biomedical Research Core Facilities. I would like to thank Dr. Pavel Morozov for sharing the scripts and reference set used for the data analyses. I am grateful to Drs. David Turner, Huanqing Zhang, Sebla Kutluay and Karin Musier-Forsyth for their help and feedback.

In **Chapter 4**, I availed of the results from a proteomics screen carried out previously in the lab. I would like to thank Dr. Jingga Inlora for collecting that data.

Table of Contents

List of Figures

Abstract

The HIV-1 structural polyprotein Gag drives the virus particle assembly specifically at the plasma membrane (PM). Gag binding to the PM is regulated by cellular factors including PM-specific phospholipid PI(4,5)P2 and RNAs, both of which bind the highly basic region (HBR) in the matrix domain (MA) of Gag. While it is well-established that the interaction between the MA-HBR of Gag and the PM-enriched lipid PI(4,5)P2 is crucial for Gag localization to the PM, the role of MA-bound RNA in this process was less well-defined.

In this thesis, I examined the role of MA-bound RNA in the specific localization of HIV-1 Gag to the PM. The strategy that I employed was the comparison of Gag derivatives in which two of the eight basic amino acids in MA-HBR are substituted from Lys to Arg (K→R) or from Lys to Thr (K→T). Using a cell-based crosslinking assay, I determined the amount of RNA that is bound to the MA of the Gag derivatives in cells. Using microscopy, I determined the subcellular localization of these MA-HBR Gag mutants. Comparison of these data showed that a strong correlation exists between the amount of MA-bound RNA in cells and the PM-specific localization of Gag. Overall, this study provided cell-based evidence supporting a model that MA-bound RNA prevents mislocalization of Gag to intracellular membranes, and in conjunction with PI(4,5)P2, helps Gag localize specifically to the PM. I also determined that the presence of Lys, but not Arg, at MA-HBR residues 29 and 31, especially 31, is important for WT-level RNA binding in cells. This indicates that the sequence of the MA-HBR, and not just the MA-HBR overall basic charge, is a determinant of MA-RNA binding in cells.

The predominant RNA species that binds MA-HBR in cells has been previously identified as transfer RNA (tRNA) with specific tRNAs bound to MA. It was not clear whether these tRNAs were selected by MA and if yes, then what were the determinants of selection of the specific tRNAs on MA. Using a Gag derivative that was designed to allow the capture of all the tRNAs bound to MA, and comparing the relative abundance of these tRNAs to their cellular abundances, I found that the tRNAs bound to MA were not just the highly abundant cellular tRNAs. These data suggest that specific tRNAs are selected by MA, and that the selection may be based on specific characteristics of tRNAs. The data also support that the tRNA sequence/structure as well as tRNA modifications are likely to contribute to the enrichment of preferred tRNAs to MA. I identified two tRNAs, SeCTCA (coding for selenocysteine [SeC]) and PheGAA, as being selected by MA in an MA-HBR dependent manner. These data support the role of the MA-HBR in selecting for specific tRNAs in cells. Comparisons of the relative abundances of SeCTCA and PheGAA between Gag derivatives that are either capable of membrane binding or not further suggest that these two tRNAs may regulate the membrane binding of Gag in cells in two different ways. SeCTCA could be a tRNA that is resistant to removal by PI(4,5)P2 and therefore prevents the binding of Gag to all cellular membranes, including the PM. PheGAA may be a tRNA that is sensitive to removal by PI(4,5)P2 and therefore allows Gag to bind specifically to the PM by preventing nonspecific binding of Gag to intracellular membranes.

SeCTCA and PheGAA have not been previously implicated in HIV-1 assembly and thus, future studies could provide a wealth of new knowledge regarding the interaction of MA with these specific tRNAs and their effect on the membrane binding of Gag. The analyses of such MA-tRNA interactions could help inform the design and development of RNA aptamers with high binding affinity towards Gag such that they resistant to removal by PI(4,5)P2. Such RNA aptamers could serve as anti-retroviral agents that prevent the binding of Gag to the PM, and hence, block HIV-1 assembly.

Chapter 1

Introduction

Human immunodeficiency virus type 1 (HIV-1) is the principal causative agent of acquired immunodeficiency syndrome (AIDS). It is a persistent major global health problem with 37.9 million people living with HIV/AIDS worldwide as of 2018. AIDS-related illnesses claimed 770,000 lives worldwide in 2018 and 1.7 million people were newly infected. Certain populations are particularly vulnerable due to legal and social inequities and at an increased risk of HIV infection including sex workers, men who have sex with men, people who are incarcerated, and transgender people (1, 2). This is a disease without any cure. Lifelong antiretroviral therapy (ART) is effective in reducing HIV mortality and curbing HIV transmission. In June 2019, 24.5 million people were receiving ART. There was a 37% decrease in new HIV infections and a 45% decrease in HIV-related deaths between 2000 and 2018, with 13.6 million deaths prevented due to ART (1). However, emerging HIV-1 drug resistance, as well as drug toxicity, undercuts the long-term success of ART. Therefore, there is a constant need for new anti-HIV drugs. Currently, there are no drugs targeting the production of progeny HIV-1 virus particles at the plasma membrane (PM) (3).

Out of (West Central) Africa

Simian immunodeficiency viruses (SIVs) circulating in wild chimpanzees (*Pan troglodytes troglodytes*) and gorillas (*Gorilla gorilla gorilla*) in West Central Africa are the closest relatives of HIV-1. SIVs are primarily monkey viruses with species-specific SIVs infecting more than 40 species of African monkeys. The crossover of SIV from monkeys to apes is reportedly via cross-species transmission originally to chimpanzees (4). Phylogenetic analyses assign the origins of HIV-1 to have arisen by cross-species

transmission to humans from chimpanzees and gorillas. SIV infection of wild chimpanzees causes $CD4^+$ T cell depletion and increased mortality (5), which is also the hallmark of HIV infection. Presumably then, the origin of AIDS predates the origin of HIV-1 (6, 7).

HIV classification

HIV belongs to the genus Lentivirus within the family of Retroviridae, subfamily Orthoretrovirinae. Types 1 and 2 (HIV-1 and HIV-2) constitute the two types of HIV. HIV-1 is the major type with four phylogenetic lineages, the groups M and N which originated from independent transmissions of SIV from chimpanzees to humans, and groups O and P which originated by transmission from gorillas to humans (7-9). Group M is the 'major' group and has nine subtypes (A, B, C, D, F, G, H, J, and K) as well as ~102 circulating recombinant forms (CRFs) (10, 11). HIV-1 subtype C accounts for approximately half of the global infection burden being prevalent in Southern Africa, Ethiopia, and regions of India (12). HIV-1 subtype B is the major subtype prevalent in Western and Central Europe, Latin and North America, and Oceania (12, 13). While it accounts for 12% of global infections (12), there is an overrepresentation of this subtype B in prevalent HIV-1 research.

HIV-1 life cycle

HIV-1 is an enveloped virus. The HIV-1 genome consists of a positive sense single-stranded RNA. The viral RNA is 9.2Kb in length (14). Two copies of this genome are enclosed within the viral core. The genome encodes for nine viral proteins: three structural polyproteins (Gag, Pol, Env), two regulatory proteins (Rev and Tat), and four accessory proteins (Nef, Vif, Vpu, and Vpr) (Figure 1.1).

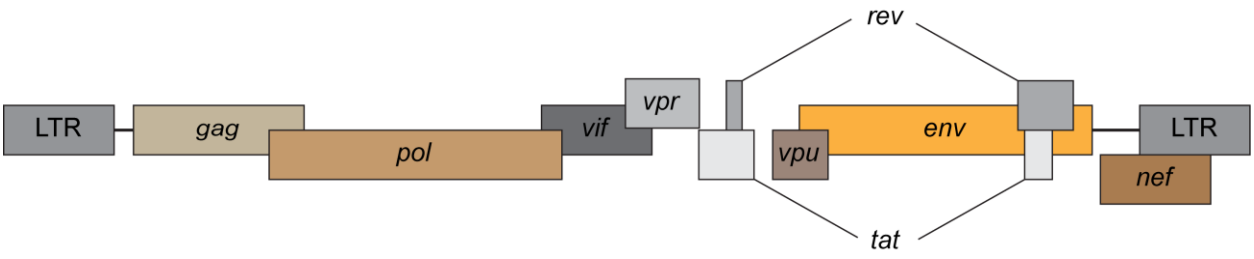

Figure 1.1. Schematic illustration of the HIV-1 genome. HIV-1 genome encodes nine viral proteins: Gag and Pol from unspliced RNA, Vif, Vpr, Vpu and Env from singly spliced RNA, and Tat, Rev, and Nef from completely spliced RNA.

Natural host cell targets of HIV-1 are $CD4^+$ T lymphocytes and cells of the myeloid lineage including macrophages, dendritic cells, and bone osteoclasts.

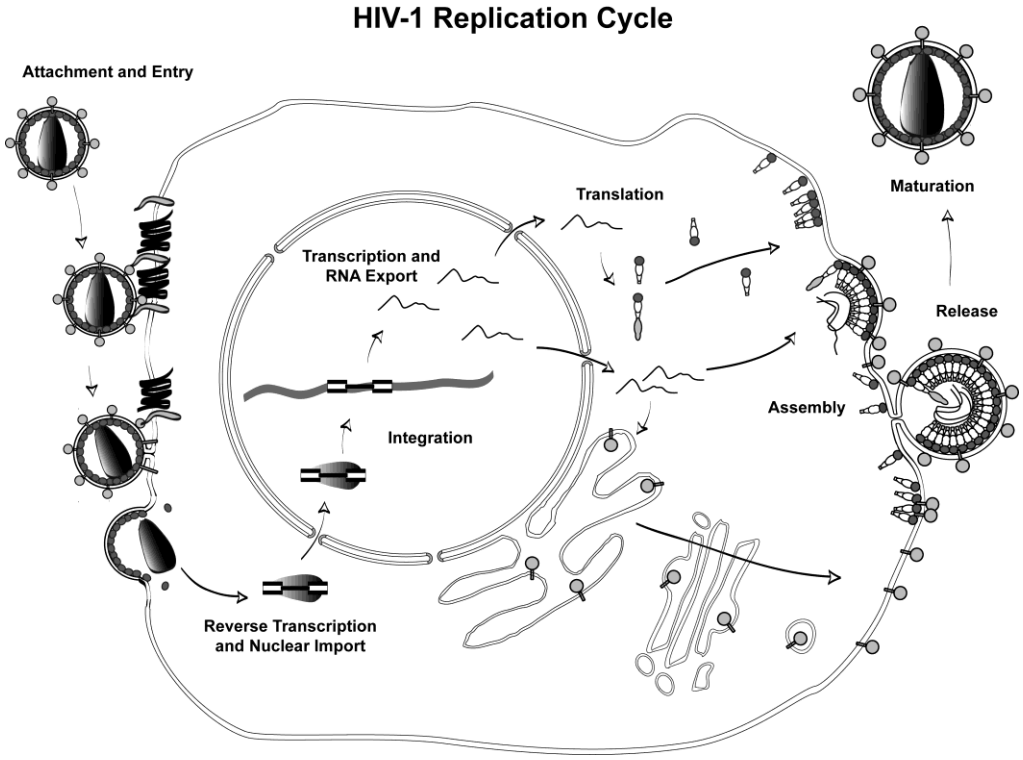

Figure 1.2. HIV life cycle. The HIV replication cycle starts with the binding of the viral envelope protein (Env) to the major cellular receptor CD4 and co-receptors. Env mediates fusion of the viral and cellular membranes, allowing the viral core to enter the cell. The viral reverse transcriptase (RT) converts the viral RNA into double stranded DNA. Following nuclear import, the viral DNA is integrated into the host genome by the viral integrase (IN). The integrated DNA is transcribed and translated. Translation of the structural polyprotein Gag initiates the virus assembly at the plasma membrane. Gag also mediates the release of the virus particle along with viral protein Vpu. The viral protease (PR) is involved in the maturation of the virus particle resulting in the production of the infectious progeny.

i. Attachment and Entry: The first step in the HIV-1 replication cycle is mediated by the viral envelope glycoprotein (Env). The Env precursor protein (gp160) is cleaved into two subunits, gp120 and gp41, by a host furin-like protease. The two subunits remain associated as heterodimers and form trimers on the surface of the virion, with gp41 serving as the transmembrane anchor into HIV-1 envelope (15, 16). The gp120 engages the primary virion receptor, CD4, on the surface of the target cell (17). This exposes the

coreceptor binding site on gp120 and facilitates the binding of gp120 to one of the two HIV co-receptors, CXCR4 or CCR5 chemokine receptors, based on its tropism. An important determinant for this tropism of gp120 is the v3 loop, one of the five hypervariable regions of gp120, which interacts with CXCR4 or CCR5 (18, 19). Binding to the receptors leads to the translocation and insertion of the N terminal fusion peptide (FP) of gp41 into the target cell membrane. Subsequent conformational changes in gp41 leads to the formation of a six-helix bundle which brings the FP and transmembrane segments at the same end of gp41 and leads to the generation of a fusion pore between the viral and the target cell membranes (15, 16).

ii. Uncoating, Reverse transcription, and Integration: After fusion, the viral core or capsid is released into the cytosol of the infected cell (15, 20). The core is formed by the assembly of ~ 1000-1,500 capsid proteins (CA, p24) into a fullerene-like cone. The core comprises ~ 200-250 CA hexamers and 12 CA pentamers in an entirely closed shell. Recent studies have revealed that the highly charged polyanion inositol hexakisphosphate (IP6) promotes the assembly as well as stability of the HIV-1 capsid (21, 22). After entry into the target cell, the capsid travels from the PM to the nucleus. Apart from protecting the viral RNA, the capsid is also required for reverse transcription of the viral RNA and nuclear import of the viral DNA (22-24).

The viral reverse transcriptase enzyme (RT) (25, 26) is a heterodimer composed of two subunits, p66 and p51. RT has DNA polymerase and RNase H activities to convert the viral genomic RNA to double-stranded DNA (27). The host tRNALys3 serves as the primer for the initiation of reverse transcription and synthesis of the first DNA strand. While the DNA polymerase copies either a DNA or an RNA template, the RNase H degrades RNA that is part of an RNA/DNA duplex. The p66 subunit harbors the active sites for both the polymerase as well as RNase H while the p51 contributes to the structure of the RT.

After nuclear import, the linear double-stranded viral DNA is then integrated into the host cell genome by the viral integrase enzyme (IN). This integrated DNA copy is termed provirus and is the source of both viral genomic RNA and viral messenger RNAs (mRNAs) encoding the nine viral proteins.

iii. Transcription, nuclear export, and translation*:* The integrated proviral DNA is transcribed by the host cellular DNA-dependent RNA polymerase II (RNAPII) from the promoter contained in the HIV-1 5' long terminal repeat (LTR) (27, 28). Initially, binding of cellular factors such as RNAPII, NF-κB, Sp1, the TATA box binding protein to the HIV promoter generates low levels of viral transcripts which are spliced and translated to produce the early viral proteins, Tat, Nef, and Rev. The transcriptional activator (Tat) protein then stimulates transcription from the viral promoter by binding to the Trans-Activating Response (TAR) hairpin in the 5' end of nascent RNA transcript. Tat-TAR binding enhances RNAPII-mediated elongation by recruiting positive transcription elongation factor b (P-TEFb). P-TEFb is a RNAPII elongation factor which induces the phosphorylation and activation of the paused RNAPII and modulates elongation at cellular genes (29-32).

Nef hijacks the cellular membrane trafficking and degradative processes to modulate its cellular targets including CD4 and Class I MHC on the cell surface. CD4 downregulation prevents the negative effects of CD4 on HIV-1 infectivity and virus production. Class I MHC downregulation prevents foreign viral peptide presentation and cytotoxic T lymphocyte activity (33, 34).

Rev pushes the HIV gene expression from the early phase to the late phase. Normally, only completely spliced RNAs can exit from the nucleus to the cytoplasm. Rev facilitates the export of the incompletely spliced and unspliced RNAs to the cytoplasm for the translation of the rest of the viral proteins (from the late genes). Rev is imported back to the nucleus through its nuclear localization signal (NLS) which is an arginine-rich motif (ARM). Rev also binds the highly structured Rev response element (RRE) contained in the Env sequence via its ARM. The Chromosome maintenance factor 1 (CRM1) normally

exports cellular proteins bearing a leucine-rich NES. Rev usurps CRM1-mediated cellular protein export by engaging with Crm1 through its leucine-rich NES facilitating the viral RNA export (35). An additional function of Rev is to regulate HIV transcription by reducing Tat protein levels (31).

The Gag precursor polyprotein $Pr55^{Gag}$ and the Gag-Pol precursor polyprotein (p160) are generated from the unspliced transcripts. The Gag-Pol precursor is generated by a programmed -1 ribosomal frame shifting (-1PRF) event, which is triggered when the translating ribosome binds two cis-acting elements in the mRNA, a slippery site and a short stem loop structure downstream of this slippery site (36-38). Recently, an interferon-stimulated gene product, Shiftless, was identified as a trans-acting -1PRF inhibitor of HIV-1 (and 5 other retroviruses) which interacts with the ribosome and the -1PRF signal containing mRNA to bring about translation termination. Shiftless was shown to inhibit Gag-Pol expression and also inhibit HIV-1 replication (39). The efficiency of this Gag/Gag-Pol shift is ~10% in human cells yielding a 20:1 ratio between Gag to Gag-Pol levels. This ratio is crucial for the production of infectious virus particles (36).

iv. Assembly and release: The initiation of the virus assembly process takes place when the $Pr55^{Gag}$ is produced (Figure 1.3 b). Gag has four major domains: matrix (MA, p17), capsid (CA, p24), nucleocapsid (NC, p7) and p6. Additionally, Gag contains two spacer peptides (SP1 and SP2) (Fig 1.3 a). The MA domain mediates the targeting and binding of Gag to the site of virus assembly. This is the major subject of my thesis research and I provide more details on this in the subsequent sections. MA is also involved in the incorporation of the Env glycoproteins into the virus particle (3). The CA and the NC domains mediate the multimerization of Gag. The CA drives the multimerization of Gag through dimerization of its C-terminal domain (CA-CTD) and is responsible for the formation of the hexameric Gag lattice in the immature virion (40). The Sp1 is involved in the formation of a six-helix bundle along with the CA-CTD. The six-helix bundle is important as a structural element of the Gag hexamer (40). IP6 (mentioned before) stabilizes the six-helix bundle by binding to the central hexameric pore made of two rings of lysine residues and is important

for the immature lattice formation as a structural element (21, 22, 24). The NC domain binds the viral genome for incorporation into the virion (41). The NC contains two zinc finger domains which interact with the packaging signal located in the 5'UTR of the genomic RNA (42, 43). The NC driven multimerization of Gag is also through a scaffold of RNA (44). The p6 is involved in the pinching off of the virus bud by recruiting the host endosomal sorting complex required for transport (ESCRT) machinery through its PTAP and YPXL late domains (3, 45, 46).

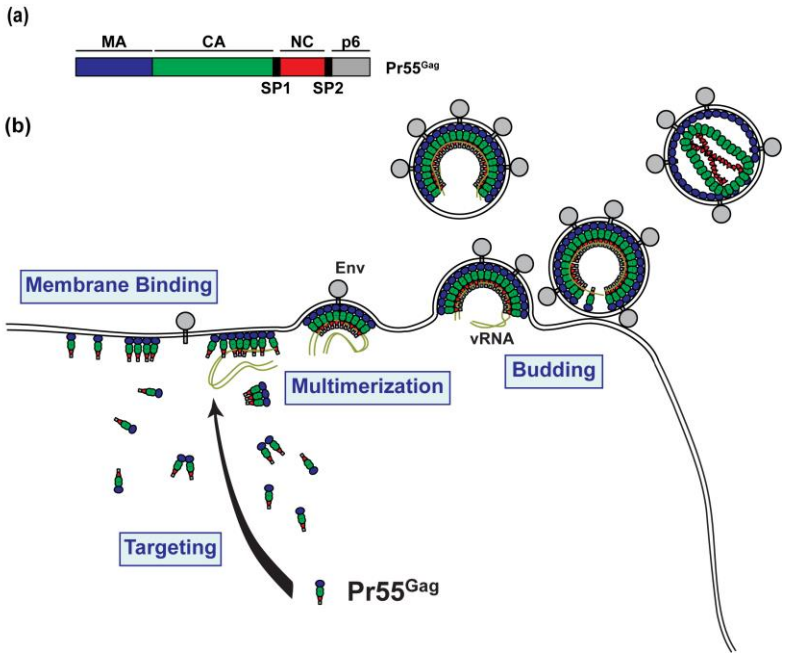

Figure 1.3. HIV-1 assembly. (a) Schematic illustration of HIV-1 Gag showing the different Gag domains. (b) Cartoon depicting the stages of HIV-1 assembly. MA is involved in targeting and membrane binding of Gag. CA mediates oligomerization of Gag. NC is involved in multimerization of Gag and binding the viral genome. p6 mediates the pinching off of the virus bud.

Apart from Gag, the viral RNA, the Gag-Pol fusion protein, Env, and several host factors such as tRNALys3, are further required to be packaged in the viral particle for the virus to be infectious. During the process of viral maturation that takes place during or shortly after the release of the assembled virus particle, the viral protease enzyme (PR) cleaves the Gag-Pol precursor to separate Pol from Gag. Gag is further cleaved by PR into its constituent domains: MA, CA, NC and p6. The six-helix bundle is involved in the modulation of the Gag maturation (40). IP6 also promotes the formation of the mature capsid (21, 22,

24). Pol is further cleaved by PR to generate the individual enzymes: PR, RT, and IN. This cleavage of the polyproteins into the individual proteins renders the virus particle infectious. The interferon-inducible membrane protein, Tetherin, acts as a host cellular restriction factor by preventing the release of the enveloped virus particles. Tetherin is a type II membrane glycoprotein with an N-terminal transmembrane domain anchor and a C-terminal glycosylphosphatidyl inositol (GPI) anchor. Tetherin dimers form a physical tether that traps the budded virus particle the PM by insertion of either of the two anchors into the viral envelope. It was reported that there is a preference for insertion of the GPI anchor into the tethered virions (47). Vpu counteracts tetherin by triggering its surface downregulation and degradation by engaging with the tetherin transmembrane domain (34, 47-52). Interaction of Vpr (viral protein R) with the p6 domain of Gag leads to its specific incorporation into the virus particle. Vpr is evolutionarily conserved across human and primate lentiviruses. Vpr is necessary for efficient HIV infection and spread in non-dividing cells such as macrophages (31, 53).

The roles played by PI(4,5)P2 in specific localization of Gag

Specific localization of Gag to the PM is mediated by the MA domain (3, 54, 55). MA employs a bipartite signal to stably interact with lipid bilayers; an N-terminal myristate moiety and a highly basic region within its globular domain (MA-HBR) (56-62). The myristate moiety is a 14-carbon fatty acid co-translationally attached to the N-terminal glycine of MA (63). When the myristate moiety is not sequestered within the MA globular head, it mediates non-specific hydrophobic interactions of Gag with membranes (64-71). By itself, the myristate moiety is not sufficient to stably anchor Gag to the lipid bilayer (63). The second determinant for the membrane binding of HIV-1 Gag is the MA-HBR (Figure 1.4 a), a conserved patch of basic amino acids encompassing MA residues 14-31, which interacts with negatively charged lipids (59, 72, 73). Earlier in vitro studies showed that HIV-1 MA can bind lipid membranes containing acidic phospholipids such as phosphatidylserine (PS) (59, 74, 75). However, as described below, multiple lines of evidence indicate that MA-HBR preferentially binds to an anionic lipid enriched at the

PM, phosphatidylinositol-(4,5)-bisphosphate [PI(4,5)P2], and that this interaction promotes specific binding of Gag to the PM (62, 69, 76-86).

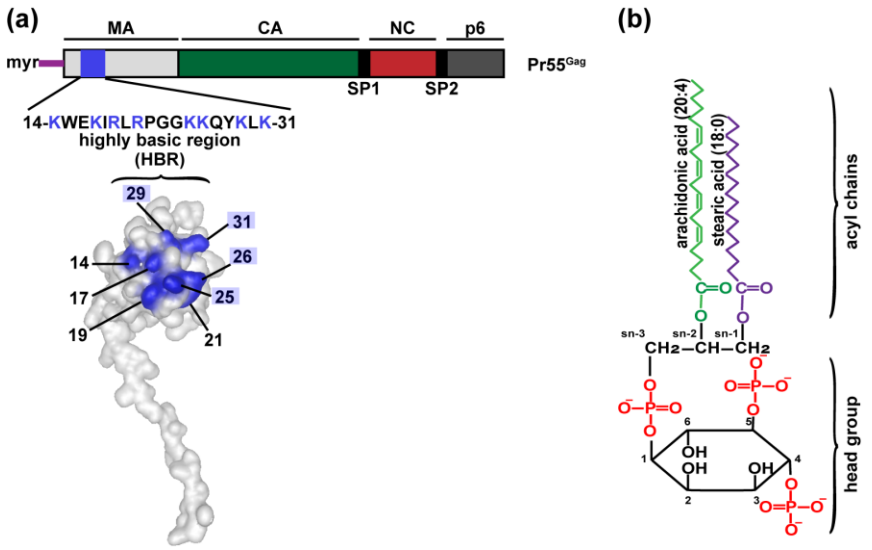

Figure 1.4. Cartoons depicting HIV-1 Gag MA-HBR and PI(4,5)P2: (a) Schematic illustration of HIV-1 Gag with the structure of HIV-1 MA (PDB accession number 2HMX) showing the basic residues of the MA-HBR in blue. The key basic residues studied in detail in chapter 2 are indicated (in the nomenclature for MA amino acid residues used in this review, the first methionine removed upon myristylation is not counted). (b) Illustration of 38:4 PI(4,5)P2, the predominant molecular species of PI(4,5)P2 in many primary mammalian cells.

PI(4,5)P2 is a polyphosphoinositide bearing a glycerol backbone, with two acyl chains esterified at the sn−1 and sn−2 positions and a phosphate and a myo-inositol ring the sn−3 position (Figure 1.4 b). The myo-inositol ring in PI(4,5)P2 is phosphorylated at the fourth and the fifth positions. PI(4,5)P2 is primarily present in the inner leaflet of the PM, with minor populations distributed at other subcellular compartments (87-89). Phosphatidylinositol phosphate (PIP) kinases (PIPKs), which generate PI(4,5)P2 at specific membranes, can be divided into two groups: type I (PIPKIs) and type II (PIPKIIs). Type I phosphatidylinositol 4-phosphate 5-kinases (PI4P5KI, one of PIPKIs), which preferentially phosphorylate the 5-hydroxyl group on the inositol ring of PI(4)P to produce PI(4,5)P2, are the dominant PIPKs in mammalian cells. A relatively lesser pool of PI(4,5)P2 is produced by PIPKIIs, which use PI(5)P as substrate and phosphorylate PI(5)P at the 4-hydroxyl position. Various polyphosphoinositide kinases and phosphatases act in concert to cycle PIs between different phosphorylation states. PI(4,5)P2 can be

dephosphorylated by a subset of polyphosphoinositide phosphatases. The polyphosphoinositide 5-phosphatase INPP5E, also known as 5-phosphatase IV, converts PI(4,5)P2 to PI(4)P by dephosphorylating at 5-hydroxyl position of the inositol ring (90). Thus, spatio-temporal distribution of PI(4,5)P2 is orchestrated by the presence of PIPKs, PI(4,5)P2 phosphatases, the enzyme substrates [PI(4)P and PI(5)P], as well as PI(4,5)P2 binding/effector proteins (87, 88, 91-96).

When PI(4,5)P2 was depleted from the PM by the overexpression of 5-phosphatase IV or when localization of PI(4,5)P2 was altered by inducing formation of PI(4,5)P2-laden endosomal vesicles, the PM localization and subsequent virus-like particle (VLP) release of HIV-1 Gag were severely decreased (62, 77, 78, 82, 84, 97-99), emphasizing the importance of PI(4,5)P2 in HIV-1 assembly and release. Another study showed that inhibition of Rab27-dependent trafficking of PI4KIIα, an enzyme that catalyzes the production of PM-specific PI4P, reduced PI(4,5)P2 at the PM and suppressed Gag localization to the PM in T cells, highlighting the complexity of the PI cycle regulating HIV-1 assembly (100). In HeLa-derived cells, knockdown of PI4P5KIα and γ, but not β, impaired the targeting of Pr55Gag to the PM and caused mislocalization of Gag to intracellular compartments (101). Therefore, it is conceivable that HIV-1 Gag binds to a specific pool of PI(4,5)P2 in cells. Perturbation of cellular PI(4,5)P2 or other phosphoinositides have been shown to reduce particle production of other retroviruses although some retroviruses are less sensitive to 5-phosphatase IV expression (78, 82, 102-108).

Determinants for Gag binding to PI(4,5)P2

PI(4,5)P2 headgroup is more negatively charged than a ubiquitous acidic phospholipid PS {the net charge of PI(4,5)P2, -3 or -4; PS, -1 (109)}. Supporting the charge-based preference of Gag for PI(4,5)P2, a modeling study on MA-membrane interactions predicted that non-specific electrostatic interactions between MA and PI(4,5)P2 are sufficient to significantly enhance membrane binding (73). However, in vitro studies showed that HIV-1 Gag or MA binds more efficiently to PI(4,5)P2-containing lipid membranes

than to charge-matched liposomes containing PS, suggesting that PI(4,5)P2 enhances Gag-membrane binding by specific interaction beyond mere electrostatic attraction (77, 80, 83, 84, 110-114). Membrane flotation-based studies showed that PI(3,5)P2 and PI(3,4,5)P3 are also able to enhance binding of Gag to liposomes although the former is not as efficient (77). Likewise, an NMR-based analysis showed enhanced binding of MA to liposomes containing PI(3,5)P2 as well, though not as efficiently as PI(4,5)P2 (115). Therefore, both negative charge density of the inositol headgroup and distribution of the phosphate residues on the inositol ring are likely determinants for the optimal interaction between MA and PI(4,5)P2. Recent genetic and structural studies collectively suggest that HBR residues Lys 29 and Lys 31, especially Lys 31, play key roles in the interaction with the PI(4,5)P2 headgroup although other basic residues may also be involved (80, 115-118). In addition, as we discuss later, binding of RNA to MA-HBR residues is also likely to contribute to lipid specificity.

The sn-2 position of glycerol backbone of PI(4,5)P2 is most commonly decorated with arachidonic acid. The 1-stearoyl-2-arachidonyl (38:4) form of PI(4,5)P2 is found to be a dominant species across multiple primary mammalian cells (89, 92, 119-121) (Figure 1.4 b). The preference of enzymes involved in the PI cycle, such as diacylglycerol kinase ε (DGKε), for substrates displaying 38:4 fatty acyl chains likely explains the enrichment of 38:4 PI(4,5)P2 (91, 120). Although an earlier structural study using water-soluble PI(4,5)P2 derivatives with short acyl chains proposed that the sn-2 acyl chain interacts with a hydrophobic cleft of the MA globular domain (69), subsequent structural and in silico studies suggest that PI(4,5)P2 acyl chains with native lengths are unlikely to directly interact with MA (115, 122). Nonetheless, acyl chains of PI(4,5)P2 may play an indirect role in MA binding. An in vitro study using giant unilamellar vesicles (GUVs) showed that Gag prefers PI(4,5)P2 with at least one unsaturated acyl chain (123). In the same experimental system, the pleckstrin homology domain of phospholipase Cδ1 ($PH_{PLC\delta1}$), which interacts with the headgroup of PI(4,5)P2, did not show a bias towards specific PI(4,5)P2 acyl chains unlike Gag (123). In the presence of cholesterol or a higher concentration of PS, HIV-1 Gag binding to liposomes

can be detected even in the absence of PI(4,5)P2. Under these conditions, HIV-1 Gag shows a preference for PS with unsaturated acyl chains over PS with saturated acyl chains (124) whereas RSV Gag, which lacks N-terminal myristoyl moiety, does not show such preference (125, 126). It will be intriguing to examine whether the myristoyl moiety plays a role in the observed acyl chain preference, for example, by favoring a loose packing (warranted by unsaturated acyl chains) around the acidic phospholipid Gag binds. Lipidomics studies showed that unsaturated acyl chain species, including 38:4, were the major PI(4,5)P2 acyl chain species found in the HIV-1 particle (78, 127), but this can be largely accounted for by the abundance in the PM. Currently, whether unsaturation of acyl chains is necessary for Gag binding to PI(4,5)P2 in cells remain unclear.

Enrichment of PI(4,5)P2 in HIV-1 particles

The estimated amounts of PI(4,5)P2 vary depending on the type of cells. PI(4,5)P2 resides mainly in the inner leaflet of the PM at ~1-2 mol% with ~5,000–20,000 molecules of PI(4,5)P2 per μm^2 of PM (91). PI(4,5)P2 is found to be enriched in the HIV-1 envelope as compared to the PM of the producer cell (78, 127-129), and this enrichment is dependent on MA (78). There are an estimated 8,000 molecules of PI(4,5)P2 in an HIV-1 particle (127). Total surface area for one HIV-1 particle will be 0.07 um^2 assuming an average diameter of 150 nm for each virus particle. Thus, there is a ~5.6 to 22.4-fold increase in PI(4,5)P2 density on HIV-1 compared to that on the PM. A new nanodisc-based study determined that ~1 PI(4,5)P2 molecule recruits one MA molecule (6 molecules of PI(4,5)P2 versus 5 molecules of MA per leaflet of the nanodisc) (117). However, assuming an average of 2500 Gag molecules per virus particle, the ratio of PI(4,5)P2 to Gag is 3:1 in a virus particle as per the latest HIV-1 lipidomics study (127). How does HIV-1 achieve such an enrichment of PI(4,5)P2 in its envelope?

The PM is not a homogeneous sea of lipid and proteins. Instead, the PM is a dynamic mosaic of various nanoscale or mesoscale domains (herein collectively referred to as microdomains) that have

distinct lipid and protein signatures. As for PI(4,5)P2, super-resolution microscopy studies in PC12 cells showed that PI(4,5)P2 exists in ~65-73 nm diameter clusters in the inner leaflet of the PM (130, 131). In model membranes, PI(4,5)P2 cluster formation can be driven by multivalent metal ions (132, 133). Metal ions generate PI(4,5)P2 clusters even at low PI(4,5)P2 concentrations of 0.02 mol% (133). One can speculate that given that MA-HBR is the established interface for the PI(4,5)P2-Gag association, the increase in PI(4,5)P2:Gag ratio in virus particle compared to nanodisc may be a result of PI(4,5)P2 clustering. In fact, a previous modeling study showed that a single basic peptide can induce clustering of PI(4,5)P2 (134). Combination of PI(4,5)P2 clustering and Gag multimerization is likely to lead to incorporation of larger numbers of PI(4,5)P2 into the virus particle than what initially engaged Gag.

The balance between MA binding to PI(4,5)P2 and RNA

The MA-HBR has been shown to bind not only acidic lipids but also RNA (116, 135-140). Notably, in experimental systems where full-length Gag translated in vitro using eukaryotic cell lysates is examined for binding to liposomes containing PS, RNA that is present in the cell lysates acts as a negative regulator for Gag membrane binding. Only when RNA is removed by treatment with RNase or when PI(4,5)P2 is included in the liposomes, in vitro transcribed Gag binds liposomes efficiently (77, 80, 84, 123). Thus, RNA bound to Gag via MA inhibits Gag binding to PS, but PI(4,5)P2 is able to overcome the negative regulation by RNA (Figure 1.5).

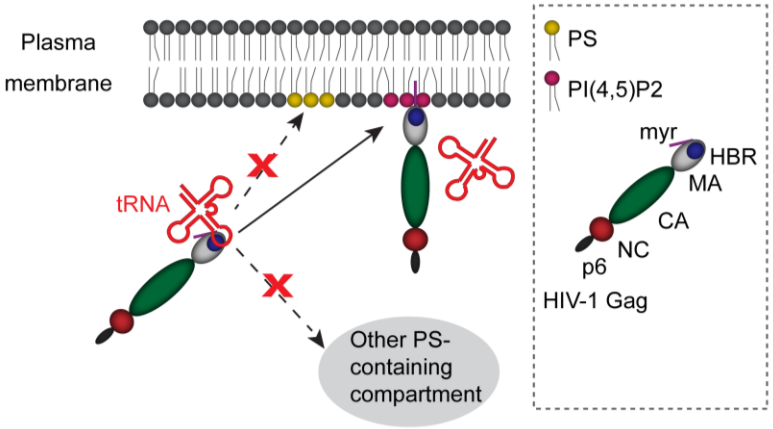

Figure 1.5. Model for regulation of Gag binding to the plasma membrane (PM): Interactions of Gag with PI(4,5)P2 and tRNA ensure specific localization of Gag to the PM. Binding of Gag to tRNA prevents localization of Gag to intracellular membranes that contain PS but not PI(4,5)P2. Interaction of Gag with PI(4,5)P2-containing membrane overcomes the block on membrane binding by tRNA, thereby recruiting Gag to the PM

The in vitro observations of competition between RNA/nucleotide and acidic lipids (80, 85) led to a proposal in which RNA binding to MA prevents MA interaction with PS, an acidic phospholipid ubiquitously distributed in cells, and thereby ensures specific binding of Gag to the PM, which contains PI(4,5)P2 (Figure 1.5). In support of this model, Gag binding to RNA via MA in cells has been observed (116, 137, 141). Moreover, RNA bound to MA in cells suppresses membrane binding of Gag molecules present in the cytosol of HIV-expressing cells regardless of whether the membrane is PS-containing liposomes (141) or total cellular membranes (137). But does RNA binding to MA prevent Gag from mislocalizing to the intracellular membranes containing PS in cells? Our comparison of HIV-1 Gag chimeras containing MA domains of various retroviruses showed that MA domains sensitive to RNA-mediated inhibition of Gag-liposome binding direct Gag chimeras to the PM, whereas Gag chimeras containing MA domains that are insensitive to RNA-mediated inhibition show promiscuous subcellular localization (82, 84). However, whether MA-RNA binding was important for the specific localization of Gag to the PM in the context of HIV-1 MA remained to be determined. My thesis study described in chapter 2 addressed this question and demonstrated the presence of a strong correlation between MA-RNA binding in cells and the inhibition of Gag binding to nonspecific intracellular compartments.

The majority of RNA that binds MA-HBR in cells has been identified as transfer RNA (tRNA) with specific tRNA species selected on MA (137). What determined the specificity of those select tRNAs for MA and whether the specific MA bound tRNAs were involved in the regulation of Gag membrane binding in cells remained to be determined. My thesis study described in chapter 3 addressed this knowledge gap and elucidated that MA-HBR as well as specific characteristics of select tRNAs may be involved in enrichment of particular tRNAS on MA. Furthermore, my thesis study identified that MA-bound tRNAs

may be sensitive or resistant to PI(4,5)P2-mediated removal and, thus may be differentially regulating Gag-membrane binding in cells.

Interestingly, the affinity of MA binding to tRNA (138, 142) surpasses its affinity to PI(4,5)P2 (110, 115, 117). The affinity of MA to PI(4,5)P2 can be augmented when PS or cholesterol is included in the PI(4,5)P2-containing membranes (110), when MA is artificially trimerized (117) or when MA is myristoylated (110). However, there has been no side-by-side comparison of MA binding affinity to membranes versus tRNA using same experimental conditions and methods thus far. Of note, in the in vitro liposome binding assays where full-length Gag produced in rabbit reticulocyte lysates is examined for liposome binding, RNase treatment drastically increases Gag binding to liposomes containing PS , but it also increases Gag binding to PI(4,5)P2-containing liposomes (80). This observation suggests that Gag binding to PI(4,5)P2 can be susceptible to the RNA-mediated inhibition depending on the condition. Consistent with this notion, in other in vitro systems where purified MA or Gag are added to lipid membranes, addition of tRNAs reduces membrane binding of MA/Gag to various degrees even when the membranes contain PI(4,5)P2 (111, 113, 138). Therefore, the balance between MA binding to PI(4,5)P2 and tRNA can be affected by factors that differ among experimental systems. These factors may include the state of Gag multimerization, the presence of other lipids, effects of cations on tRNAs and membranes, and clustering of PI(4,5)P2.

MA-RNA binding is mediated by the MA region containing HBR (76, 135-138, 141, 143-149). Therefore, it is likely that tRNA binding suppresses Gag membrane binding through inhibition of the interaction between HBR and acidic phospholipids. Interestingly, however, our previous study has shown that removal of RNA from Gag by RNase treatment increases not only Gag binding to negatively charged liposomes but also, to a lesser extent, binding to liposomes containing only a neutral lipid PC (80). Therefore, hydrophobic interactions mediated by the myristoyl moiety may also be regulated by RNA binding to MA-HBR. A similar observation was also made in another in vitro study that used a purified Gag

and yeast tRNA (113). Of note, myristoylated MA under conditions that favor myristate exposure has a weakened affinity to tRNA compared to when the myristate moiety is sequestered (138). Therefore, there may be interplay between myristoyl exposure and MA-tRNA binding.

In **Chapters 3 and 4**, I focus on the role of transfer RNAs (tRNAs) in HIV-1 assembly. Therefore, I am providing a brief overview of tRNA structure, regulation, and post-transcriptional modifications in cells in the following section. Additionally, while I have reviewed the role of tRNAs in HIV-1 assembly, I am presenting a summary of relevant research on the involvement of specific tRNAs in other steps of the HIV-1 life cycle.

tRNA structure, regulation, and function in cells

tRNAs are transcribed by RNA polymerase III, have a characteristic structure, and undergo heavy post-transcriptional modifications.

i. tRNA structure: tRNAs are small (~75-90 nt) noncoding RNA adaptors for protein translation that decode the mRNA. They are highly structured, with most tRNAs folded into the characteristic cloverleaf secondary structure (Figure 1.6), and an L-shaped tertiary structure. Each tRNA consists of an acceptor stem with the 3' CCA tail; the D-arm and the TΨC-arm (also known as the T-arm), which mediate the stabilization of the L-shaped structure of the tRNA; the variable loop (V-loop), the size of which is extended in certain tRNA species (termed as type II tRNAs); and, the anticodon arm, which houses the anticodon which through pairing with the corresponding mRNA codon allows for protein synthesis (150). Mg^{2+} ions are required for tRNA folding and stabilization (151).

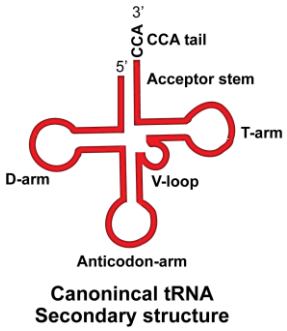

Figure 1.6. Schematic representation of the secondary structure of tRNA. Schematic illustration of the generic tRNA cloverleaf secondary structure. The acceptor stem bearing the 3' CCA tail, the D-arm, the T-arm, the V-loop and the anticodon arm are depicted.

ii. tRNA transcription and processing: There are 416 tRNA genes predicted with high confidence in the human genome [hg19, (152, 153)]. RNA polymerase III (RNAPIII) is responsible for the transcription of tRNAs. RNAPIII is recruited to tRNA genes by the transcription factors TFIIIB and TFIIIC, which recognize two internal promotor elements, box A (nucleotides 8–19, D-loop) and box B (nucleotides 52–62, T-loop). All tRNAs show high conservation in nucleotides 8, 14, 18 and 19 in box A, and nucleotides 53–56, 58 and 61 in box B. Out of the remaining variable regions, human tRNA genes vary at 6.4% in box A, and 12.3% in box B. This variation can potentially mediate differential tRNA expression in various tissues (154-156). After transcription, the precursor tRNA (pre-tRNA) transcript undergoes a complex, multistep, and highly regulated maturation process in order to become functional. The steps for maturation of pre-tRNA to mature tRNA involve the deletion of the 5' leader, 3' trailer, and introns, as well as the addition of a cytosine-cytosine-adenine sequence to the 3' terminus (CCA tail), and nuclear export of the mature tRNA molecule to the cytoplasm. Aminoacyl-tRNA synthetases (aaRS) load the cognate amino acid to the CCA tail of the tRNA (termed as tRNA charging) which is an essential step in protein translation.

iii. tRNA post-transcriptional modifications: The pre-tRNA transcripts also undergo heavy post-transcriptional nucleoside modifications by tRNA modification enzymes throughout the maturation process (157, 158). These enzymes recognize local structure as well as certain motifs in the tRNA, and their activity is also dependent on presence of other modifications, temperature, and various stabilization

factors such as Mg^{2+} ions (159). Till date, 172 RNA modifications have been catalogued with a major bulk of these modifications found in tRNAs (160, 161). There is a whole gamut of tRNA modifications from simple sugar or base methylations to modifications requiring multiple enzymatic steps to realize, such as wybutosine (yW). tRNA modifications impact a number of aspects of tRNA biology including tRNA folding and structure, stability in the cell, and even in tRNA decoding function affecting efficiency and fidelity (151, 162-168). The modifications of tRNAs show dynamic changes in response to cellular environmental cues and the translational status of the cells (159, 162, 165, 169-173). Finally, stress-induced fragmentation of tRNAs to generate tRNA halves (tiRNAs) and shorter tRNA-derived RNA fragments (tRFs) further expand the tRNA functional repertoire (150, 164, 168, 174, 175).

Summary of relevant research on the role of specific tRNAs in HIV-1 life cycle

Apart from tRNALys3, other specific tRNAs may be playing an important role in HIV-1 life cycle.

i. tRNALys3 in HIV-1 reverse transcription: The host tRNALys3 (also known as LysTTT) serves as the primer for the initiation of reverse transcription and synthesis of the first DNA strand. tRNALys3 is selectively incorporated into the newly assembled viruses. This selective incorporation of tRNALys3 is shown to be facilitated by its cognate aminoacyl-tRNA synthetases, lysyl-tRNA synthetase (LysRS) (176), that binds and charges tRNALys3 with its corresponding amino acid, lysine. Of note, tRNALys3 binding to LysRS is needed for tRNALys3 packaging into the HIV-1 virus particle; but tRNALys3 aminoacylation is not required (177). HIV-1 Gag is required for this selective packaging of tRNALys3 (174). LysRS has been shown to interact with the CA-CTD of Gag. Further Gag-Pol, particularly RT, promotes preferred incorporation of tRNALys3 in the virion (178). The primer binding site (PBS) of the genome is not important for selective packaging of the tRNA primer. The tRNA-like element (TLE) in the 5'UTR of HIV-1 genome resembles the anticodon arm of tRNA (179-181). LysRS binds this TLE which causes the release of tRNALys3 which can then anneal to the PBS (150, 182). The HIV-1 Gag NC domain has been shown to promote the annealing of tRNALys3

to the PBS (150, 174, 178, 182). An 18 nucleotide segment at the 3' end of tRNALys3 is hybridized to the complementary PBS (27, 150, 183, 184). The 1-methyladenosine at position 58 (m1A58) of tRNALys3 acts as a stop signal for RT in order to copy precisely the last 18 nucleotides of tRNALys3 in the positive strand (150, 185, 186).

ii. Other tRNAs in HIV-1 reverse transcription: Apart from tRNALys3, select tRNAs, including tRNALys1,2, have been reported to be packaged into HIV-1 (184, 187, 188). It has been recently suggested, based on PBS sequence analysis from infected human plasma samples as well as from the PBS mutation frequencies across the HIV database, that tRNALys5, tRNALys6, and tRNALys1,2 could potentially prime reverse transcription in humans at lower frequencies (189). In addition, when the PBS is altered to be complementary to tRNAs other than tRNALys3, HIV-1 exhibits a preference for some select tRNAs, tRNALys1,2, tRNAMet, tRNAHis, and tRNAGlu, as alternative primers in vitro (174, 190).

iii. tRNAs in HIV-1 translation: A-ending codons, including UUA, are rare in the human genome but enriched in HIV-1 genome (191, 192). tRNALeu that reads UUA codon is also rare in the HIV-1 target T lymphocytes. The frameshifting efficiency is reported to be modulated by the availability of cellular tRNALeu that decodes the UUA codon at the slippery site (36). Microarray based data suggested that tRNAs selectively packaged in HIV-1 virons were potentially those that decode the rare codons required for translation of the HIV-1 late genes (191). The interferon-inducible schlafen 11 (SLFN11) was reported to inhibit the translation of the HIV-1 proteins in a codon usage-dependent manner. Microarray data revealed that HIV-1 transfection alters the tRNA population in cells in which the SLFN11 gene was knocked down, but not in the SLFN11 expressing cells. Notably, SLFN11 expression in CD4+ T cells is enhanced in HIV-1 elite controllers (individuals who suppress HIV-1 viral loads to undetectable levels even in the absence of ART) as compared to both untreated non-controllers and ART-treated individuals (150, 193). The P-element-induced wimpy-like (Piwi-like) protein 2, human Piwil2/Hili, was also found to inhibit replication of HIV-1 in a codon-specific manner. Unlike SLFN11 which does not bind to any specific tRNAs,

the mouse Hili equivalent, Mili, bound select tRNAs, including ArgUCU and IleUAU which are rare tRNAs in the cell, but enriched in the HIV-1 genome. HIV-1 translation was inhibited by expression of Hili in activated T cells, potentially due to the unavailability of the rare tRNAs needed for the HIV-1 protein translation (150, 194).

Overview of thesis

The work presented in this thesis illustrates the role of MA-RNA binding in cells and their effect on HIV-1 localization and membrane binding. **Chapter 2** demonstrates MA-RNA binding in cells is important for preventing the mislocalization of HIV-1 Gag to nonspecific intracellular compartments in cells. The importance of the MA-HBR sequence as well as charge in MA-RNA binding in cells is also described in **chapter 2**. **Chapter 3** discusses the specific interactions of select tRNAs with MA and proposes that there may be differential regulation of Gag-membrane binding in cells by different tRNAs. Specific characteristics of tRNAs that may potentially determine the specificity of select tRNAs for MA are also discussed. **Chapter 4** summarizes the data from chapters **2 and 3** and discusses the implications and future directions of the work presented.

References

1. WHO U. 2019. Global HIV & AIDS statistics.
2. Zalla LC, Herce ME, Edwards JK, Michel J, Weir SS. 2019. The burden of HIV among female sex workers, men who have sex with men and transgender women in Haiti: results from the 2016 Priorities for Local AIDS Control Efforts (PLACE) study. J Int AIDS Soc 22:e25281.
3. Freed EO. 2015. HIV-1 assembly, release and maturation. Nat Rev Microbiol 13:484-96.
4. Bailes E, Gao F, Bibollet-Ruche F, Courgnaud V, Peeters M, Marx PA, Hahn BH, Sharp PM. 2003. Hybrid origin of SIV in chimpanzees. Science 300:1713.
5. Keele BF, Jones JH, Terio KA, Estes JD, Rudicell RS, Wilson ML, Li Y, Learn GH, Beasley TM, Schumacher-Stankey J, Wroblewski E, Mosser A, Raphael J, Kamenya S, Lonsdorf EV, Travis DA, Mlengeya T, Kinsel MJ, Else JG, Silvestri G, Goodall J, Sharp PM, Shaw GM, Pusey AE, Hahn BH. 2009. Increased mortality and AIDS-like immunopathology in wild chimpanzees infected with SIVcpz. Nature 460:515-9.
6. Locatelli S, Peeters M. 2012. Cross-species transmission of simian retroviruses: how and why they could lead to the emergence of new diseases in the human population. AIDS 26:659-73.
7. Sharp PM, Hahn BH. 2011. Origins of HIV and the AIDS pandemic. Cold Spring Harb Perspect Med 1:a006841.
8. D'arc M, Ayouba A, Esteban A, Learn GH, Boué V, Liegeois F, Etienne L, Tagg N, Leendertz FH, Boesch C, Madinda NF, Robbins MM, Gray M, Cournil A, Ooms M, Letko M, Simon VA, Sharp PM, Hahn BH, Delaporte E, Mpoudi Ngole E, Peeters M. 2015. Origin of the HIV-1 group O epidemic in western lowland gorillas. Proc Natl Acad Sci U S A 112:E1343-52.
9. Sharp PM, Hahn BH. 2010. The evolution of HIV-1 and the origin of AIDS. Philos Trans R Soc Lond B Biol Sci 365:2487-94.
10. Hemelaar J. 2012. The origin and diversity of the HIV-1 pandemic. Trends Mol Med 18:182-92.
11. **HIV Sequence Compendium 2018** Foley B LT, Apetrei C, Hahn B, Mizrachi I, Mullins J, Rambaut A, Wolinsky S, and Korber B, Eds. Published by Theoretical Biology and Biophysics Group, Los Alamos National Laboratory, NM, LA-UR 18-25673.
12. Hemelaar J, Elangovan R, Yun J, Dickson-Tetteh L, Fleminger I, Kirtley S, Williams B, Gouws-Williams E, Ghys PD, Characterisation WUNfHI. 2019. Global and regional molecular epidemiology of HIV-1, 1990-2015: a systematic review, global survey, and trend analysis. Lancet Infect Dis 19:143-155.
13. Gartner MJ, Roche M, Churchill MJ, Gorry PR, Flynn JK. 2020. Understanding the mechanisms driving the spread of subtype C HIV-1. EBioMedicine 53:102682.
14. Muesing MA, Smith DH, Cabradilla CD, Benton CV, Lasky LA, Capon DJ. 1985. Nucleic acid structure and expression of the human AIDS/lymphadenopathy retrovirus. Nature 313:450-8.
15. Chen B. 2019. Molecular Mechanism of HIV-1 Entry. Trends Microbiol 27:878-891.
16. Wilen CB, Tilton JC, Doms RW. 2012. HIV: cell binding and entry. Cold Spring Harb Perspect Med 2.
17. Klatzmann D, Champagne E, Chamaret S, Gruest J, Guetard D, Hercend T, Gluckman JC, Montagnier L. 1984. T-lymphocyte T4 molecule behaves as the receptor for human retrovirus LAV. Nature 312:767-8.

18. Yang ZY, Chakrabarti BK, Xu L, Welcher B, Kong WP, Leung K, Panet A, Mascola JR, Nabel GJ. 2004. Selective modification of variable loops alters tropism and enhances immunogenicity of human immunodeficiency virus type 1 envelope. J Virol 78:4029-36.
19. Sattentau QJ, Moore JP. 1991. Conformational changes induced in the human immunodeficiency virus envelope glycoprotein by soluble CD4 binding. J Exp Med 174:407-15.
20. Joseph SB, Arrildt KT, Sturdevant CB, Swanstrom R. 2015. HIV-1 target cells in the CNS. J Neurovirol 21:276-89.
21. Dick RA, Zadrozny KK, Xu C, Schur FKM, Lyddon TD, Ricana CL, Wagner JM, Perilla JR, Ganser-Pornillos BK, Johnson MC, Pornillos O, Vogt VM. 2018. Inositol phosphates are assembly co-factors for HIV-1. Nature 560:509-512.
22. Mallery DL, Márquez CL, McEwan WA, Dickson CF, Jacques DA, Anandapadamanaban M, Bichel K, Towers GJ, Saiardi A, Böcking T, James LC. 2018. IP6 is an HIV pocket factor that prevents capsid collapse and promotes DNA synthesis. Elife 7.
23. Ganser-Pornillos BK, Pornillos O. 2019. Restriction of HIV-1 and other retroviruses by TRIM5. Nat Rev Microbiol 17:546-556.
24. Mallery DL, Faysal KMR, Kleinpeter A, Wilson MSC, Vaysburd M, Fletcher AJ, Novikova M, Böcking T, Freed EO, Saiardi A, James LC. 2019. Cellular IP. Cell Rep 29:3983-3996.e4.
25. Baltimore D. 1970. RNA-dependent DNA polymerase in virions of RNA tumour viruses. Nature 226:1209-11.
26. Temin HM, Mizutani S. 1970. RNA-dependent DNA polymerase in virions of Rous sarcoma virus. Nature 226:1211-3.
27. Hu WS, Hughes SH. 2012. HIV-1 reverse transcription. Cold Spring Harb Perspect Med 2.
28. Nchioua R, Bosso M, Kmiec D, Kirchhoff F. 2020. Cellular Factors Targeting HIV-1 Transcription and Viral RNA Transcripts. Viruses 12.
29. Das AT, Harwig A, Berkhout B. 2011. The HIV-1 Tat protein has a versatile role in activating viral transcription. J Virol 85:9506-16.
30. Rice AP. 2017. The HIV-1 Tat Protein: Mechanism of Action and Target for HIV-1 Cure Strategies. Curr Pharm Des 23:4098-4102.
31. Faust TB, Binning JM, Gross JD, Frankel AD. 2017. Making Sense of Multifunctional Proteins: Human Immunodeficiency Virus Type 1 Accessory and Regulatory Proteins and Connections to Transcription. Annu Rev Virol 4:241-260.
32. Ajasin D, Eugenin EA. 2020. HIV-1 Tat: Role in Bystander Toxicity. Front Cell Infect Microbiol 10:61.
33. Pereira EA, daSilva LL. 2016. HIV-1 Nef: Taking Control of Protein Trafficking. Traffic 17:976-96.
34. Ramirez PW, Sharma S, Singh R, Stoneham CA, Vollbrecht T, Guatelli J. 2019. Plasma Membrane-Associated Restriction Factors and Their Counteraction by HIV-1 Accessory Proteins. Cells 8.
35. Neville M, Stutz F, Lee L, Davis LI, Rosbash M. 1997. The importin-beta family member Crm1p bridges the interaction between Rev and the nuclear pore complex during nuclear export. Curr Biol 7:767-75.
36. Korniy N, Goyal A, Hoffmann M, Samatova E, Peske F, Pöhlmann S, Rodnina MV. 2019. Modulation of HIV-1 Gag/Gag-Pol frameshifting by tRNA abundance. Nucleic Acids Res 47:5210-5222.
37. Jacks T, Power MD, Masiarz FR, Luciw PA, Barr PJ, Varmus HE. 1988. Characterization of ribosomal frameshifting in HIV-1 gag-pol expression. Nature 331:280-3.
38. Parkin NT, Chamorro M, Varmus HE. 1992. Human immunodeficiency virus type 1 gag-pol frameshifting is dependent on downstream mRNA secondary structure: demonstration by expression in vivo. J Virol 66:5147-51.

39. Wang X, Xuan Y, Han Y, Ding X, Ye K, Yang F, Gao P, Goff SP, Gao G. 2019. Regulation of HIV-1 Gag-Pol Expression by Shiftless, an Inhibitor of Programmed -1 Ribosomal Frameshifting. Cell 176:625-635.e14.
40. Novikova M, Zhang Y, Freed EO, Peng K. 2019. Multiple Roles of HIV-1 Capsid during the Virus Replication Cycle. Virol Sin 34:119-134.
41. Levin JG, Guo J, Rouzina I, Musier-Forsyth K. 2005. Nucleic acid chaperone activity of HIV-1 nucleocapsid protein: critical role in reverse transcription and molecular mechanism. Prog Nucleic Acid Res Mol Biol 80:217-86.
42. Gorelick RJ, Nigida SM, Bess JW, Arthur LO, Henderson LE, Rein A. 1990. Noninfectious human immunodeficiency virus type 1 mutants deficient in genomic RNA. J Virol 64:3207-11.
43. McBride MS, Panganiban AT. 1996. The human immunodeficiency virus type 1 encapsidation site is a multipartite RNA element composed of functional hairpin structures. J Virol 70:2963-73.
44. Muriaux D, Mirro J, Harvin D, Rein A. 2001. RNA is a structural element in retrovirus particles. Proc Natl Acad Sci U S A 98:5246-51.
45. Fujii K, Munshi UM, Ablan SD, Demirov DG, Soheilian F, Nagashima K, Stephen AG, Fisher RJ, Freed EO. 2009. Functional role of Alix in HIV-1 replication. Virology 391:284-92.
46. Huang M, Orenstein JM, Martin MA, Freed EO. 1995. p6Gag is required for particle production from full-length human immunodeficiency virus type 1 molecular clones expressing protease. J Virol 69:6810-8.
47. Venkatesh S, Bieniasz PD. 2013. Mechanism of HIV-1 virion entrapment by tetherin. PLoS Pathog 9:e1003483.
48. Neil SJ. 2017. Exercising Restraint. Cell Host Microbe 21:274-277.
49. Foster TL, Pickering S, Neil SJD. 2017. Inhibiting the Ins and Outs of HIV Replication: Cell-Intrinsic Antiretroviral Restrictions at the Plasma Membrane. Front Immunol 8:1853.
50. Neil SJ, Zang T, Bieniasz PD. 2008. Tetherin inhibits retrovirus release and is antagonized by HIV-1 Vpu. Nature 451:425-30.
51. Perez-Caballero D, Zang T, Ebrahimi A, McNatt MW, Gregory DA, Johnson MC, Bieniasz PD. 2009. Tetherin inhibits HIV-1 release by directly tethering virions to cells. Cell 139:499-511.
52. Van Damme N, Goff D, Katsura C, Jorgenson RL, Mitchell R, Johnson MC, Stephens EB, Guatelli J. 2008. The interferon-induced protein BST-2 restricts HIV-1 release and is downregulated from the cell surface by the viral Vpu protein. Cell Host Microbe 3:245-52.
53. Yin X, Langer S, Zhang Z, Herbert KM, Yoh S, König R, Chanda SK. 2020. Sensor Sensibility-HIV-1 and the Innate Immune Response. Cells 9.
54. Jouvenet N, Neil SJ, Bess C, Johnson MC, Virgen CA, Simon SM, Bieniasz PD. 2006. Plasma membrane is the site of productive HIV-1 particle assembly. PLoS Biol 4:e435.
55. Finzi A, Orthwein A, Mercier J, Cohen EA. 2007. Productive human immunodeficiency virus type 1 assembly takes place at the plasma membrane. J Virol 81:7476-90.
56. Göttlinger HG, Sodroski JG, Haseltine WA. 1989. Role of capsid precursor processing and myristoylation in morphogenesis and infectivity of human immunodeficiency virus type 1. Proc Natl Acad Sci U S A 86:5781-5.
57. Bryant M, Ratner L. 1990. Myristoylation-dependent replication and assembly of human immunodeficiency virus 1. Proc Natl Acad Sci U S A 87:523-7.
58. Yuan X, Yu X, Lee TH, Essex M. 1993. Mutations in the N-terminal region of human immunodeficiency virus type 1 matrix protein block intracellular transport of the Gag precursor. J Virol 67:6387-94.
59. Zhou W, Parent LJ, Wills JW, Resh MD. 1994. Identification of a membrane-binding domain within the amino-terminal region of human immunodeficiency virus type 1 Gag protein which interacts with acidic phospholipids. J Virol 68:2556-69.

60. Freed EO, Orenstein JM, Buckler-White AJ, Martin MA. 1994. Single amino acid changes in the human immunodeficiency virus type 1 matrix protein block virus particle production. J Virol 68:5311-20.
61. Ono A, Orenstein JM, Freed EO. 2000. Role of the Gag matrix domain in targeting human immunodeficiency virus type 1 assembly. J Virol 74:2855-66.
62. Ono A, Ablan SD, Lockett SJ, Nagashima K, Freed EO. 2004. Phosphatidylinositol (4,5) bisphosphate regulates HIV-1 Gag targeting to the plasma membrane. Proc Natl Acad Sci U S A 101:14889-94.
63. Resh MD. 2016. Fatty acylation of proteins: The long and the short of it. Prog Lipid Res 63:120-31.
64. Zhou W, Resh MD. 1996. Differential membrane binding of the human immunodeficiency virus type 1 matrix protein. J Virol 70:8540-8.
65. Ono A, Freed EO. 1999. Binding of human immunodeficiency virus type 1 Gag to membrane: role of the matrix amino terminus. J Virol 73:4136-44.
66. Paillart JC, Göttlinger HG. 1999. Opposing effects of human immunodeficiency virus type 1 matrix mutations support a myristyl switch model of gag membrane targeting. J Virol 73:2604-12.
67. Hermida-Matsumoto L, Resh MD. 1999. Human immunodeficiency virus type 1 protease triggers a myristoyl switch that modulates membrane binding of Pr55(gag) and p17MA. J Virol 73:1902-8.
68. Tang C, Loeliger E, Luncsford P, Kinde I, Beckett D, Summers MF. 2004. Entropic switch regulates myristate exposure in the HIV-1 matrix protein. Proc Natl Acad Sci U S A 101:517-22.
69. Saad JS, Miller J, Tai J, Kim A, Ghanam RH, Summers MF. 2006. Structural basis for targeting HIV-1 Gag proteins to the plasma membrane for virus assembly. Proc Natl Acad Sci U S A 103:11364-9.
70. Saad JS, Loeliger E, Luncsford P, Liriano M, Tai J, Kim A, Miller J, Joshi A, Freed EO, Summers MF. 2007. Point mutations in the HIV-1 matrix protein turn off the myristyl switch. J Mol Biol 366:574-85.
71. Li H, Dou J, Ding L, Spearman P. 2007. Myristoylation is required for human immunodeficiency virus type 1 Gag-Gag multimerization in mammalian cells. J Virol 81:12899-910.
72. Hill CP, Worthylake D, Bancroft DP, Christensen AM, Sundquist WI. 1996. Crystal structures of the trimeric human immunodeficiency virus type 1 matrix protein: implications for membrane association and assembly. Proc Natl Acad Sci U S A 93:3099-104.
73. Murray PS, Li Z, Wang J, Tang CL, Honig B, Murray D. 2005. Retroviral matrix domains share electrostatic homology: models for membrane binding function throughout the viral life cycle. Structure 13:1521-31.
74. Dalton AK, Ako-Adjei D, Murray PS, Murray D, Vogt VM. 2007. Electrostatic interactions drive membrane association of the human immunodeficiency virus type 1 Gag MA domain. Journal of Virology 81:6434-6445.
75. Ehrlich LS, Fong S, Scarlata S, Zybarth G, Carter C. 1996. Partitioning of HIV-1 Gag and Gag-related proteins to membranes. Biochemistry 35:3933-43.
76. Shkriabai N, Datta SA, Zhao Z, Hess S, Rein A, Kvaratskhelia M. 2006. Interactions of HIV-1 Gag with assembly cofactors. Biochemistry 45:4077-83.
77. Chukkapalli V, Hogue IB, Boyko V, Hu WS, Ono A. 2008. Interaction between the human immunodeficiency virus type 1 Gag matrix domain and phosphatidylinositol-(4,5)-bisphosphate is essential for efficient gag membrane binding. J Virol 82:2405-17.

78. Chan R, Uchil PD, Jin J, Shui G, Ott DE, Mothes W, Wenk MR. 2008. Retroviruses human immunodeficiency virus and murine leukemia virus are enriched in phosphoinositides. J Virol 82:11228-38.
79. Alfadhli A, Barklis RL, Barklis E. 2009. HIV-1 matrix organizes as a hexamer of trimers on membranes containing phosphatidylinositol-(4,5)-bisphosphate. Virology 387:466-72.
80. Chukkapalli V, Oh SJ, Ono A. 2010. Opposing mechanisms involving RNA and lipids regulate HIV-1 Gag membrane binding through the highly basic region of the matrix domain. Proc Natl Acad Sci U S A 107:1600-5.
81. Anraku K, Fukuda R, Takamune N, Misumi S, Okamoto Y, Otsuka M, Fujita M. 2010. Highly sensitive analysis of the interaction between HIV-1 Gag and phosphoinositide derivatives based on surface plasmon resonance. Biochemistry 49:5109-16.
82. Inlora J, Chukkapalli V, Derse D, Ono A. 2011. Gag localization and virus-like particle release mediated by the matrix domain of human T-lymphotropic virus type 1 Gag are less dependent on phosphatidylinositol-(4,5)-bisphosphate than those mediated by the matrix domain of HIV-1 Gag. J Virol 85:3802-10.
83. Chukkapalli V, Ono A. 2011. Molecular determinants that regulate plasma membrane association of HIV-1 Gag. J Mol Biol 410:512-24.
84. Inlora J, Collins DR, Trubin ME, Chung JY, Ono A. 2014. Membrane binding and subcellular localization of retroviral Gag proteins are differentially regulated by MA interactions with phosphatidylinositol-(4,5)-bisphosphate and RNA. MBio 5:e02202.
85. Alfadhli A, Still A, Barklis E. 2009. Analysis of human immunodeficiency virus type 1 matrix binding to membranes and nucleic acids. J Virol 83:12196-203.
86. Alfadhli A, McNett H, Tsagli S, Bächinger HP, Peyton DH, Barklis E. 2011. HIV-1 matrix protein binding to RNA. J Mol Biol 410:653-66.
87. Sun Y, Thapa N, Hedman AC, Anderson RA. 2013. Phosphatidylinositol 4,5-bisphosphate: targeted production and signaling. Bioessays 35:513-22.
88. Tan X, Thapa N, Choi S, Anderson RA. 2015. Emerging roles of PtdIns(4,5)P2--beyond the plasma membrane. J Cell Sci 128:4047-56.
89. Dickson EJ, Hille B. 2019. Understanding phosphoinositides: rare, dynamic, and essential membrane phospholipids. Biochem J 476:1-23.
90. Kisseleva MV, Wilson MP, Majerus PW. 2000. The isolation and characterization of a cDNA encoding phospholipid-specific inositol polyphosphate 5-phosphatase. J Biol Chem 275:20110-6.
91. Balla T. 2013. Phosphoinositides: tiny lipids with giant impact on cell regulation. Physiol Rev 93:1019-137.
92. D'Souza K, Epand RM. 2014. Enrichment of phosphatidylinositols with specific acyl chains. Biochim Biophys Acta 1838:1501-8.
93. Majerus PW, York JD. 2009. Phosphoinositide phosphatases and disease. J Lipid Res 50 Suppl:S249-54.
94. Gericke A, Leslie NR, Lösche M, Ross AH. 2013. PtdIns(4,5)P2-mediated cell signaling: emerging principles and PTEN as a paradigm for regulatory mechanism. Adv Exp Med Biol 991:85-104.
95. Hsu F, Mao Y. 2015. The structure of phosphoinositide phosphatases: Insights into substrate specificity and catalysis. Biochim Biophys Acta 1851:698-710.
96. Hammond GRV, Burke JE. 2020. Novel roles of phosphoinositides in signaling, lipid transport, and disease. Curr Opin Cell Biol 63:57-67.
97. Monde K, Chukkapalli V, Ono A. 2011. Assembly and replication of HIV-1 in T cells with low levels of phosphatidylinositol-(4,5)-bisphosphate. J Virol 85:3584-95.
98. Mücksch F, Laketa V, Müller B, Schultz C, Kräusslich HG. 2017. Synchronized HIV assembly by tunable PIP. Elife 6.

99. Chan J, Dick RA, Vogt VM. 2011. Rous Sarcoma Virus Gag Has No Specific Requirement for Phosphatidylinositol-(4,5)-Bisphosphate for Plasma Membrane Association In Vivo or for Liposome Interaction In Vitro.
100. Gerber PP, Cabrini M, Jancic C, Paoletti L, Banchio C, von Bilderling C, Sigaut L, Pietrasanta LI, Duette G, Freed EO, Basile GeS, Moita CF, Moita LF, Amigorena S, Benaroch P, Geffner J, Ostrowski M. 2015. Rab27a controls HIV-1 assembly by regulating plasma membrane levels of phosphatidylinositol 4,5-bisphosphate. J Cell Biol 209:435-52.
101. Gonzales B, de Rocquigny H, Beziau A, Durand S, Burlaud-Gaillard J, Lefebvre A, Krull S, Emond P, Brand D, Piver E. 2020. Type I phosphatidylinositol-4-phosphate 5-kinase α and γ play a key role in targeting HIV-1 Pr55. J Virol.
102. Nadaraia-Hoke S, Bann DV, Lochmann TL, Gudleski-O'Regan N, Parent LJ. 2013. Alterations in the MA and NC domains modulate phosphoinositide-dependent plasma membrane localization of the Rous sarcoma virus Gag protein. J Virol 87:3609-15.
103. Fernandes F, Chen K, Ehrlich LS, Jin J, Chen MH, Medina GN, Symons M, Montelaro R, Donaldson J, Tjandra N, Carter CA. 2011. Phosphoinositides direct equine infectious anemia virus gag trafficking and release. Traffic 12:438-51.
104. Stansell E, Apkarian R, Haubova S, Diehl WE, Tytler EM, Hunter E. 2007. Basic residues in the Mason-Pfizer monkey virus gag matrix domain regulate intracellular trafficking and capsid-membrane interactions. J Virol 81:8977-88.
105. Hamard-Peron E, Juillard F, Saad JS, Roy C, Roingeard P, Summers MF, Darlix JL, Picart C, Muriaux D. 2010. Targeting of murine leukemia virus gag to the plasma membrane is mediated by PI(4,5)P2/PS and a polybasic region in the matrix. J Virol 84:503-15.
106. Saad JS, Ablan SD, Ghanam RH, Kim A, Andrews K, Nagashima K, Soheilian F, Freed EO, Summers MF. 2008. Structure of the myristylated human immunodeficiency virus type 2 matrix protein and the role of phosphatidylinositol-(4,5)-bisphosphate in membrane targeting. J Mol Biol 382:434-47.
107. Chan J, Dick RA, Vogt VM. 2011. Rous sarcoma virus gag has no specific requirement for phosphatidylinositol-(4,5)-bisphosphate for plasma membrane association in vivo or for liposome interaction in vitro. J Virol 85:10851-60.
108. Ramos AR, Ghosh S, Erneux C. 2019. The impact of phosphoinositide 5-phosphatases on phosphoinositides in cell function and human disease. J Lipid Res 60:276-286.
109. McLaughlin S, Murray D. 2005. Plasma membrane phosphoinositide organization by protein electrostatics. Nature 438:605-11.
110. Barros M, Heinrich F, Datta SAK, Rein A, Karageorgos I, Nanda H, Lösche M. 2016. Membrane Binding of HIV-1 Matrix Protein: Dependence on Bilayer Composition and Protein Lipidation. J Virol 90:4544-4555.
111. Carlson LA, Bai Y, Keane SC, Doudna JA, Hurley JH. 2016. Reconstitution of selective HIV-1 RNA packaging in vitro by membrane-bound Gag assemblies. Elife 5.
112. Keller H, Kräusslich HG, Schwille P. 2013. Multimerizable HIV Gag derivative binds to the liquid-disordered phase in model membranes. Cell Microbiol 15:237-47.
113. Tran RJ, Lalonde MS, Sly KL, Conboy JC. 2019. Mechanistic Investigation of HIV-1 Gag Association with Lipid Membranes. J Phys Chem B 123:4673-4687.
114. Dick RA, Kamynina E, Vogt VM. 2013. Effect of multimerization on membrane association of Rous sarcoma virus and HIV-1 matrix domain proteins. J Virol 87:13598-608.
115. Mercredi PY, Bucca N, Loeliger B, Gaines CR, Mehta M, Bhargava P, Tedbury PR, Charlier L, Floquet N, Muriaux D, Favard C, Sanders CR, Freed EO, Marchant J, Summers MF. 2016. Structural and Molecular Determinants of Membrane Binding by the HIV-1 Matrix Protein. J Mol Biol 428:1637-55.

116. Thornhill D, Olety B, Ono A. 2019. Relationships between MA-RNA Binding in Cells and Suppression of HIV-1 Gag Mislocalization to Intracellular Membranes. J Virol 93.
117. Murphy RE, Samal AB, Vlach J, Mas V, Prevelige PE, Saad JS. 2019. Structural and biophysical characterizations of HIV-1 matrix trimer binding to lipid nanodiscs shed light on virus assembly. J Biol Chem 294:18600-18612.
118. Junková P, Pleskot R, Prchal J, Sýs J, Ruml T. 2020. Differences and commonalities in plasma membrane recruitment of the two morphogenetically distinct retroviruses HIV-1 and MMTV. J Biol Chem 295:8819-8833.
119. Traynor-Kaplan A, Kruse M, Dickson EJ, Dai G, Vivas O, Yu H, Whittington D, Hille B. 2017. Fatty-acyl chain profiles of cellular phosphoinositides. Biochim Biophys Acta Mol Cell Biol Lipids 1862:513-522.
120. Epand RM, So V, Jennings W, Khadka B, Gupta RS, Lemaire M. 2016. Diacylglycerol Kinase-ε: Properties and Biological Roles. Front Cell Dev Biol 4:112.
121. Barneda D, Cosulich S, Stephens L, Hawkins P. 2019. How is the acyl chain composition of phosphoinositides created and does it matter? Biochem Soc Trans 47:1291-1305.
122. Charlier L, Louet M, Chaloin L, Fuchs P, Martinez J, Muriaux D, Favard C, Floquet N. 2014. Coarse-grained simulations of the HIV-1 matrix protein anchoring: revisiting its assembly on membrane domains. Biophys J 106:577-85.
123. Olety B, Veatch SL, Ono A. 2015. Phosphatidylinositol-(4,5)-Bisphosphate Acyl Chains Differentiate Membrane Binding of HIV-1 Gag from That of the Phospholipase Cδ1 Pleckstrin Homology Domain. J Virol 89:7861-73.
124. Dick RA, Goh SL, Feigenson GW, Vogt VM. 2012. HIV-1 Gag protein can sense the cholesterol and acyl chain environment in model membranes. Proc Natl Acad Sci U S A 109:18761-6.
125. Dick RA, Datta SA, Nanda H, Fang X, Wen Y, Barros M, Wang YX, Rein A, Vogt VM. 2015. Hydrodynamic and Membrane Binding Properties of Purified Rous Sarcoma Virus Gag Protein. J Virol 89:10371-82.
126. Wen Y, Dick RA, Feigenson GW, Vogt VM. 2016. Effects of Membrane Charge and Order on Membrane Binding of the Retroviral Structural Protein Gag. J Virol 90:9518-32.
127. Mücksch F, Citir M, Lüchtenborg C, Glass B, Traynor-Kaplan A, Schultz C, Brügger B, Kräusslich HG. 2019. Quantification of phosphoinositides reveals strong enrichment of PIP. Sci Rep 9:17661.
128. Brügger B, Glass B, Haberkant P, Leibrecht I, Wieland FT, Kräusslich HG. 2006. The HIV lipidome: a raft with an unusual composition. Proc Natl Acad Sci U S A 103:2641-6.
129. Lorizate M, Sachsenheimer T, Glass B, Habermann A, Gerl MJ, Kräusslich HG, Brügger B. 2013. Comparative lipidomics analysis of HIV-1 particles and their producer cell membrane in different cell lines. Cell Microbiol 15:292-304.
130. van den Bogaart G, Meyenberg K, Risselada HJ, Amin H, Willig KI, Hubrich BE, Dier M, Hell SW, Grubmüller H, Diederichsen U, Jahn R. 2011. Membrane protein sequestering by ionic protein-lipid interactions. Nature 479:552-5.
131. Wang J, Richards DA. 2012. Segregation of PIP2 and PIP3 into distinct nanoscale regions within the plasma membrane. Biol Open 1:857-62.
132. Levental I, Christian DA, Wang YH, Madara JJ, Discher DE, Janmey PA. 2009. Calcium-dependent lateral organization in phosphatidylinositol 4,5-bisphosphate (PIP2)- and cholesterol-containing monolayers. Biochemistry 48:8241-8.
133. Wen Y, Vogt VM, Feigenson GW. 2018. Multivalent Cation-Bridged PI(4,5)P. Biophys J 114:2630-2639.
134. Wang J, Gambhir A, McLaughlin S, Murray D. 2004. A computational model for the electrostatic sequestration of PI(4,5)P2 by membrane-adsorbed basic peptides. Biophys J 86:1969-86.

135. Purohit P, Dupont S, Stevenson M, Green MR. 2001. Sequence-specific interaction between HIV-1 matrix protein and viral genomic RNA revealed by in vitro genetic selection. RNA 7:576-84.
136. Hearps AC, Wagstaff KM, Piller SC, Jans DA. 2008. The N-terminal basic domain of the HIV-1 matrix protein does not contain a conventional nuclear localization sequence but is required for DNA binding and protein self-association. Biochemistry 47:2199-210.
137. Kutluay SB, Zang T, Blanco-Melo D, Powell C, Jannain D, Errando M, Bieniasz PD. 2014. Global changes in the RNA binding specificity of HIV-1 gag regulate virion genesis. Cell 159:1096-1109.
138. Gaines CR, Tkacik E, Rivera-Oven A, Somani P, Achimovich A, Alabi T, Zhu A, Getachew N, Yang AL, McDonough M, Hawkins T, Spadaro Z, Summers MF. 2018. HIV-1 Matrix Protein Interactions with tRNA: Implications for Membrane Targeting. J Mol Biol 430:2113-2127.
139. Jones CP, Datta SA, Rein A, Rouzina I, Musier-Forsyth K. 2011. Matrix domain modulates HIV-1 Gag's nucleic acid chaperone activity via inositol phosphate binding. J Virol 85:1594-603.
140. Kroupa T, Datta SAK, Rein A. 2020. Distinct Contributions of Different Domains within the HIV-1 Gag Polyprotein to Specific and Nonspecific Interactions with RNA. Viruses 12.
141. Chukkapalli V, Inlora J, Todd GC, Ono A. 2013. Evidence in support of RNA-mediated inhibition of phosphatidylserine-dependent HIV-1 Gag membrane binding in cells. J Virol 87:7155-9.
142. Todd GC, Duchon A, Inlora J, Olson ED, Musier-Forsyth K, Ono A. 2017. Inhibition of HIV-1 Gag-membrane interactions by specific RNAs. RNA 23:395-405.
143. Burniston MT, Cimarelli A, Colgan J, Curtis SP, Luban J. 1999. Human immunodeficiency virus type 1 Gag polyprotein multimerization requires the nucleocapsid domain and RNA and is promoted by the capsid-dimer interface and the basic region of matrix protein. J Virol 73:8527-40.
144. Ott DE, Coren LV, Gagliardi TD. 2005. Redundant roles for nucleocapsid and matrix RNA-binding sequences in human immunodeficiency virus type 1 assembly. J Virol 79:13839-47.
145. Cimarelli A, Luban J. 1999. Translation elongation factor 1-alpha interacts specifically with the human immunodeficiency virus type 1 Gag polyprotein. J Virol 73:5388-401.
146. Webb JA, Jones CP, Parent LJ, Rouzina I, Musier-Forsyth K. 2013. Distinct binding interactions of HIV-1 Gag to Psi and non-Psi RNAs: implications for viral genomic RNA packaging. RNA 19:1078-88.
147. Ramalingam D, Duclair S, Datta SA, Ellington A, Rein A, Prasad VR. 2011. RNA aptamers directed to human immunodeficiency virus type 1 Gag polyprotein bind to the matrix and nucleocapsid domains and inhibit virus production. J Virol 85:305-14.
148. Lochrie MA, Waugh S, Pratt DG, Clever J, Parslow TG, Polisky B. 1997. In vitro selection of RNAs that bind to the human immunodeficiency virus type-1 gag polyprotein. Nucleic Acids Res 25:2902-10.
149. Chang CY, Chang YF, Wang SM, Tseng YT, Huang KJ, Wang CT. 2008. HIV-1 matrix protein repositioning in nucleocapsid region fails to confer virus-like particle assembly. Virology 378:97-104.
150. Nunes A, Ribeiro DR, Marques M, Santos MAS, Ribeiro D, Soares AR. 2020. Emerging Roles of tRNAs in RNA Virus Infections. Trends Biochem Sci.
151. Lorenz C, Lünse CE, Mörl M. 2017. tRNA Modifications: Impact on Structure and Thermal Adaptation. Biomolecules 7.
152. Chan PP, Lowe TM. 2016. GtRNAdb 2.0: an expanded database of transfer RNA genes identified in complete and draft genomes. Nucleic Acids Res 44:D184-9.
153. Chan PP, Lowe TM. 2009. GtRNAdb: a database of transfer RNA genes detected in genomic sequence. Nucleic Acids Res 37:D93-7.
154. Paule MR, White RJ. 2000. Survey and summary: transcription by RNA polymerases I and III. Nucleic Acids Res 28:1283-98.

155. Geiduschek EP, Kassavetis GA. 2001. The RNA polymerase III transcription apparatus. J Mol Biol 310:1-26.
156. Goodenbour JM, Pan T. 2006. Diversity of tRNA genes in eukaryotes. Nucleic Acids Res 34:6137-46.
157. Hopper AK, Nostramo RT. 2019. tRNA Processing and Subcellular Trafficking Proteins Multitask in Pathways for Other RNAs. Front Genet 10:96.
158. Schaffer AE, Pinkard O, Coller JM. 2019. tRNA Metabolism and Neurodevelopmental Disorders. Annu Rev Genomics Hum Genet 20:359-387.
159. Hori H. 2019. Regulatory Factors for tRNA Modifications in Extreme- Thermophilic Bacterium. Front Genet 10:204.
160. Boccaletto P, Machnicka MA, Purta E, Piatkowski P, Baginski B, Wirecki TK, de Crécy-Lagard V, Ross R, Limbach PA, Kotter A, Helm M, Bujnicki JM. 2018. MODOMICS: a database of RNA modification pathways. 2017 update. Nucleic Acids Res 46:D303-D307.
161. Cantara WA, Crain PF, Rozenski J, McCloskey JA, Harris KA, Zhang X, Vendeix FA, Fabris D, Agris PF. 2011. The RNA Modification Database, RNAMDB: 2011 update. Nucleic Acids Res 39:D195-201.
162. Koh CS, Sarin LP. 2018. Transfer RNA modification and infection - Implications for pathogenicity and host responses. Biochim Biophys Acta Gene Regul Mech 1861:419-432.
163. El Yacoubi B, Bailly M, de Crécy-Lagard V. 2012. Biosynthesis and function of posttranscriptional modifications of transfer RNAs. Annu Rev Genet 46:69-95.
164. Schimmel P. 2018. The emerging complexity of the tRNA world: mammalian tRNAs beyond protein synthesis. Nat Rev Mol Cell Biol 19:45-58.
165. Pan T. 2018. Modifications and functional genomics of human transfer RNA. Cell Res 28:395-404.
166. Väre VY, Eruysal ER, Narendran A, Sarachan KL, Agris PF. 2017. Chemical and Conformational Diversity of Modified Nucleosides Affects tRNA Structure and Function. Biomolecules 7.
167. Pereira M, Francisco S, Varanda AS, Santos M, Santos MAS, Soares AR. 2018. Impact of tRNA Modifications and tRNA-Modifying Enzymes on Proteostasis and Human Disease. Int J Mol Sci 19.
168. Huber SM, Leonardi A, Dedon PC, Begley TJ. 2019. The Versatile Roles of the tRNA Epitranscriptome during Cellular Responses to Toxic Exposures and Environmental Stress. Toxics 7.
169. Alings F, Sarin LP, Fufezan C, Drexler HC, Leidel SA. 2015. An evolutionary approach uncovers a diverse response of tRNA 2-thiolation to elevated temperatures in yeast. RNA 21:202-12.
170. Chionh YH, McBee M, Babu IR, Hia F, Lin W, Zhao W, Cao J, Dziergowska A, Malkiewicz A, Begley TJ, Alonso S, Dedon PC. 2016. tRNA-mediated codon-biased translation in mycobacterial hypoxic persistence. Nat Commun 7:13302.
171. Roundtree IA, Evans ME, Pan T, He C. 2017. Dynamic RNA Modifications in Gene Expression Regulation. Cell 169:1187-1200.
172. Arimbasseri AG, Blewett NH, Iben JR, Lamichhane TN, Cherkasova V, Hafner M, Maraia RJ. 2015. RNA Polymerase III Output Is Functionally Linked to tRNA Dimethyl-G26 Modification. PLoS Genet 11:e1005671.
173. Chan C, Pham P, Dedon PC, Begley TJ. 2018. Lifestyle modifications: coordinating the tRNA epitranscriptome with codon bias to adapt translation during stress responses. Genome Biol 19:228.
174. Jin D, Musier-Forsyth K. 2019. Role of host tRNAs and aminoacyl-tRNA synthetases in retroviral replication. J Biol Chem 294:5352-5364.

175. Torres AG, Reina O, Stephan-Otto Attolini C, Ribas de Pouplana L. 2019. Differential expression of human tRNA genes drives the abundance of tRNA-derived fragments. Proc Natl Acad Sci U S A 116:8451-8456.
176. Cen S, Khorchid A, Javanbakht H, Gabor J, Stello T, Shiba K, Musier-Forsyth K, Kleiman L. 2001. Incorporation of lysyl-tRNA synthetase into human immunodeficiency virus type 1. J Virol 75:5043-8.
177. Javanbakht H, Cen S, Musier-Forsyth K, Kleiman L. 2002. Correlation between tRNALys3 aminoacylation and its incorporation into HIV-1. J Biol Chem 277:17389-96.
178. Mak J, Jiang M, Wainberg MA, Hammarskjöld ML, Rekosh D, Kleiman L. 1994. Role of Pr160gag-pol in mediating the selective incorporation of tRNA(Lys) into human immunodeficiency virus type 1 particles. J Virol 68:2065-72.
179. Jones CP, Saadatmand J, Kleiman L, Musier-Forsyth K. 2013. Molecular mimicry of human tRNALys anti-codon domain by HIV-1 RNA genome facilitates tRNA primer annealing. RNA 19:219-29.
180. Jones CP, Cantara WA, Olson ED, Musier-Forsyth K. 2014. Small-angle X-ray scattering-derived structure of the HIV-1 5' UTR reveals 3D tRNA mimicry. Proc Natl Acad Sci U S A 111:3395-400.
181. Liu S, Comandur R, Jones CP, Tsang P, Musier-Forsyth K. 2016. Anticodon-like binding of the HIV-1 tRNA-like element to human lysyl-tRNA synthetase. RNA 22:1828-1835.
182. Duchon AA, St Gelais C, Titkemeier N, Hatterschide J, Wu L, Musier-Forsyth K. 2017. HIV-1 Exploits a Dynamic Multi-aminoacyl-tRNA Synthetase Complex To Enhance Viral Replication. J Virol 91.
183. Ratner L, Haseltine W, Patarca R, Livak KJ, Starcich B, Josephs SF, Doran ER, Rafalski JA, Whitehorn EA, Baumeister K. 1985. Complete nucleotide sequence of the AIDS virus, HTLV-III. Nature 313:277-84.
184. Jiang M, Mak J, Ladha A, Cohen E, Klein M, Rovinski B, Kleiman L. 1993. Identification of tRNAs incorporated into wild-type and mutant human immunodeficiency virus type 1. J Virol 67:3246-53.
185. Zhang C, Jia G. 2018. Reversible RNA Modification N. Genomics Proteomics Bioinformatics 16:155-161.
186. Auxilien S, Keith G, Le Grice SF, Darlix JL. 1999. Role of post-transcriptional modifications of primer tRNALys,3 in the fidelity and efficacy of plus strand DNA transfer during HIV-1 reverse transcription. J Biol Chem 274:4412-20.
187. Huang Y, Mak J, Cao Q, Li Z, Wainberg MA, Kleiman L. 1994. Incorporation of excess wild-type and mutant tRNA(3Lys) into human immunodeficiency virus type 1. J Virol 68:7676-83.
188. Pavon-Eternod M, Wei M, Pan T, Kleiman L. 2010. Profiling non-lysyl tRNAs in HIV-1. RNA 16:267-73.
189. Fennessey CM, Camus C, Immonen TT, Reid C, Maldarelli F, Lifson JD, Keele BF. 2019. Low-level alternative tRNA priming of reverse transcription of HIV-1 and SIV in vivo. Retrovirology 16:11.
190. Ni N, Morrow CD. 2007. Impact of forced selection of tRNAs on HIV-1 replication and genome stability highlight preferences for selection of certain tRNAs. Virus Res 124:29-37.
191. van Weringh A, Ragonnet-Cronin M, Pranckeviciene E, Pavon-Eternod M, Kleiman L, Xia X. 2011. HIV-1 modulates the tRNA pool to improve translation efficiency. Mol Biol Evol 28:1827-34.
192. Berkhout B, Grigoriev A, Bakker M, Lukashov VV. 2002. Codon and amino acid usage in retroviral genomes is consistent with virus-specific nucleotide pressure. AIDS Res Hum Retroviruses 18:133-41.
193. Li M, Kao E, Gao X, Sandig H, Limmer K, Pavon-Eternod M, Jones TE, Landry S, Pan T, Weitzman MD, David M. 2012. Codon-usage-based inhibition of HIV protein synthesis by human schlafen 11. Nature 491:125-8.

194. Peterlin BM, Liu P, Wang X, Cary D, Shao W, Leoz M, Hong T, Pan T, Fujinaga K. 2017. Hili Inhibits HIV Replication in Activated T Cells. J Virol 91.

Chapter 2

Title: Relationships between MA-RNA Binding in Cells and Suppression of HIV-1 Gag Mislocalization to Intracellular Membranes

Abstract

The HIV-1 Gag matrix (MA) domain mediates localization of Gag to the plasma membrane (PM), the site for infectious virion assembly. The MA highly basic region (HBR) interacts with phosphatidylinositol-(4,5)-bisphosphate [PI(4,5)P2], a PM-specific acidic lipid. MA-HBR also binds RNAs. To test whether acidic lipids alone determine PM-specific localization of Gag or whether MA-RNA binding also plays a role, we compared a panel of MA-HBR mutants that contain two types of substitutions at MA residues 25/26 or 29/31: Lys->Arg (KR) (25/26KR and 29/31KR) and Lys->Thr (KT) (25/26KT and 29/31KT). Consistent with the importance of the HBR charge in RNA binding, both KT mutants failed to bind RNA via MA efficiently unlike the corresponding KR mutants. Both 25/26KT Gag-YFP and 29/31KT Gag-YFP bound non-specifically to PM and intracellular membranes, presumably via the myristoyl moiety and remaining MA basic residues. In contrast, 25/26KR Gag-YFP bound specifically to the PM, suggesting a role for the total positive charge and/or MA-bound RNA in navigating Gag to the PM. Unlike 29/31KT Gag-YFP, 29/31KR Gag-YFP was predominantly cytosolic and showed little intracellular membrane binding despite having a higher HBR charge. Therefore, it is likely that MA-RNA binding blocks promiscuous Gag membrane binding in cells. Notably, introduction of a heterologous multimerization domain restored PI(4,5)P2-dependent PM-specific localization for 29/31KR Gag-YFP, suggesting that the blocking of PM binding is more readily reversed than that of intracellular membrane binding. Altogether, these cell-based data support a model

in which MA-RNA binding ensures PM-specific localization of Gag via suppression of non-specific membrane binding.

Introduction

HIV-1 progeny virions exit most cells at the plasma membrane (PM) (1, 2). The matrix (MA) domain of the HIV-1 structural polyprotein Gag mediates the targeting and binding of Gag to the PM, which is a crucial stage of virus particle production (3-9). The two essential features of the MA domain required for the PM-specific localization and binding of Gag are an N-terminal myristate moiety and a highly basic region (HBR) (10-16). The myristate moiety allows Gag to form hydrophobic interactions with membranes when it is not sequestered in the MA globular domain (17-24). The MA-HBR comprises a highly conserved cluster of basic residues spanning residues 14-31 (13, 14, 23, 25). This basic patch drives electrostatic and head group-specific interactions of Gag with phosphatidylinositol (4,5)-bisphosphate [PI(4,5)P2], an acidic phospholipid found primarily in the inner leaflet of the PM (15, 20, 26-34). In addition to acidic phospholipids, RNA, which has been shown to bind the MA domain (35-43), may play an important role in regulation of Gag-membrane binding (28, 32, 44-48). Among the HBR basic residues, an NMR-based study showed that the residues 29 and 31 are particularly important for PI(4,5)P2 interaction in the absence of RNA (49).

WT Gag that is translated *in vitro* using rabbit reticulocyte lysates binds liposomes consisting of a neutral lipid, phosphatidylcholine (PC), and an acidic lipid, phosphatidylserine (PS) (PC+PS liposomes) poorly but shows enhanced membrane binding either when Gag is treated with RNase or when PI(4,5)P2 is included in the liposomes (32, 34, 50). In cells, besides NC, MA-HBR mediates significant RNA binding to WT Gag (46, 47). Notably, regardless of the presence of NC, Gag present in the cytosol binds to PC+PS liposomes only upon RNase treatment (46), suggesting a role for MA-bound RNA in cells. In good

agreement with these studies, RNase treatment of cell homogenates derived from HIV-1-expressing cells resulted in significant shift of Gag from cytosolic to membrane fraction (47). These observations suggest that WT Gag is susceptible to negative regulation of membrane binding by MA-bound RNA and that Gag-membrane binding occurs only when this RNA is removed by RNase or counteracted by PI(4,5)P2. Sequencing of RNAs cross-linked to MA revealed that the major RNA species bound to MA in cells is tRNA and that MA-tRNA binding is reduced with membrane-bound Gag compared to cytosolic Gag (47). Consistent with the role for MA-tRNA binding, tRNA-mediated inhibition of Gag-liposome binding has been observed in vitro (46, 48, 51-53).

Based on these studies, our working model is that RNA bound to MA-HBR prevents Gag from electrostatically binding to acidic phospholipids such as PS, which are present ubiquitously in the cell (54). In this model, PI(4,5)P2 helps Gag overcome RNA-mediated negative regulation, thereby promoting Gag binding to the PM, while RNA prevents Gag from binding to other acidic lipids present in non-PM membranes (32, 44). The hypothesis that MA-RNA binding prevents promiscuous localization of Gag has not been directly investigated in the context of HIV-1 Gag expressed in cells. Our previous study of Gag chimeras containing various retroviral MA domains showed a correlation between the size of basic patches, RNA sensitivity in the *in vitro* liposome binding assay, and PM-specific Gag localization in cells (29). However, MA-RNA binding in cells was not measured in that study. Moreover, confounding effects of structural variations of the various retroviral MA domains, other than the size of the basic patches, could not be excluded. In addition, although unlikely, it remains possible that Gag chimeras with different retroviral MA domains may be differentially endocytosed after nascent virion assembly at the PM, resulting in apparent differences in Gag localization.

In the current study, to examine the correlation between MA-RNA binding and subcellular Gag localization while addressing the limitations in the previous studies, we compared the effects of two types of amino acid substitutions in HIV-1 MA-HBR on the ability of MA to bind RNA in cells and on the specificity

of subcellular localization of HIV-1 Gag. The first type is Lys-to-Thr (KT) changes. We previously showed that MA-HBR mutants with KT changes at MA residues 25 and 26 (25/26KT) or MA residues 29 and 31 (29/31KT) display promiscuous subcellular localization to both PM and intracellular membranes (14, 32). MA-RNA binding is reduced upon substitutions of Lys in MA-HBR to neutral amino acids such as Thr in previous *in vitro* studies (35, 36). In cells, such substitutions caused a reduction in tRNA populations bound to Gag relative to total RNA populations bound to Gag (47). However, the magnitude of the effect of the HBR mutations on the RNA binding ability of MA in cells remained to be determined. The second type of amino acid substitutions in MA-HBR that we introduced is Lys-to-Arg (KR) changes. These changes, which do not affect the overall basic charge of MA-HBR unlike the KT changes, are expected to preserve the RNA binding ability, since liposome binding of a mutant Gag in which all basic residues of MA-HBR were switched (K->R and R->K) is still sensitive to RNA-mediated block of PC+PS liposome binding (55). However, this prediction had neither been tested in cells nor tested for specific HBR residues. The comparison of KT and KR substitutions in MA-HBR in this study revealed that basic-to-neutral changes in two Lys residues are sufficient to diminish MA-RNA binding in cells to the background level and that there is a strong correlation between MA-RNA binding and subcellular localization of Gag. Altogether, the findings in this study support our working model that MA-RNA binding inhibits promiscuous localization of Gag, thereby ensuring Gag localization to the PM in the presence of PI(4,5)P2.

Results

Gag derivatives with Lys-to-Arg (KR) changes in MA-HBR bind RNA more efficiently than those with Lys-to-Thr (KT) changes in cells

To compare the RNA binding capacity of MA, we introduced three modifications into Gag constructs and examined RNA binding to WT MA and MA HBR mutants in cells using photoactivatable ribonucleoside-enhanced crosslinking and immunoprecipitation (PAR-CLIP). The first modification is an

MA amino acid substitution (1GA) that blocks N-terminal myristoylation and thereby prevents Gag from binding membranes. The previous cell-based PAR-CLIP study (47) was conducted using Gag constructs that can bind membranes, which would cause dissociation of RNA from MA according to the model described above (see Introduction). Therefore, we eliminated membrane binding so as to allow us to determine the total RNA binding capacity of Gag. Second, to focus on the RNA binding ability of the MA domain, we deleted most of the NC domain (delNC), which is the major RNA binding domain of Gag. Lastly, we fused YFP to the Gag C-terminus (Gag-YFP) to facilitate microscopy analysis of the same constructs analyzed for MA-RNA binding.

The 1GA/delNC/Gag-YFP constructs containing KR or KT mutations in MA residues 25 and 26 (25/26KR and 25/26KT) or MA residues 29 and 31 (29/31KR and 29/31KT) (Figure 2.1) were compared with isogenic constructs with the WT HBR sequence or a mutant HBR sequence in which all MA-HBR basic residues were switched to neutral residues (6A2T) (Figure 2.1). To determine the amount of RNA bound to MA in cells, we employed a PAR-CLIP assay (47, 56) with modifications (Figure 2.1 A.). HeLa cells were transfected with one of the constructs described above or a non-Gag control, pUC19, cultured in a medium containing 4-thiouridine (4-SU), a photoactivatable ribonucleoside analogue, and subsequently exposed to UV light, which crosslinks RNA-binding proteins and 4-SU-containing RNA bound to the proteins. Following cell lysis, Gag constructs were immunoprecipitated using HIV-Ig, and the RNA bound to the constructs was end-labeled with ^{32}P prior to SDS-PAGE and electrotransfer to PVDF membrane. The RNA binding efficiency of the constructs was determined through comparison of the signal intensity of RNA by phosphorimager analysis versus the signal intensity of Gag constructs detected by immunoblotting on the same membrane.

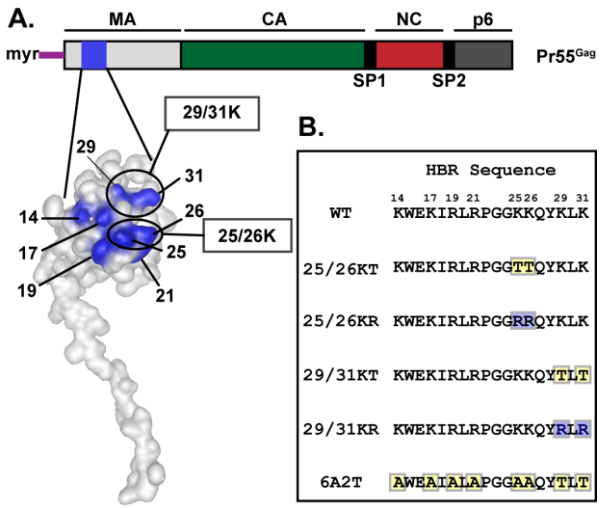

Figure 2.1. Amino acid substitutions introduced in MA-HBR. (A.) Schematic illustration of HIV-1 Gag with the structure of HIV-1 MA (PDB 2HMX) showing the basic residues of HBR in blue with residues mutated in this study circled. (B.) Sequences of HIV-1 Gag MA-HBR analyzed in this study are shown. Lys-to-Arg (KR) or Lys-to-Thr (KT) changes were introduced at MA residues 25 and 26 or 29 and 31. In the 6A2T mutant, all MA-HBR basic residues were switched to neutral Ala or Thr.

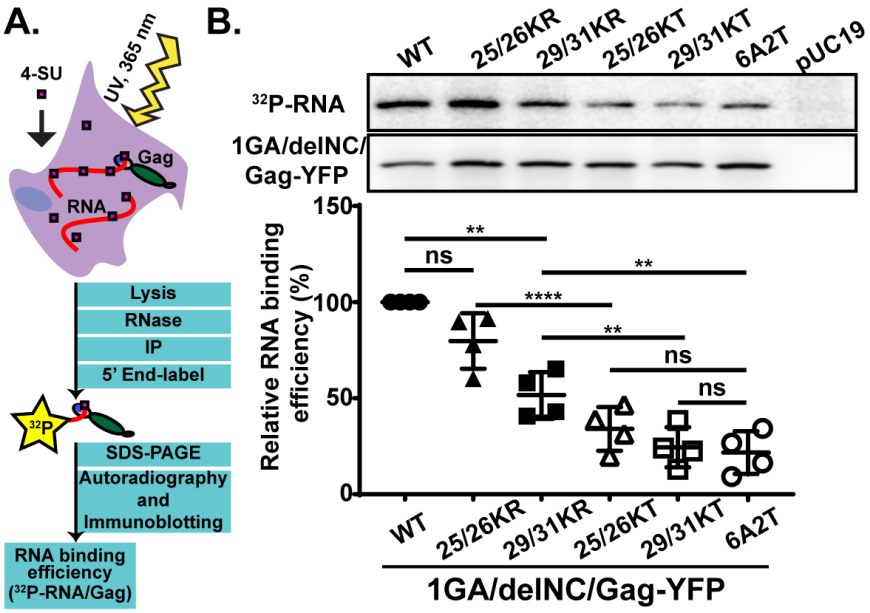

Figure 2.2 Gag derivatives with KR mutations in MA-HBR bind RNA efficiently compared to those with KT mutations. (A.) Schematic illustration of the PAR-CLIP assay. A CMV promoter-driven Gag-YFP construct lacking the myristoylation site (1GA) and most of the NC domain (delNC) was used as the backbone for the Gag derivatives analyzed in this assay. A mutant Gag with all MA-HBR basic residues switched to neutral Ala or Thr, 6A2T, was used as a negative control. To identify bands representing Gag, non-Gag plasmid, pUC19, was used as an additional control. The 1GA/delNC/Gag-YFP constructs were expressed in HeLa cells and crosslinked to 4-SU containing RNA in the cells. Gag proteins were recovered by immunoprecipitation, Gag-bound RNA was end-labeled with ^{32}P, and signals for Gag proteins and Gag-bound RNA were detected by SDS-PAGE followed by immunoblotting and

autoradiography, respectively. (B.) Representative results for ^{32}P-labelled Gag-bound RNA detected by autoradiography and total Gag detected by immunoblotting and chemiluminescence are shown on the top. Relative RNA binding efficiency (%) of MA-HBR mutants was determined by quantifying the intensity of RNA signals normalized by the Gag band intensity on the same PVDF membrane. Results from 4 independent experiments are shown as means +/- standard deviations. P values were determined using Student's t-test, using raw data. ns, not significant; **, P ≤ 0.01; ****, P ≤ 0.0001.

Consistent with previous results (46), the Gag construct bearing 6A2T MA did not bind RNA efficiently, showing ~4-fold reduction in the amount of RNA bound relative to WT (Figure 2.2 B.). Both the constructs bearing 25/26KT and 29/31KT MA bound significantly less RNA than the WT construct, similar to what was observed for 6A2T, indicating that both Lys 25 and 26 and Lys 29 and 31 contribute to MA-RNA binding to similar extent in cells. On the other hand, there was no statistically significant difference in the RNA binding efficiency between the 25/26KR MA and the WT MA. The Gag construct with the other KR changes, 29/31KR, also bound significantly more RNA compared to its KT counterpart, albeit less efficiently than WT. These results indicate that the RNA binding efficiency of MA is dependent on the overall positive charge of the MA-HBR basic patch. Additionally, the identity of basic amino acids at residues 29 and/or 31 also plays a role in WT-level RNA binding. Having observed differential effects on MA-RNA binding between KR and KT substitutions, we investigated below the correlation (or lack thereof) between MA-RNA binding and subcellular localization of Gag, first focusing on the effects of the substitutions at MA residues 25/26, and next on those at the residues 29/31.

Gag derivatives containing 25/26KR substitutions exhibit PM-specific localization unlike those with 25/26KT changes

To compare subcellular distribution of Lys 25/26 mutants, we expressed myristoylated and YFP-tagged Gag constructs bearing these changes, both in the full-length and delNC contexts, in HeLa cells and observed the YFP localization in cells (Figure 2.3). Based on the YFP distribution patterns, we identified 4 different phenotypes (Figure 2.3 A. and B.): (i) localization predominantly at the PM (green bar), (ii) localization to both PM and intracellular compartments (blue bar), (iii) localization to only intracellular

compartments (orange bar), and (iv) only hazy cytosolic localization with no punctate intensities (pink bar). These 4 distribution patterns were also validated by comparison of the YFP signal with that of Alexa Fluor 594-conjugated Concanavalin A (ConA-AF594), which serves as the PM marker (Figure 2.3 C.).

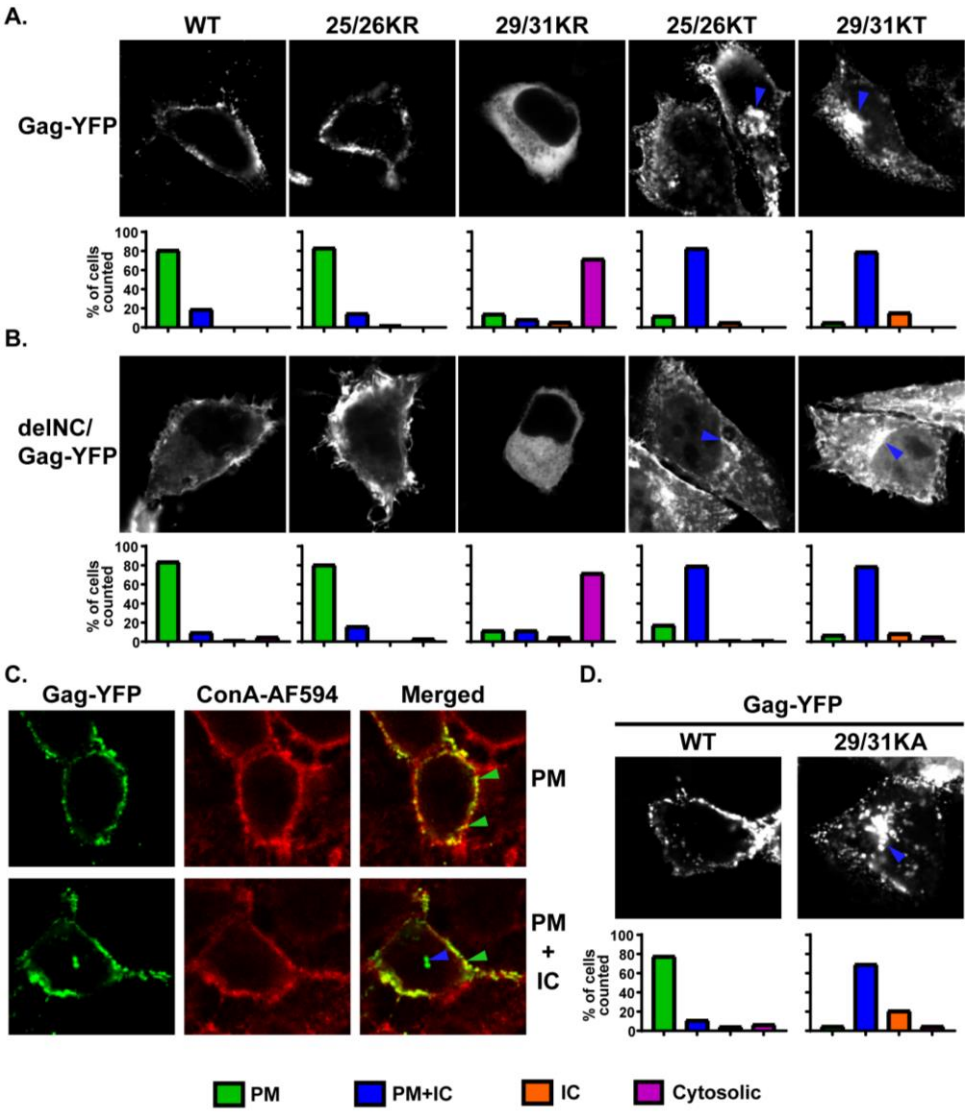

Figure 2.3. Gag derivatives containing KR substitutions in the MA-HBR region do not show promiscuous localization in cells unlike those with KT changes. (A. and B.) HeLa cells were transfected with full-length Gag-YFP. (A.) or delNC/Gag-YFP (B.), which contain WT MA sequence or 25/26KR, 25/26KT, 29/31KR or 29/31KT. At 14 hours post transfection, cells were stained with Alexa Fluor 594-conjugated concanavalin A (ConA-AF594), fixed with 4% paraformaldehyde in PBS, and analyzed using a fluorescence microscope. Note that subcellular distributions of delNC/Gag-YFP constructs mirror those of the corresponding full-length Gag-YFP constructs for both WT and MA-HBR mutants. Forty-two to 85 cells were analyzed per condition across 3 independent experiments. The localization patterns determined by epifluorescence microscopy were confirmed by confocal microscopy. Representative confocal images are shown in the top panels. The blue arrowhead indicates Gag-YFP signal in the intracellular

compartments. Bar graphs in the bottom panels represent percentages of cells showing indicated patterns of subcellular distribution for each Gag-YFP construct. ConA-AF594 staining was used as PM marker (not shown). PM, Plasma membrane; PM+IC, Plasma membrane + Intracellular compartments; IC, Intracellular compartments. (C.) Images in the top row show an example of Gag-YFP showing PM-specific localization and ConA-AF594 staining of the PM in which green arrowheads indicate overlap of the two signals at the cell surface in a merged image. Images in the bottom row show an example of Gag-YFP exhibiting PM+IC localization. The blue arrowhead indicates Gag-YFP signal in the intracellular compartments. (D.) HeLa cells were transfected with full-length WT Gag-YFP or 29/31KA Gag-YFP. At 16 hours post transfection, cells were stained with ConA-AF594, fixed with 4% paraformaldehyde in PBS, and analyzed using a fluorescence microscope. A total of 45 to 62 cells in 3 independent experiments were analyzed. The localization patterns determined by epifluorescence microscopy were confirmed by confocal microscopy. Representative confocal images are shown in top panel. The blue arrowhead indicates Gag-YFP signal in the intracellular compartments. Bar graphs in bottom panel represent percentages of cell populations as described above.

As seen previously, the 25/26KT mutant bound both PM and intracellular membranes. In contrast, the 25/26KR mutant presented PM-specific localization similar to WT. Importantly for correlating the localization data with MA-RNA binding results (Figure 2.2), the subcellular localization patterns of delNC/Gag-YFP were similar to that of the corresponding full-length Gag-YFP for both WT and the MA-HBR mutants. When we examined the VLP release efficiency of full-length Gag-YFP construct, we found that despite the difference in subcellular localization, both the Lys 25/26 mutants displayed 2-fold increase in VLP release efficiency compared to WT (Figure 2.4). A previous study showed that 25/26KT Gag produced *in vitro* using rabbit reticulocyte lysates binds neutral PC-only liposomes efficiently unlike WT Gag. Gag binding to neutral lipid membranes is via hydrophobic, and not electrostatic, interactions. Therefore, the efficient binding of 25/26KT Gag to PC-only liposomes reflects enhanced myristate-driven hydrophobic interactions, most likely dues to increased myristate exposure (32). Using the same liposome binding assay, we found that the 25/26KR mutant also exhibits increased hydrophobic interactions (Figure 2.5 A., 2.5 B.). Of note, myristoylation-deficient full-length Gag-YFP (1GA/Gag-YFP) containing the 25/26KR or 25/26KT MA sequence were unable to bind any cellular membranes (Figure 2.5 C.), eliminating the involvement of an alternative, myristate-independent mechanism for membrane binding of Lys 25/26 mutants. Although it is formally possible that an unknown cellular function promotes release of myristoylated Lys 25/26 mutants but not WT, these in vitro and cell-based data collectively suggest that

the enhanced VLP release efficiency of Gag constructs with the Lys 25/26 substitutions is likely a result of increased hydrophobic interactions dependent on the myristoyl moiety.

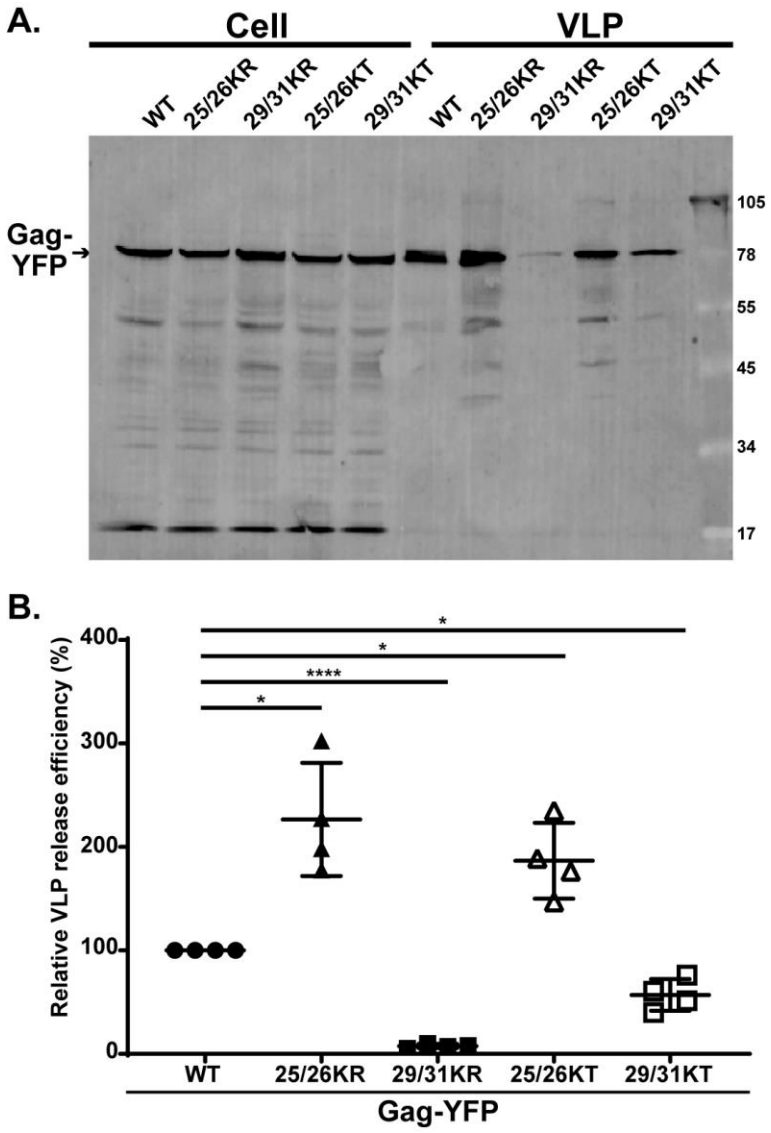

Figure 2.4. MA-HBR mutations alter VLP release efficiency. (A.) HeLa cells were transfected with WT Gag-YFP or Gag-YFP containing 25/26KR, 25/26KT, 29/31KR or 29/31KT changes. At 14 hours post transfection, cell and virus like particle (VLP) lysates were collected and subjected to SDS-PAGE, and Gag proteins were detected by immunoblotting using HIV immunoglobulin. (B.) Relative VLP release efficiency represents the amount of VLP-associated Gag as a fraction of total Gag present in VLP and cell lysates and is normalized to the VLP release efficiency of WT Gag. Results from 4 independent experiments are shown as means +/- standard deviations. The average VLP release efficiency of WT Gag was 8.3%. P values were determined from raw data using Student's t- test. *, $P \leq 0.05$; ****, $P \leq 0.0001$.

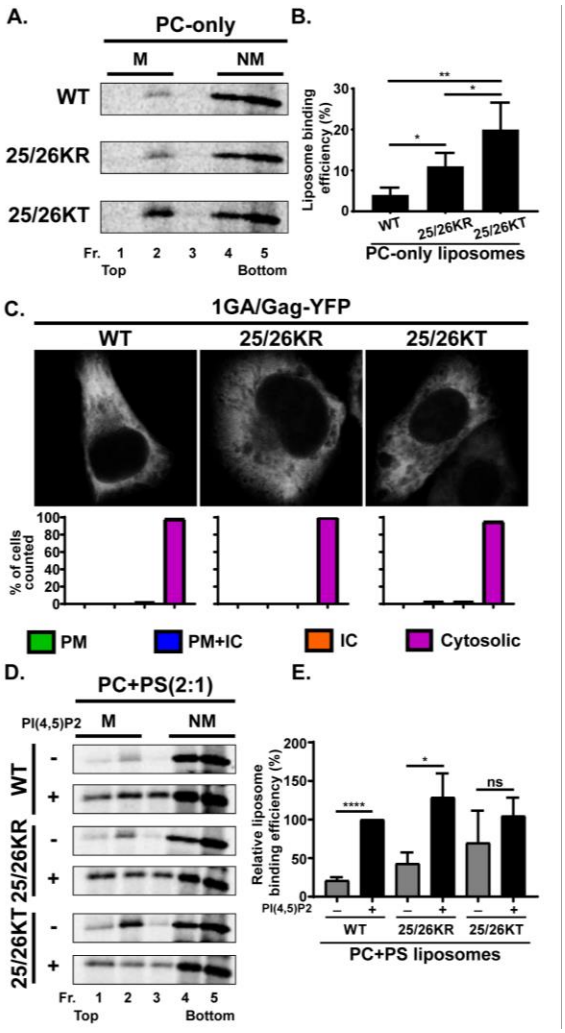

Figure 2.5. Membrane binding of Gag derivatives containing Lys 25/26 substitutions. (A.) ^{35}S-labeled HIV-1 WT Gag, 25/26KR Gag and 25/26KT Gag were synthesized in vitro using rabbit reticulocyte lysates and incubated with PC-only liposomes. The reaction mixtures were subjected to membrane flotation centrifugation, and a total of five 1-ml fractions were collected from each sample. M, membrane bound Gag; NM, non-membrane-bound Gag. (B.) The liposome binding efficiency was calculated as the percentage of membrane-bound Gag (M) to the total Gag (M+NM) synthesized in the reaction. Results from four independent experiments are shown as means ± standard deviations. P values were determined by Student's t test. *, P ≤ 0.05; **, P ≤ 0.01. (C.) HeLa cells were transfected with non-myristoylated Gag-YFP (1GA/Gag-YFP), which contains WT MA sequence or 25/26KR or 25/26KT, substitutions. At 16 hours post transfection, cells were stained with ConA-AF594, fixed with 4% paraformaldehyde in PBS, and analyzed using a fluorescence microscope. Forty to 52 cells were analyzed per condition across 3 independent experiments. The localization patterns determined by epifluorescence microscopy were confirmed by confocal microscopy. Representative confocal images are shown. Bar graphs in the represent percentages of cells showing indicated patterns of subcellular distribution for each Gag-YFP construct. ConA-AF594 staining was used as PM marker as in Figure 2.3 C. (not shown). PM, Plasma membrane; PM+IC, Plasma membrane + Intracellular compartments; IC, Intracellular compartments. (D.) ^{35}S-labeled HIV-1 WT Gag, 25/26KR Gag and 25/26KT Gag were synthesized in vitro using rabbit reticulocyte lysates and incubated with PC+PS (2:1) liposomes (-) or liposomes containing 7.25 mol% PI(4,5)P2 (+). The reaction mixtures were analyzed as in (A). M, membrane bound Gag; NM, non-membrane-bound Gag. (E.) The relative liposome binding efficiency was calculated as the percentage of membrane-bound Gag (M) to the total Gag (M+NM) synthesized in the reaction and normalized to the efficiency of

WT Gag binding to PI(4,5)P2-containing liposomes. The average efficiency of WT Gag binding to PI(4,5)P2-containing liposome was 42.5%. Results from three independent experiments are presented as means ± standard deviations. P values were determined by Student's t test. ns, not significant; *, P ≤0.05; ****, P ≤ 0.0001.

25/26KR Gag is dependent on PI(4,5)P2 for efficient membrane binding unlike 25/26KT Gag

While 25/26KR MA shows WT-level RNA binding and mediates PM-specific localization of Gag-YFP, unlike WT MA it engaged in increased hydrophobic interactions with membranes similar to its corresponding KT mutant MA (32) (Figure 2.5 A., 2.5 B.). An earlier study has demonstrated that the 25/26KT mutant exhibits increased PI(4,5)P2-independent liposome binding (32). Therefore, we examined whether 25/26KR MA still shows PI(4,5)P2-dependent liposome binding. We found that the presence of PI(4,5)P2 significantly increased the liposome binding efficiency of the 25/26KR mutant but does not affect the 25/26KT mutant (Figure 2.5 D., 2.5 E.). These results indicate that the 25/26KR mutant is dependent on PI(4,5)P2 for efficient membrane binding unlike the 25/26KT mutant even though both showed increased hydrophobic interactions relative to WT.

Upon depletion of cellular PI(4,5)P2, 25/26KR Gag-YFP exhibits promiscuous subcellular localization

PM localization of WT Gag is dependent on PI(4,5)P2 (15, 26, 27). To investigate whether the PM localization of 25/26KR Gag is also dependent on PI(4,5)P2, we next examined the effect of expression of 5-phosphatase IV (5ptaseIV), which depletes cellular PI(4,5)P2, on subcellular distribution of Gag-YFP derivatives. We co-expressed WT Gag-YFP or Gag-YFP with Lys 25/26 substitutions with full-length 5ptaseIV (FL) or its catalytically inactive derivative (Δ1) (Figure 2.6). As previously reported (26), WT Gag-YFP lost PM-specific localization and displayed predominantly hazy cytosolic but sometimes intracellular punctate distribution when co-expressed with FL 5ptaseIV. The 25/26KT mutant showed predominantly promiscuous localization regardless of the presence of FL or Δ1 5ptaseIV, demonstrating that this MA substitution mutant is not dependent on PI(4,5)P2 for cellular membrane binding. In contrast, the localization of the 25/26KR mutant changed from predominantly PM-specific localization to more

promiscuous localization when it was co-expressed with the FL but not Δ1 5ptaseIV. These results indicate that the PM-specific localization of the 25/26KR Gag is dependent on the presence of PI(4,5)P2 in the cell.

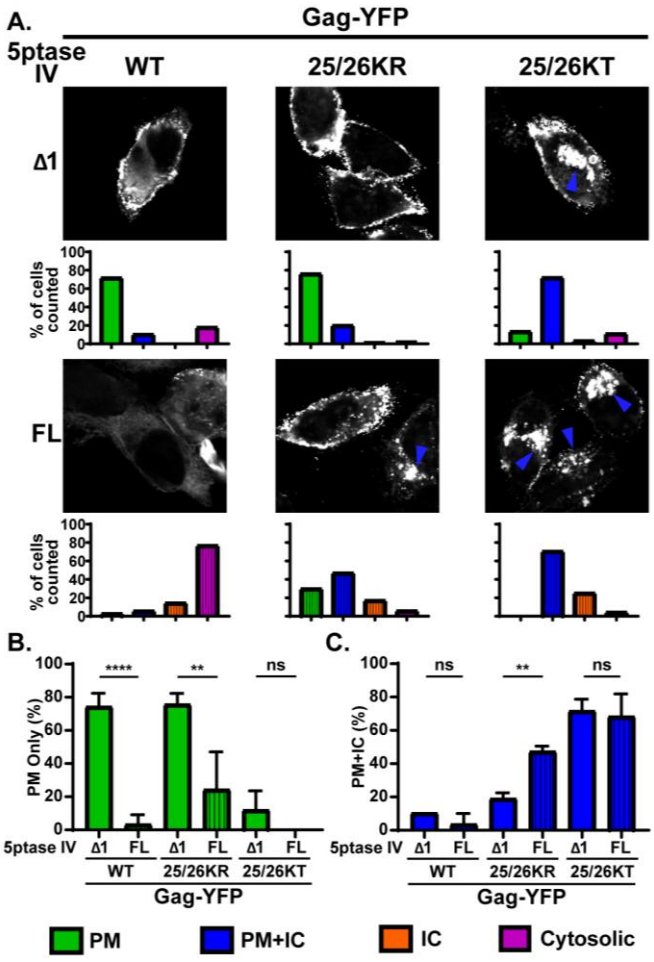

Figure 2.6. Depletion of cellular PI(4,5)P2 leads to promiscuous subcellular localization of 25/26KR Gag-YFP. (A.) HeLa cells were transfected with WT Gag-YFP, 25/26KR Gag-YFP or 25/26KT Gag-YFP along with myc-tagged 5ptaseIV FL or the catalytically inactive Δ1 derivative. At 14 hours post transfection, cells were stained with ConA-AF594 (not shown), fixed with 4% paraformaldehyde in PBS, permeabilized, immunostained with mouse monoclonal anti-Myc antibody and anti-mouse IgG conjugated with Alexa Fluor 405 (not shown), and analyzed using a fluorescence microscope. Only cells positive for both myc-tagged 5ptaseIV and Gag-YFP were included in the analysis. Sixty-nine to 134 cells were analyzed per condition across 3 independent experiments. Representative confocal images of Gag-YFP are shown. The blue arrowhead indicates Gag-YFP signal in the intracellular compartments. The localization patterns were examined as in Figure 2.3, and the percentages of total number of cells showing indicated subcellular distribution patterns under each condition are shown in bar graphs. PM, Plasma membrane; PM+IC, Plasma membrane + Intracellular; IC, Intracellular. (B. and C.) The percentages of cells showing PM-only distribution of Gag-YFP (B.) and PM+IC distribution of Gag-YFP (C.) are compared between cells expressing 5ptaseIV FL and Δ1 across 3 independent experiments and are presented as means ± standard deviations. P values were determined by Student's t test. ns, not significant; **, $P \leq 0.01$; ****, $P \leq 0.0001$.

Overall, our results shown thus far suggest that in the case of the Lys 25/26 mutants, Gag that binds RNA efficiently maintains PI(4,5)P2-dependent PM-specific localization, while Gag that binds RNA poorly shows PI(4,5)P2-independent promiscuous localization. Thus, these results indicate that for Gag derivatives containing Lys 25/26 substitutions, there is a correlation between RNA-binding and PI(4,5)P2-dependent PM-specific localization as previously observed with Gag chimeras containing heterologous retroviral MA domains (29).

Gag derivatives containing 29/31KR substitutions show predominantly cytosolic distribution

Since 29/31KR MA exhibits significantly higher RNA binding than 29/31KT MA (Figure 2.2), we next sought to test whether RNA binding efficiency correlates with subcellular localization in the case of Gag constructs containing changes at MA residues 29/31 as were observed for Gag mutants with changes at residues 25/26. To this end, we first examined distribution of myristoylated full-length Gag-YFP and delNC/Gag-YFP derivatives (Figure 2.3). Consistent with previous reports, Gag-YFP with the 29/31KT changes displayed promiscuous localization with its signals present at both PM and intracellular membranes. Interestingly, the 29/31KR mutant displayed a predominantly cytosolic distribution of Gag-YFP indicating a loss of efficient membrane binding. It is important to note that unlike 29/31KT Gag-YFP, 29/31KR Gag-YFP showed negligible intracellular membrane binding despite having a higher positive charge than 29/31KT MA, which could mediate electrostatic interactions with acidic lipids more efficiently. We found that both delNC and full-length Gag-YFP showed analogous subcellular patterns for each Lys 29/31 mutant. Of note, substitution of Lys 29 and 31 to not only Thr but also to another neutral amino acid Ala (Figure 2.3 D.) or acidic amino acid Glu (14) led to a promiscuous Gag localization. Therefore, it is unlikely that promiscuous localization of 29/31KT Gag-YFP is due to inadvertent introduction of a motif targeting Gag to intracellular compartments. Rather, these observations suggest that any changes in Lys residues 29 and 31, except for the Lys-to-Arg changes, which maintain the total basic charge of MA HBR, would result in promiscuous Gag localization. These results, together with the results of the comparison

between two Lys 25/26 mutants, strongly suggest that MA-RNA binding prevents Gag binding to intracellular membranes regardless of whether Gag can bind the PM. In congruence with the microscopy results, we found that the VLP release efficiency determined in the context of full-length Gag-YFP was significantly impaired for the 29/31KT mutant and almost abolished for the 29/31KR mutant (Figure 2.4).

Replacing the NC domain with a heterologous dimerization motif enables 29/31KR Gag-YFP to localize specifically to the PM in a PI(4,5)P2-dependent fashion

Even though the lack of binding to intracellular membranes is a shared phenotype between 25/26KR Gag-YFP and 29/31KR Gag-YFP, 29/31KR Gag-YFP showed cytosolic distribution in most cells unlike 25/26KR Gag-YFP. We hypothesized that 29/31KR Gag, unlike WT and 25/26KR Gag, is unable to counteract the negative regulation of membrane binding by RNA that is bound to its MA-HBR. A previous study suggests that while overall positive charge of HBR is sufficient for RNA-mediated suppression of Gag-liposome binding irrespective of the identity of the residues, the identity of at least one of the basic residues is important for MA-PI(4,5)P2 interaction (55). In addition, a recent NMR study found that Lys 29 and 31 are important for binding of MA to PI(4,5)P2, even in an experimental system in which RNA is absent (49).

Based on these observations, we reasoned that due to attenuated MA-PI(4,5)P2 binding, 29/31KR Gag is unable to counteract RNA-mediated suppression of membrane binding. It is then conceivable, according to our model, that if membrane binding of this mutant Gag can be enhanced enough to offset the negative regulation imposed by MA-RNA interactions, then this mutant would localize specifically to the PM but not the intracellular compartments because MA-bound RNA would still prevent promiscuous membrane binding. Multimerization increases binding of HIV-1 MA to the PM as well as to liposomes of different compositions (48). Thus, we sought to test the hypothesis above by attempting to augment multimerization of 29/31KR Gag. Previous studies reported that a leucine zipper dimerization motif (LZ)

promotes Gag multimerization more efficiently than the NC domain (57, 58). Therefore, in order to improve Gag multimerization, we replaced the NC domain of Gag with LZ (38, 59-62). We then expressed WT and the Lys 29/31 substitution mutants in the context of Gag-YFP and GagLZ-YFP in cells and examined their subcellular localization patterns (Figure 2.7).

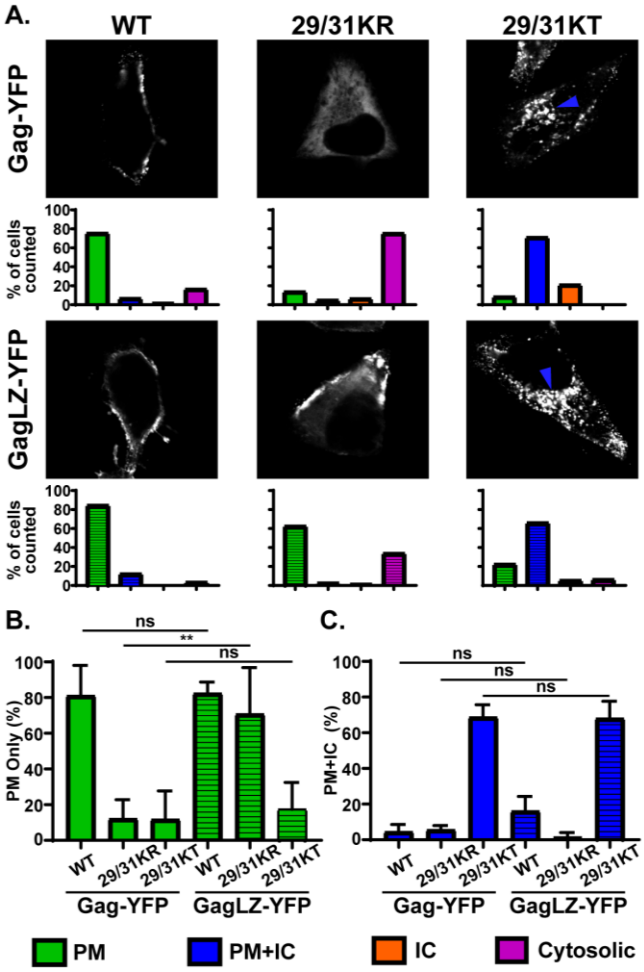

Figure 2.7. 29/31KR Gag exhibits increased PM-specific localization when the NC domain is exchanged for leucine dimerization motif (LZ). (A.) HeLa cells were transfected with WT Gag-YFP, WT GagLZ-YFP or their derivatives with 29/31K substitutions. At 14 hours post transfection, cells were stained with ConA-AF594 (not shown), fixed with 4% paraformaldehyde in PBS, and analyzed using a fluorescence microscope. Sixty-one to 125 cells were analyzed per condition across 3 independent experiments. Representative confocal images of Gag-YFP are shown (top panels). The blue arrowhead indicates Gag-YFP signal in the intracellular compartments. The localization patterns were examined as in Figure 2.3, and the percentages of total number of cells showing indicated subcellular distribution patterns are shown in bar graphs (bottom panels). PM, Plasma membrane; PM+IC, Plasma membrane + Intracellular; IC, Intracellular. (B. and C.) The percentages of cells showing PM only (B.) and PM+IC (C.) distribution are compared between Gag-YFP and GagLZ-YFP across 3 independent experiments and are shown as means ± standard deviations. P values were determined by Student's t test. ns, not significant; **, $P \leq 0.01$.

We found that WT GagLZ-YFP predominantly localized at the PM as observed for WT Gag-YFP. The 29/31KT GagLZ-YFP showed a promiscuous localization like the 29/31KT Gag-YFP, indicating that merely replacing the NC domain with LZ did not lead to the plasma membrane-specific localization. Consistent with our prediction, the 29/31KR GagLZ-YFP demonstrated a significantly enhanced PM localization compared to the 29/31KR Gag-YFP. Importantly, this construct showed very little promiscuous localization unlike the 29/31KT GagLZ-YFP, suggesting that MA with 29/31KR changes retains the ability to ensure PM-specific localization. Unexpectedly, the 29/31KR GagLZ-YFP still failed to release VLPs efficiently (Figure 2.8).

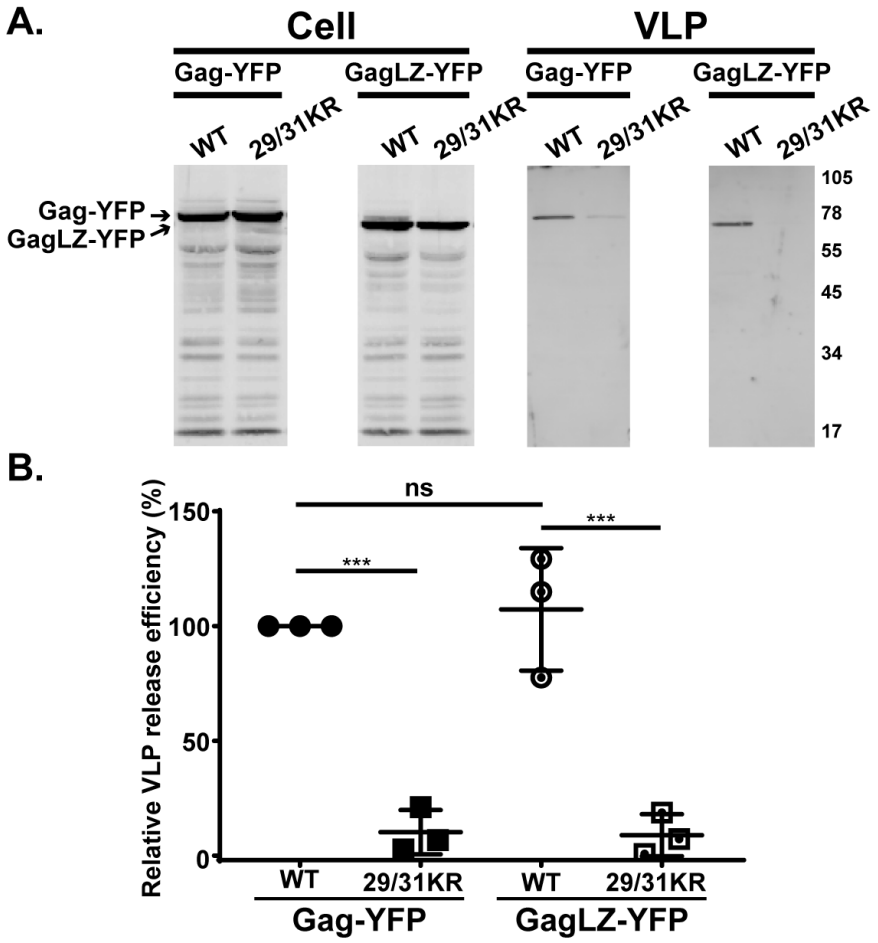

Figure 2.8. 29/31KR GagLZ-YFP fails to release VLP. (A.) HeLa cells were transfected with Gag-YFP or GagLZ-YFP containing WT MA or 29/31KR MA sequences. At 16 hours post transfection, cell and VLP lysates were collected and analyzed as in Figure 2.4. (B.) Relative VLP release efficiency represents the amount of VLP-associated Gag as a fraction of total Gag present in VLP and cell lysates and is normalized to the VLP release efficiency of WT Gag. Results

from 3 independent experiments are shown as means +/- standard deviations. The average VLP release efficiency of WT Gag was 9.6%. ns, not significant; ***, P ≤ 0.001.

We then wanted to test directly in cells whether LZ-driven PM localization is still PI(4,5)P2-dependent. To this end, we co-expressed GagLZ-YFP constructs with FL and Δ1 5ptaseIV enzyme (Figure 2.9). We found that both the WT GagLZ-YFP and 29/31KR GagLZ-YFP lost the PM-specific localization when the FL 5ptaseIV enzyme was co-expressed. These results suggest that the WT GagLZ-YFP and the 29/31KR GagLZ-YFP bind the PM in a PI(4,5)P2-dependent manner. Interestingly, in the presence of FL 5ptaseIV, WT GagLZ-YFP showed promiscuous localization to intracellular compartments and the PM, whereas 29/31KR GagLZ-YFP showed predominantly cytosolic localization as observed for WT Gag-YFP (Figure 2.6).

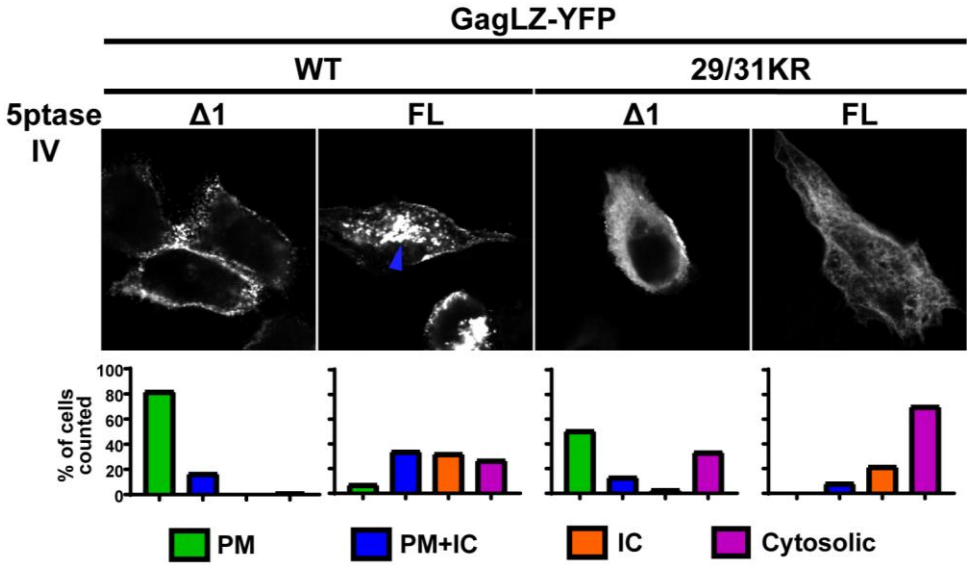

Figure 2.9. 29/31KR GagLZ-YFP localizes to the PM in a PI(4,5)P2-dependent manner. HeLa cells were transfected with WT GagLZ-YFP or 29/31KR GagLZ-YFP along with myc-tagged 5ptaseIV FL or the catalytically inactive Δ1 derivative. At 14-16 hours post transfection, cells were stained with ConA-AF594 (not shown), fixed with 4% paraformaldehyde in PBS, immunostained with mouse monoclonal anti-Myc antibody and anti-mouse IgG conjugated with Alexa Fluor 405 (not shown), and analyzed as in Figure 2.6. Thirty-seven to 78 cells in 3 independent experiments were analyzed per condition. Representative confocal images of Gag-YFP are shown (top panels). The blue arrowhead indicates Gag-YFP signal in the intracellular compartments. The localization patterns were examined as in Figure 2.3, and the percentages of cells showing indicated subcellular distribution patterns are shown in bar graphs (bottom panels). PM, Plasma membrane; PM+IC, Plasma membrane + Intracellular; IC, Intracellular.

Overall, the presented data suggest that when MA-HBR in Gag binds RNA, Gag localizes specifically to the PM if it can counteract the RNA-mediated block on membrane binding either via interaction with

PI(4,5)P2, which occurs natively in the case of WT and 25/26KR Gag, or when enhanced by improved multimerization as observed for 29/31KR GagLZ. In contrast, when Gag is deficient in MA-RNA binding as observed for KT mutants, it fails to localize specifically to the PM and instead, binds promiscuously to different cellular membrane compartments. Altogether the analyses of Lys 25/26 and Lys 29/31 substitutions in MA-HBR revealed a strong correlation between MA-RNA binding and suppression of non-specific Gag localization to intracellular membranes (summarized in Figure 2.10).

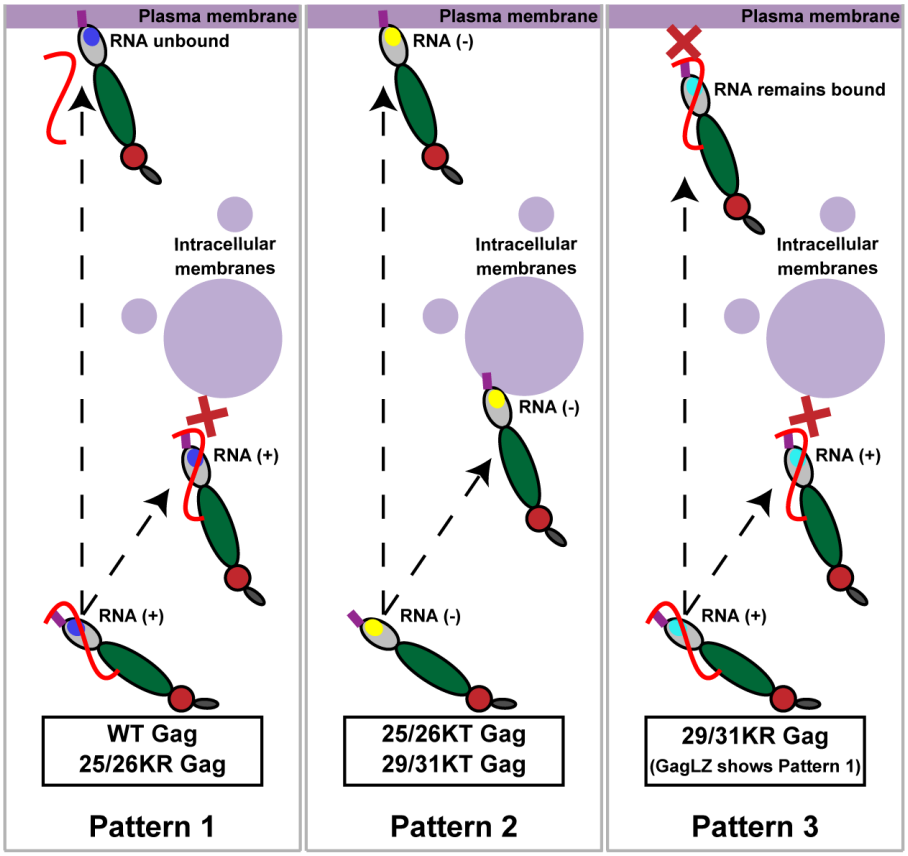

Figure 2.10. Relationships between MA-RNA binding and subcellular localization of Gag. Note that the full-length Gag constructs and the corresponding delNC Gag constructs show similar subcellular localization patterns for both WT and MA-HBR mutants.

Discussion

In the current study, we examined the effects of amino acid substitutions in MA-HBR on the relative amount of RNA bound to HIV-1 Gag in cells and on the subcellular localization of Gag. We found

that MA-HBR mutants that were incapable of binding RNA efficiently displayed a promiscuous subcellular localization (i.e., 25/26KT Gag and 29/31KT Gag), consistent with earlier observations obtained with Gag chimeras containing heterologous retroviral MA sequences (29). In contrast, MA-HBR mutants that bound RNA efficiently did not show a promiscuous localization; they either localized specifically to the PM (25/26KR Gag) or mainly remained in the cytosol (29/31KR Gag). The latter presented PM-specific and not promiscuous localization when its membrane binding ability was enhanced via LZ-mediated multimerization. The correlation established between MA-RNA binding and the lack of Gag localization to intracellular membranes in this study further provides support for our current working model in which RNA-mediated inhibition of Gag membrane binding ensures PM-specific localization of Gag.

The liposome binding experiments using neutral liposomes indicate that both 25/26KT and 25/26KR Gag engage in greater hydrophobic interactions with membranes than WT Gag, likely due to increased myristate exposure relative to WT Gag (this study and (32)). Despite the enhanced hydrophobic interactions with membranes, 25/26KR Gag maintains PM-specific localization like WT Gag. However, the outcomes of PI(4,5)P2 depletion differ between WT and 25/26KR Gag. Upon FL 5ptaseIV expression, WT Gag loses membrane binding and exhibits predominantly cytosolic distribution, whereas 25/26KR Gag retains membrane binding albeit localizing promiscuously in the majority of the Gag-YFP expressing cells. The two different outcomes of PI(4,5)P2 depletion highlight the two functions of PI(4,5)P2, enhancing membrane binding of Gag and supporting PM-specific localization.

We found that 25/26KR Gag exhibits increased VLP release efficiency compared to WT Gag, likely due to enhanced membrane binding as discussed above. Therefore, the Lys-to-Arg mutation at residues 25 and 26 should confer fitness advantage to HIV-1. However, Lys 25 and 26 are highly conserved across various clades of HIV-1 (63). We speculate that Arg, instead of Lys, at positions 25 and 26 may negatively affect other aspects of the HIV-1 life cycle. Similar to 25/26KR Gag, 25/26KT Gag also shows superior VLP release efficiency even though 25/26KT Gag does not localize specifically to the PM unlike its KR

counterpart. The high VLP release efficiency of 25/26KT Gag may be due to even more robust hydrophobic interactions with membranes than 25/26KR Gag (Figure 2.5), which may make up for the Gag mislocalization. The increased hydrophobic interactions of 25/26KT Gag, which does not bind RNA, relative to 25/26KR Gag, which binds RNA at the WT level, is consistent with the observation that removal of RNA increases myristate-dependent hydrophobic interactions (32). However, the 25/26KR Gag still showed the enhanced hydrophobic membrane binding relative to WT Gag. Therefore, further investigation is required to determine the mechanism(s) by which Lys 25/26 modulates myristate exposure.

We found that RNA binding of 29/31KR Gag was not as efficient as WT Gag although it was better than that of 29/31KT Gag. While we observed previously that RNA sensitivity of Gag-liposome binding is maintained when all Lys and Arg in MA-HBR are switched with each other (55), the presence of Lys, but not Arg, at residues 29 and 31 seems to be important for WT-level RNA binding of Gag. Although both Arg and Lys are positively charged basic amino acids, Arg has a terminal guanidium group, while Lys has a single terminal amino group. These groups also differ in their geometry (i.e., planar versus tetrahedral). Therefore, it is possible that Lys and Arg participate in different number and/or orientation of electrostatic interactions with RNA or lipids (64-67).

Even though 29/31KR Gag showed reduced RNA binding, this level of MA-RNA binding was sufficient for suppressing binding to intracellular membranes. It is noteworthy that 29/31KR Gag failed to bind even the PM in most cells. Strongly cationic model proteins have been shown to associate with the PM (68). However, in the case of HIV-1 Gag, the high positive charge retained in 29/31KR MA is insufficient for the PM localization, likely due to the RNA-mediated block. As mentioned above, Lys 29 and 31 are important for PI(4,5)P2 interaction even in the absence of RNA (49). Based on this knowledge, we speculate that due to inefficient interaction with PI(4,5)P2, 29/31KR Gag is unable to overcome the negative regulation by RNA. Therefore, the balance between MA-RNA and MA-PI(4,5)P2 binding, which is

carefully orchestrated for WT Gag, is tipped in the favor of MA-RNA binding in case of 29/31KR Gag. In an attempt to find a mutant that retains partial ability to interact with PI(4,5)P2, which could result in a partial shift of balance back to MA-PI(4,5)P2 binding, we created single mutants 29KR Gag and 31KR Gag and examined their subcellular localization in HeLa cells. However, we found that 31KR Gag fully recapitulated the phenotype of 29/31KR by exhibiting predominantly cytosolic distribution, while 29KR Gag showed mainly WT-like PM-specific localization (data not shown). Thus, Lys but not Arg is required at MA residue 31, whereas residue 29 can be either Lys or Arg for WT-like membrane binding and PM-specific localization of Gag.

The PM-specific localization of 29/31KR GagLZ is likely a manifestation of the enhanced multimerization of 29/31KR Gag restoring the balance towards MA-PI(4,5)P2 binding. Probable mechanisms through which LZ may promote membrane binding may be an avidity effect due to increased multimerization, myristate exposure induced by multimerization (22), a reduction in the amount of RNA bound to MA associated with myristate exposure (53), or some combination of these factors. We cannot rule out the possibility that the 29/31KR mutation affects MA-MA interaction in the context of LZ-mediated Gag multimerization and thereby affects membrane binding of Gag; however, the MA-HBR residues Lys 29 and 31 are not among the residues identified as important for MA trimerization (69).

Previous studies have shown that NC deletion abrogates Gag localization to specific PM domains such as uropods in polarized T cells or the virus-containing compartments (VCCs) in macrophages, whereas insertion of LZ restores such localization (70, 71). In contrast, we do not see a difference in the subcellular localization of Gag between full-length Gag and delNC Gag for any of the MA mutants examined (Figure 2.3). Taken together, these data suggest that presence of NC and hence NC-dependent multimerization do not dictate overall Gag localization to the PM but are important for the subsequent movement of Gag to specific domains within the PM.

We observed no commensurate increase in VLP release for 29/31KR GagLZ-YFP compared to 29/31KR despite the shift in Gag localization from the cytosol to the PM. Analogous to our observation, a recent study found that when the MA domain of HIV-1 Gag was replaced with the N-terminal PI(4,5)P2 binding region of avian sarcoma virus Gag, the chimeric Gag localized to the PM but did not release VLP efficiently (72). The order of Gag-PM binding and multimerization into Gag puncta varies between different retroviruses (73, 74), suggesting that membrane binding and multimerization need to be coordinated for optimal particle assembly. Thus, it is conceivable that the release defect of 29/31KR GagLZ-YFP may be in part due to a change in Gag multimerization caused by the absence of the native NC domain or the presence of the LZ motif or YFP-tag that becomes apparent in the context of the 29/31KR mutation.

Overall, this paper provides a strong correlation between the ability of HIV-1 Gag to bind RNA via MA and the specificity of Gag localization to the PM. In the absence of PI(4,5)P2, WT Gag and 29/31KR GagLZ remain in the cytosol (Figures 2.6 and 2.9). Therefore, RNA binding is likely sufficient for preventing non-specific binding to other membranes for these Gag proteins. On the other hand, 25/26KR Gag and WT GagLZ, which are likely to have higher affinities to lipid bilayers due to increased myristate exposure or avidity, show promiscuous localization upon PI(4,5)P2 depletion (Figure 2.6 and 2.9). In these cases, both RNA and PI(4,5)P2 likely work in conjunction to prevent promiscuous localization. Altogether, the comparisons between the MA HBR mutants indicate the role of MA-bound RNA as an important player in targeting Gag specifically to the PM.

Materials and Methods

Plasmids.

pCMVNLGagPolRRE Gag-YFP, which expresses HIV-1 Gag_{NL4-3} fused to YFP in an HIV-1 Rev-dependent manner, was constructed as described previously for pCMVNLGagPolRRE Gag-mRFP (75) using standard

molecular cloning techniques. pCMVNLGagPolRRE delNC/Gag-YFP was generated by replacing the SpeI-XmaI region of pCMVNLGagPolRRE (76) with the corresponding region of pNL4-3/delNC/Gag-YFP described previously (77). pCMVNL GagLZ-YFP (previously named pCMVNLGag Venus LZ) was described in prior reports (29, 55). pGEMNLNR, an expression vector used for *in vitro* transcription and translation of Gag, was described previously (26). To create pCMVNLGagPolRRE 25/26KR Gag-YFP,pCMVNLGagPolRRE 29/31KR Gag-YFP, pCMVNLGagPolRRE 29KR Gag-YFP, pCMVNLGagPolRRE 31KR Gag-YFP, and pCMVNLGagPolRRE 29/31KA Gag-YFP, the corresponding MA-HBR point mutations were introduced using PCR mutagenesis into pCMVNLGagPolRRE Gag-YFP. pCMVNLGagPolRRE 25/26KT Gag-YFP and pCMVNLGagPolRRE 29/31KT Gag-YFP were constructed by replacing the SpeI-BssHII region of pCMVNLGagPolRRE Gag-YFP with corresponding region of pGEMNLNR 25/26KT Gag and pGEMNLNR 29/31KT Gag (26, 32). pCMVNLGagPolRRE delNC/Gag-YFP containing the MA-HBR mutations, i.e., 25/26KR, 25/26KT, 29/31KR and 29/31KT, were constructed using standard molecular cloning techniques. pCMVNLGagPolRRE 6A2T delNC/Gag-YFP was created by replacing the SpeI-BssHII region of pCMVNLGagPolRRE delNC/Gag-YFP with corresponding region of pGEMNLNR 6A2T Gag (26, 32). pGEMNLNR containing the MA-HBR mutations, i.e., 25/26KR and 29/31KR, were constructed using standard molecular biology techniques. 1GA mutation was introduced into the pCMVNLGagPolRRE Gag-YFP and pCMVNLGagPolRRE delNC/Gag-YFP constructs by PCR mutagenesis as described before (74). pCMVNL GagLZ-YFP containing the MA-HBR mutations, i.e., 29/31KR and 29/31KT; and pGEMNLNR containing the MA-HBR mutations, i.e., 25/26KR and 29/31KR, were constructed using standard molecular cloning techniques.

pCMV-Rev was described previously (75) (kindly provided by S. Venkatesan, National Institutes of Health). A mammalian expression plasmid encoding myc-tagged 5-phosphatase IV (FL 5ptaseIV), pcDNA4TO/Myc5ptaseIV, and its catalytically inactive Δ1 derivative (Δ1 5ptaseIV) were previously

described (26, 78). pCMV-Vphu, which encodes the codon-optimized version of the HIV-1 Vpu gene, was previously described (79) (a kind gift from K. Strebel).

Cells and transfection.

HeLa cells were cultured as described previously (32). For microscopy, 30,000 HeLa cells were plated into each well of eight-well chamber slides (Lab-Tek; Nalgene Nunc International), cultured for 24 h, and transfected with plasmids encoding indicated Gag-YFP derivatives using Lipofectamine 2000 (Invitrogen) as per the manufacturer's instructions. For VLP release and PAR-CLIP experiments, 4×10^5 cells were plated into each well of six-well plates (Corning), cultured for 24 h, and transfected as described above.

VLP release assay and immunoblotting.

VLP release assays were carried out as described previously (32). HIV-1 Gag in cell and VLP lysates was detected by immunoblotting using HIV immunoglobulin (HIV-Ig; AIDS Research and Reference Reagent Program) as a primary antibody. Alexa Fluor 488-conjugated goat anti-human IgG (Invitrogen) was used for the detection of primary antibodies for HIV-1 Gag. Fluorescence signals were detected and quantified using a Typhoon Trio imager (GE Healthcare).

Immunostaining and fluorescence microscopy.

Hela cells transfected with plasmids expressing Gag-YFP were incubated for 1 min at room temperature with Alexa Fluor 594-conjugated Concanavalin A (ConA-AF594; Invitrogen) for visualization of the plasma membrane cells 14-16 hours post transfection. Cells were then fixed with 4% paraformaldehyde (PFA) in PBS. The expression of 5ptaseIV (both full-length [FL] and Δ1) in cells was detected by immunostaining with mouse anti-myc antibody (9E10; Santa Cruz Biotechnologies) after permeabilizing the cells. For quantitative analysis of Gag localization phenotypes, images of about 20 fields were recorded using an Olympus IX70 inverted fluorescence microscope at 60x magnification, and a range of 37 to 134 cells were

evaluated for Gag localization pattern. For 5ptaseIV coexpression studies, only cells that were positive for both Gag and 5ptaseIV (either FL or Δ1) were chosen for evaluation. Confocal microscopy using Leica SP5 Inverted confocal microscope was carried out to further verify localization patterns determined by epifluorescence microscopy.

Liposome-binding assay.

Preparation of liposomes, *in vitro* Gag translation, and sucrose gradient flotation centrifugation were performed as described previously (32). In brief, full-length myristoylated Gag was translated *in vitro* using Promega's TnT Sp6 Coupled Reticulocyte Lysate System and incubated with sonicated liposomes composed of a neutral lipid, phosphatidylcholine, and an acidic lipid, phosphatidylserine, in a 2:1 molar ratio (PC+PS [2:1] liposomes) with or without addition of 7.25 mol% PI(4,5)P2. Following sucrose flotation centrifugation, five fractions were collected with the top two fractions representing the membrane bound, floating Gag. Following SDS-PAGE, Gag bands were detected by phosphorimager analysis and quantified using ImageQuant 1D TL v8.1 image analysis software. Liposome binding efficiency (%) was calculated as the percentage of membrane bound Gag versus the total Gag in all 5 fractions.

PAR-CLIP assay.

To determine the amount of cellular RNA bound to transfected Gag, the PAR-CLIP assay was performed as described before (47, 56) with some modifications. Briefly, in each well of a 6-well plate, $4X10^5$ HeLa cells were cultured in DMEM supplemented with 5% fetal bovine serum in the presence of penicillin and streptomycin antibiotics. The cells were then transfected with either a plasmid encoding 1GA/delNC/Gag-YFP containing the indicated MA sequence or pUC19. The cells were cultured for 24 hrs post transfection before addition of fresh media containing 100 μM 4-thiouridine (4-SU, Sigma), a photo-crosslinkable ribonucleoside analogue. After 16 hours, the cells were exposed to 354nm UV light at 300mJ/cm^2 to crosslink RNA and RNA-binding proteins. Cells were lysed with NP-40 lysis buffer (50mM HEPES buffer [pH

7.5], containing 150mM KCl, 2mM EDTA, 0.5% [v/v] NP40 substitute, 0.5mM DTT, and supplemented with protease inhibitor cocktail), and the lysate was treated with 20U/ml RNase A (Promega) and 60U/ml RQ1 DNase (Promega). Gag was immunoprecipitated by incubating the cell lysates with HIV-Ig bound to Dynabeads™ Protein G (Invitrogen) for 1 hour on a rotating shaker at 4°C. The RNA bound to Gag was first dephosphorylated at the 5' end with calf intestinal alkaline phosphatase (New England BioLabs, NEB) followed by T4 polynucleotide kinase-catalyzed (NEB) rephosphorylation of the RNA at the 5'end with ^{32}P (ATP-[γ-^{32}P], PerkinElmer). The Gag-RNA complex was eluted from Dynabeads by heating in PAR-CLIP elution buffer (50mM Tris HCL pH 6.8, containing 2mM EDTA-NaOH 10% [v/v] Glycerol, 2% [v/v] SDS, 100mM DTT, 0.1% [w/v] Bromophenol Blue) for 5 min at 95°C with shaking at 1400 RPM. After resolving the bands by SDS-PAGE and subsequent electrotransfer to a PVDF membrane, the membrane was probed with HIV-Ig as the primary antibody and corresponding secondary antibody conjugated to horseradish peroxidase (goat anti-human IgG, Invitrogen). Gag-specific bands were detected after incubation with SuperSignal West Pico chemiluminescent substrate (Pierce) on Syngene Pxi multiapplication imager, and the intensity of the bands were measured using GeneTools analysis software. The ^{32}P end-labeled RNA bands were also detected on the same membrane using autoradiography on the Typhoon FLA 9500 laser scanner and quantified using ImageQuant 1D TL v8.1 image analysis software. The relative RNA binding efficiency (%) was calculated as the percentage of total RNA band intensity versus the total Gag band intensity for each construct and compared to the normalized value for WT 1GA/delNC/Gag-YFP.

Statistical analysis.

Student's t-tests were performed using Graphpad Prism. *P* values of <0.05 were considered statistically significant.

Acknowledgements

We thank members of our laboratory for helpful discussions and critical reviews of the manuscript. We thank S. Kutluay for her helpful comments in the optimization of the PAR-CLIP technique. The following reagent was obtained through the AIDS Research and Reference Reagent Program, Division of AIDS, NIAID, NIH: HIV Ig (from NABI and NHLBI). The microscopy data presented in this study was collected at the Biomedical Research Core Facilities Microscopy core, University of Michigan. This work was supported by NIH grant R37 AI071727 (to A.O.).

References

1. Jouvenet N, Neil SJ, Bess C, Johnson MC, Virgen CA, Simon SM, Bieniasz PD. 2006. Plasma membrane is the site of productive HIV-1 particle assembly. PLoS Biol 4:e435.
2. Finzi A, Orthwein A, Mercier J, Cohen EA. 2007. Productive human immunodeficiency virus type 1 assembly takes place at the plasma membrane. J Virol 81:7476-90.
3. Adamson CS, Freed EO. 2007. Human immunodeficiency virus type 1 assembly, release, and maturation. Adv Pharmacol 55:347-87.
4. Bieniasz PD. 2009. The cell biology of HIV-1 virion genesis. Cell Host Microbe 5:550-8.
5. Freed EO. 2015. HIV-1 assembly, release and maturation. Nat Rev Microbiol 13:484-96.
6. Swanstrom R, Wills J. 1997. Synthesis, Assembly, and Processing of Viral Proteins. *Retroviruses*:p 263 – 334.
7. Sundquist WI, Kräusslich HG. 2012. HIV-1 assembly, budding, and maturation. Cold Spring Harb Perspect Med 2:a006924.
8. Garnier L, Bowzard JB, Wills JW. 1998. Recent advances and remaining problems in HIV assembly. AIDS 12 Suppl A:S5-16.
9. Balasubramaniam M, Freed EO. 2011. New insights into HIV assembly and trafficking. Physiology (Bethesda) 26:236-51.
10. Göttlinger HG, Sodroski JG, Haseltine WA. 1989. Role of capsid precursor processing and myristoylation in morphogenesis and infectivity of human immunodeficiency virus type 1. Proc Natl Acad Sci U S A 86:5781-5.
11. Bryant M, Ratner L. 1990. Myristoylation-dependent replication and assembly of human immunodeficiency virus 1. Proc Natl Acad Sci U S A 87:523-7.
12. Zhou W, Parent LJ, Wills JW, Resh MD. 1994. Identification of a membrane-binding domain within the amino-terminal region of human immunodeficiency virus type 1 Gag protein which interacts with acidic phospholipids. J Virol 68:2556-69.
13. Yuan X, Yu X, Lee TH, Essex M. 1993. Mutations in the N-terminal region of human immunodeficiency virus type 1 matrix protein block intracellular transport of the Gag precursor. J Virol 67:6387-94.
14. Ono A, Orenstein JM, Freed EO. 2000. Role of the Gag matrix domain in targeting human immunodeficiency virus type 1 assembly. J Virol 74:2855-66.
15. Ono A, Ablan SD, Lockett SJ, Nagashima K, Freed EO. 2004. Phosphatidylinositol (4,5) bisphosphate regulates HIV-1 Gag targeting to the plasma membrane. Proc Natl Acad Sci U S A 101:14889-94.
16. Freed EO, Orenstein JM, Buckler-White AJ, Martin MA. 1994. Single amino acid changes in the human immunodeficiency virus type 1 matrix protein block virus particle production. J Virol 68:5311-20.
17. Ono A, Freed EO. 1999. Binding of human immunodeficiency virus type 1 Gag to membrane: role of the matrix amino terminus. J Virol 73:4136-44.
18. Paillart JC, Göttlinger HG. 1999. Opposing effects of human immunodeficiency virus type 1 matrix mutations support a myristyl switch model of gag membrane targeting. J Virol 73:2604-12.
19. Spearman P, Horton R, Ratner L, Kuli-Zade I. 1997. Membrane binding of human immunodeficiency virus type 1 matrix protein in vivo supports a conformational myristyl switch mechanism. J Virol 71:6582-92.

20. Saad JS, Miller J, Tai J, Kim A, Ghanam RH, Summers MF. 2006. Structural basis for targeting HIV-1 Gag proteins to the plasma membrane for virus assembly. Proc Natl Acad Sci U S A 103:11364-9.
21. Saad JS, Loeliger E, Luncsford P, Liriano M, Tai J, Kim A, Miller J, Joshi A, Freed EO, Summers MF. 2007. Point mutations in the HIV-1 matrix protein turn off the myristyl switch. J Mol Biol 366:574-85.
22. Tang C, Loeliger E, Luncsford P, Kinde I, Beckett D, Summers MF. 2004. Entropic switch regulates myristate exposure in the HIV-1 matrix protein. Proc Natl Acad Sci U S A 101:517-22.
23. Zhou W, Resh MD. 1996. Differential membrane binding of the human immunodeficiency virus type 1 matrix protein. J Virol 70:8540-8.
24. Hermida-Matsumoto L, Resh MD. 1999. Human immunodeficiency virus type 1 protease triggers a myristoyl switch that modulates membrane binding of Pr55(gag) and p17MA. J Virol 73:1902-8.
25. Hill CP, Worthylake D, Bancroft DP, Christensen AM, Sundquist WI. 1996. Crystal structures of the trimeric human immunodeficiency virus type 1 matrix protein: implications for membrane association and assembly. Proc Natl Acad Sci U S A 93:3099-104.
26. Chukkapalli V, Hogue IB, Boyko V, Hu WS, Ono A. 2008. Interaction between the human immunodeficiency virus type 1 Gag matrix domain and phosphatidylinositol-(4,5)-bisphosphate is essential for efficient gag membrane binding. J Virol 82:2405-17.
27. Chan R, Uchil PD, Jin J, Shui G, Ott DE, Mothes W, Wenk MR. 2008. Retroviruses human immunodeficiency virus and murine leukemia virus are enriched in phosphoinositides. J Virol 82:11228-38.
28. Inlora J, Chukkapalli V, Derse D, Ono A. 2011. Gag localization and virus-like particle release mediated by the matrix domain of human T-lymphotropic virus type 1 Gag are less dependent on phosphatidylinositol-(4,5)-bisphosphate than those mediated by the matrix domain of HIV-1 Gag. J Virol 85:3802-10.
29. Inlora J, Collins DR, Trubin ME, Chung JY, Ono A. 2014. Membrane binding and subcellular localization of retroviral Gag proteins are differentially regulated by MA interactions with phosphatidylinositol-(4,5)-bisphosphate and RNA. MBio 5:e02202.
30. Alfadhli A, Barklis RL, Barklis E. 2009. HIV-1 matrix organizes as a hexamer of trimers on membranes containing phosphatidylinositol-(4,5)-bisphosphate. Virology 387:466-72.
31. Anraku K, Fukuda R, Takamune N, Misumi S, Okamoto Y, Otsuka M, Fujita M. 2010. Highly sensitive analysis of the interaction between HIV-1 Gag and phosphoinositide derivatives based on surface plasmon resonance. Biochemistry 49:5109-16.
32. Chukkapalli V, Oh SJ, Ono A. 2010. Opposing mechanisms involving RNA and lipids regulate HIV-1 Gag membrane binding through the highly basic region of the matrix domain. Proc Natl Acad Sci U S A 107:1600-5.
33. Shkriabai N, Datta SA, Zhao Z, Hess S, Rein A, Kvaratskhelia M. 2006. Interactions of HIV-1 Gag with assembly cofactors. Biochemistry 45:4077-83.
34. Chukkapalli V, Ono A. 2011. Molecular determinants that regulate plasma membrane association of HIV-1 Gag. J Mol Biol 410:512-24.
35. Purohit P, Dupont S, Stevenson M, Green MR. 2001. Sequence-specific interaction between HIV-1 matrix protein and viral genomic RNA revealed by in vitro genetic selection. RNA 7:576-84.
36. Hearps AC, Wagstaff KM, Piller SC, Jans DA. 2008. The N-terminal basic domain of the HIV-1 matrix protein does not contain a conventional nuclear localization sequence but is required for DNA binding and protein self-association. Biochemistry 47:2199-210.
37. Burniston MT, Cimarelli A, Colgan J, Curtis SP, Luban J. 1999. Human immunodeficiency virus type 1 Gag polyprotein multimerization requires the nucleocapsid domain and RNA and is promoted by the capsid-dimer interface and the basic region of matrix protein. J Virol 73:8527-40.

38. Chang CY, Chang YF, Wang SM, Tseng YT, Huang KJ, Wang CT. 2008. HIV-1 matrix protein repositioning in nucleocapsid region fails to confer virus-like particle assembly. Virology 378:97-104.
39. Cimarelli A, Luban J. 1999. Translation elongation factor 1-alpha interacts specifically with the human immunodeficiency virus type 1 Gag polyprotein. J Virol 73:5388-401.
40. Ott DE, Coren LV, Gagliardi TD. 2005. Redundant roles for nucleocapsid and matrix RNA-binding sequences in human immunodeficiency virus type 1 assembly. J Virol 79:13839-47.
41. Webb JA, Jones CP, Parent LJ, Rouzina I, Musier-Forsyth K. 2013. Distinct binding interactions of HIV-1 Gag to Psi and non-Psi RNAs: implications for viral genomic RNA packaging. RNA 19:1078-88.
42. Ramalingam D, Duclair S, Datta SA, Ellington A, Rein A, Prasad VR. 2011. RNA aptamers directed to human immunodeficiency virus type 1 Gag polyprotein bind to the matrix and nucleocapsid domains and inhibit virus production. J Virol 85:305-14.
43. Lochrie MA, Waugh S, Pratt DG, Clever J, Parslow TG, Polisky B. 1997. In vitro selection of RNAs that bind to the human immunodeficiency virus type-1 gag polyprotein. Nucleic Acids Res 25:2902-10.
44. Alfadhli A, Still A, Barklis E. 2009. Analysis of human immunodeficiency virus type 1 matrix binding to membranes and nucleic acids. J Virol 83:12196-203.
45. Alfadhli A, McNett H, Tsagli S, Bächinger HP, Peyton DH, Barklis E. 2011. HIV-1 matrix protein binding to RNA. J Mol Biol 410:653-66.
46. Chukkapalli V, Inlora J, Todd GC, Ono A. 2013. Evidence in support of RNA-mediated inhibition of phosphatidylserine-dependent HIV-1 Gag membrane binding in cells. J Virol 87:7155-9.
47. Kutluay SB, Zang T, Blanco-Melo D, Powell C, Jannain D, Errando M, Bieniasz PD. 2014. Global changes in the RNA binding specificity of HIV-1 gag regulate virion genesis. Cell 159:1096-1109.
48. Dick RA, Kamynina E, Vogt VM. 2013. Effect of multimerization on membrane association of Rous sarcoma virus and HIV-1 matrix domain proteins. J Virol 87:13598-608.
49. Mercredi PY, Bucca N, Loeliger B, Gaines CR, Mehta M, Bhargava P, Tedbury PR, Charlier L, Floquet N, Muriaux D, Favard C, Sanders CR, Freed EO, Marchant J, Summers MF. 2016. Structural and Molecular Determinants of Membrane Binding by the HIV-1 Matrix Protein. J Mol Biol 428:1637-55.
50. Dick RA, Vogt VM. 2014. Membrane interaction of retroviral Gag proteins. Front Microbiol 5:187.
51. Todd GC, Duchon A, Inlora J, Olson ED, Musier-Forsyth K, Ono A. 2017. Inhibition of HIV-1 Gag-membrane interactions by specific RNAs. RNA 23:395-405.
52. Carlson LA, Bai Y, Keane SC, Doudna JA, Hurley JH. 2016. Reconstitution of selective HIV-1 RNA packaging in vitro by membrane-bound Gag assemblies. Elife 5.
53. Gaines CR, Tkacik E, Rivera-Oven A, Somani P, Achimovich A, Alabi T, Zhu A, Getachew N, Yang AL, McDonough M, Hawkins T, Spadaro Z, Summers MF. 2018. HIV-1 Matrix Protein Interactions with tRNA: Implications for Membrane Targeting. J Mol Biol 430:2113-2127.
54. Leventis PA, Grinstein S. 2010. The distribution and function of phosphatidylserine in cellular membranes. Annu Rev Biophys 39:407-27.
55. Llewellyn GN, Grover JR, Olety B, Ono A. 2013. HIV-1 Gag associates with specific uropod-directed microdomains in a manner dependent on its MA highly basic region. J Virol 87:6441-54.
56. Hafner M, Landthaler M, Burger L, Khorshid M, Hausser J, Berninger P, Rothballer A, Ascano M, Jungkamp AC, Munschauer M, Ulrich A, Wardle GS, Dewell S, Zavolan M, Tuschl T. 2010. PAR-CliP--a method to identify transcriptome-wide the binding sites of RNA binding proteins. J Vis Exp.
57. Klein KC, Reed JC, Tanaka M, Nguyen VT, Giri S, Lingappa JR. 2011. HIV Gag-leucine zipper chimeras form ABCE1-containing intermediates and RNase-resistant immature capsids similar to those formed by wild-type HIV-1 Gag. J Virol 85:7419-35.

58. Li H, Dou J, Ding L, Spearman P. 2007. Myristoylation is required for human immunodeficiency virus type 1 Gag-Gag multimerization in mammalian cells. J Virol 81:12899-910.
59. Accola MA, Strack B, Göttlinger HG. 2000. Efficient particle production by minimal Gag constructs which retain the carboxy-terminal domain of human immunodeficiency virus type 1 capsid-p2 and a late assembly domain. J Virol 74:5395-402.
60. Crist RM, Datta SA, Stephen AG, Soheilian F, Mirro J, Fisher RJ, Nagashima K, Rein A. 2009. Assembly properties of human immunodeficiency virus type 1 Gag-leucine zipper chimeras: implications for retrovirus assembly. J Virol 83:2216-25.
61. Zhang Y, Qian H, Love Z, Barklis E. 1998. Analysis of the assembly function of the human immunodeficiency virus type 1 gag protein nucleocapsid domain. J Virol 72:1782-9.
62. Stauffer S, Rahman SA, de Marco A, Carlson LA, Glass B, Oberwinkler H, Herold N, Briggs JAG, Müller B, Grünewald K, Kräusslich HG. 2014. The Nucleocapsid Domain of Gag Is Dispensable for Actin Incorporation into HIV-1 and for Association of Viral Budding Sites with Cortical F-Actin, p 7893-903, J Virol, vol 88.
63. **HIV Sequence Compendium 2018** Foley B LT, Apetrei C, Hahn B, Mizrachi I, Mullins J, Rambaut A, Wolinsky S, and Korber B, Eds. Published by Theoretical Biology and Biophysics Group, Los Alamos National Laboratory, NM, LA-UR 18-25673. **HIV Sequence Compendium 2018**.
64. Calnan BJ, Tidor B, Biancalana S, Hudson D, Frankel AD. 1991. Arginine-mediated RNA recognition: the arginine fork. Science 252:1167-71.
65. Li L, Vorobyov I, Allen TW. 2013. The different interactions of lysine and arginine side chains with lipid membranes. J Phys Chem B 117:11906-20.
66. Sokalingam S, Raghunathan G, Soundrarajan N, Lee SG. 2012. A study on the effect of surface lysine to arginine mutagenesis on protein stability and structure using green fluorescent protein. PLoS One 7:e40410.
67. Wu Z, Cui Q, Yethiraj A. 2013. Why do arginine and lysine organize lipids differently? Insights from coarse-grained and atomistic simulations. J Phys Chem B 117:12145-56.
68. Yeung T, Gilbert GE, Shi J, Silvius J, Kapus A, Grinstein S. 2008. Membrane phosphatidylserine regulates surface charge and protein localization. Science 319:210-3.
69. Tedbury PR, Novikova M, Ablan SD, Freed EO. 2016. Biochemical evidence of a role for matrix trimerization in HIV-1 envelope glycoprotein incorporation. Proc Natl Acad Sci U S A 113:E182-90.
70. Llewellyn GN, Hogue IB, Grover JR, Ono A. 2010. Nucleocapsid promotes localization of HIV-1 gag to uropods that participate in virological synapses between T cells. PLoS Pathog 6:e1001167.
71. Inlora J, Chukkapalli V, Bedi S, Ono A. 2016. Molecular Determinants Directing HIV-1 Gag Assembly to Virus-Containing Compartments in Primary Macrophages. J Virol 90:8509-19.
72. Watanabe SM, Medina GN, Eastep GN, Ghanam RH, Vlach J, Saad JS, Carter CA. 2018. The matrix domain of the Gag protein from avian sarcoma virus contains a PI(4,5)P. J Biol Chem 293:18841-18853.
73. Eichorst JP, Chen Y, Mueller JD, Mansky LM. 2018. Distinct Pathway of Human T-Cell Leukemia Virus Type 1 Gag Punctum Biogenesis Provides New Insights into Enveloped Virus Assembly. MBio 9.
74. Ivanchenko S, Godinez WJ, Lampe M, Kräusslich HG, Eils R, Rohr K, Bräuchle C, Müller B, Lamb DC. 2009. Dynamics of HIV-1 Assembly and Release, PLoS Pathog, vol 5.
75. Hogue IB, Grover JR, Soheilian F, Nagashima K, Ono A. 2011. Gag induces the coalescence of clustered lipid rafts and tetraspanin-enriched microdomains at HIV-1 assembly sites on the plasma membrane. J Virol 85:9749-66.
76. Ono A, Freed EO. 2001. Plasma membrane rafts play a critical role in HIV-1 assembly and release. Proc Natl Acad Sci U S A 98:13925-30.

77. Hogue IB, Hoppe A, Ono A. 2009. Quantitative fluorescence resonance energy transfer microscopy analysis of the human immunodeficiency virus type 1 Gag-Gag interaction: relative contributions of the CA and NC domains and membrane binding. J Virol 83:7322-36.
78. Kisseleva MV, Wilson MP, Majerus PW. 2000. The isolation and characterization of a cDNA encoding phospholipid-specific inositol polyphosphate 5-phosphatase. J Biol Chem 275:20110-6.
79. Nguyen KL, llano M, Akari H, Miyagi E, Poeschla EM, Strebel K, Bour S. 2004. Codon optimization of the HIV-1 vpu and vif genes stabilizes their mRNA and allows for highly efficient Rev-independent expression. Virology 319:163-75.

Chapter 3

Title: Differential Interaction of Cellular tRNAs with the Matrix Domain of HIV-1 Gag

Abstract:

The specific localization of HIV-1 Gag to the plasma membrane (PM) is an essential early step in the infectious progeny production. Both the PM-specific phospholipid PI(4,5)P2 and tRNAs bind the highly basic region (HBR) in the matrix domain (MA) of Gag and regulate the binding of Gag to the PM. MA-bound tRNA species in cells likely represent those tRNAs bound to cytosolic Gag. To determine if specific tRNAs are displaced when Gag binds to the PM, we compared the tRNA species in 293T cells bound to WT Gag, 1GA Gag (a Gag derivative that is incapable of membrane binding despite containing the intact MA-HBR, and thus remains in the cytosol), 1GA 6A2T Gag (a Gag in which all the MA-HBR basic residues are switched to neutral residues), as well as the total tRNA repertoire in 293T cells. We identified two tRNA species of interest. SeCTCA was highly enriched on 1GA Gag and WT Gag relative to its cellular abundance, suggesting that SeCTCA may be resistant to removal from MA by PI(4,5)P2 in the cell. PheGAA was specifically enriched only on 1GA Gag relative to its cellular abundance but not on WT Gag, suggesting that PheGAA may be a tRNA that is sensitive to removal from MA by PI(4,5)P2. Both tRNAs were enriched on 1GA Gag compared to 1GA 6A2T Gag, suggesting the role of MA-HBR in selecting for specific tRNAs. Additionally, we find that differences in tRNA sequences or inferred modifications may potentially play a role in the selection of specific tRNAs by MA, suggesting that tRNA characteristics influence specificity of MA for select tRNAs. Overall, this study supports a model in which a specific subset of tRNAs blocks the binding of Gag to nonspecific intracellular membranes but is displaced by PI(4,5)P2 allowing Gag to bind

specifically to the PM, while another subset of tRNAs is resistant to removal by PI(4,5)P2 and block membrane binding of Gag to all cellular membranes, including those containing PI(4,5)P2.

Introduction

The HIV-1 Gag matrix (MA) domain mediates localization of Gag to the plasma membrane (PM), which is crucial for the generation of infectious progeny (1-9). The interaction between the MA highly basic region (HBR) and the PM-enriched lipid PI(4,5)P2 is essential for the localization of Gag to the PM (10-22). In cells, besides the nucleocapsid domain (NC) of Gag, the MA-HBR mediates significant RNA binding to Gag (23). Notably, irrespective of the presence of NC, Gag recovered from the cell cytosol binds liposomes containing a nonspecific acidic phospholipid, phosphatidylserine (PS), only upon RNase treatment, suggesting a role for MA-bound RNA in regulating Gag-membrane binding (23). Previously, we found a correlation that strongly suggests that the amount of RNA bound to MA-HBR in cells regulates the subcellular localization of Gag (24). What is the identity of this RNA species?

An earlier CLIPSeq-based study reported that in cells, most MA-bound RNA is transfer RNA (tRNA) (25). Multiple studies have shown that tRNA regulates Gag-membrane binding (23, 25-29). Interestingly, specific cellular tRNA species were reported to be preferentially bound to MA over other tRNA species (25). To reiterate our working model, which is based on data from our lab and others, PI(4,5)P2, but not other acidic lipids such as PS, displaces RNA to bind MA-HBR and enables the specific recruitment of Gag to the PM. The same CLIPSeq-based study also showed a decrease in Gag-bound tRNAs when Gag is membrane-bound compared to when Gag is free in the cytosol (25). This suggests that the tRNAs identified as selective for MA in the CLIPSeq-based study were potentially bound to Gag present in the cytosol. An in vitro liposome based study suggested that different tRNAs could have different effects on Gag-liposome binding. While one tRNA, ProTGG, inhibited binding of Gag to PS-containing liposomes,

another tRNA, LysTTT, did not (26). This gave rise to an attractive possibility that different tRNAs regulate the membrane binding of Gag differently even in cells. There could be one subset of the cellular tRNA population that inhibits the binding of Gag to nonspecific intracellular membranes but allows Gag to bind to PI(4,5)P2 present at the PM. Another subset of tRNAs could block Gag binding to all membranes, including the PI(4,5)P2-containing ones. The tRNAs bound to Gag in the cytosol could belong to either of these two possible groups of tRNAs. Thus, whether the tRNAs found bound to MA in the previous study (25) are the tRNAs that block membrane binding of Gag irrespective of the presence of PI(4,5)P2 or the tRNAs that are sensitive to removal by PI(4,5)P2 is not known. Determination of different tRNA subpopulations which either support or block the localization of Gag to the PM will help uncover the potential biological significance of MA-tRNA interactions on Gag-membrane binding in cells.

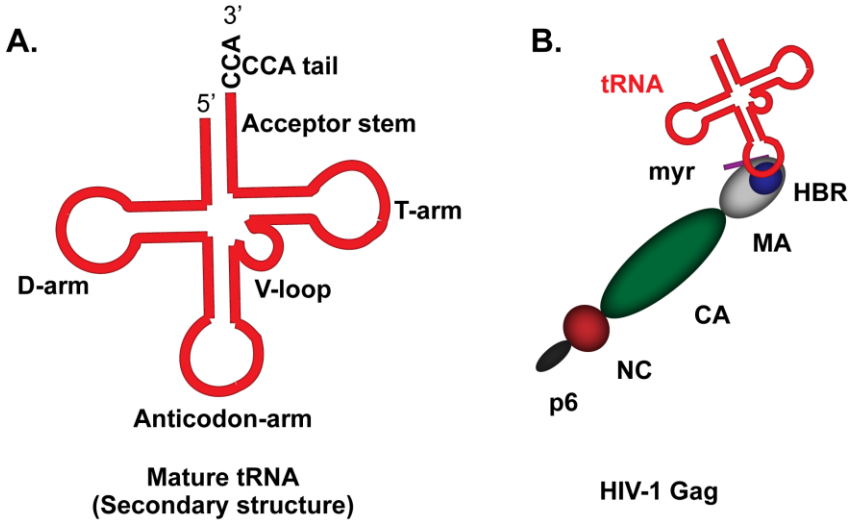

Figure 3.1. Schematic representation of the secondary structure of tRNA and the binding of tRNA to the highly basic region of the matrix domain of HIV-1 Gag (MA-HBR). (A.) Schematic illustration of the generic tRNA cloverleaf secondary structure. The acceptor stem bearing the 3' CCA tail, the D-arm, the T-arm, the V-loop and the anticodon arm are depicted. (B.) Schematic representation of tRNA binding to the HIV-1 Gag MA-HBR. Note that the site of binding is shown in this diagram arbitrarily to be the anticodon arm but could be any of the other arms or a combination of tRNA regions. tRNA binding to MA regulates Gag membrane binding in cells (25).

In this study, we set out to determine whether there are two possible MA-bound tRNA sub-populations in cells. To achieve this goal, we determined the tRNA species that are bound to a Gag construct that is capable of binding to membranes due to the presence of the N-terminal myristoyl moiety

and the intact MA-HBR (WT Gag). We compared this tRNA population to the tRNAs bound to 1GA Gag, a Gag mutant which lacks the site for myristoylation and is thus incapable of membrane binding despite containing an intact MA-HBR (30). The rationale for using the 1GA Gag mutant is to retain the entire population of tRNAs that bind MA, because membrane binding causes disassociation of tRNAs from MA (25). If we find that a certain subpopulation of tRNAs is common between WT and 1GA Gag, that subpopulation potentially represents the tRNAs that are resistant to PI(4,5)P2-mediated removal and, thus blocks the binding of Gag to all cellular membranes. In contrast, the subset of tRNAs that are displaced from WT Gag, but present on 1GA Gag, are potentially the tRNAs that prevent the binding of Gag to nonspecific intracellular membranes but can be removed upon MA-PI(4,5)P2 interaction, thus allowing the specific recruitment of Gag to the PM.

Whether the tRNA species bound to MA simply reflects the overall abundance in cells is unknown. Therefore, we tested if the selection of tRNAs on MA reflected the cellular tRNA abundance. For this, we determined the relative abundances of tRNAs that are present in the cells and examined whether the tRNAs selected on Gag were the highly abundant cellular tRNAs. Finally, we tested whether the MA-HBR basic residues are important for the selection of the specific tRNA species on Gag by determining the total tRNA species bound to a 1GA MA-HBR mutant Gag in which all the MA-HBR basic residues are switched to neutral amino acids (1GA 6A2T).

Preliminary results confirm the previously reported finding that specific tRNA species are selected on MA (25). Based on the relative abundances of these select MA-bound tRNAs on WT Gag vs. 1GA Gag, we predict that these tRNAs could be differentially regulating Gag membrane binding in cells. Further, the data suggest that the selection of tRNAs on MA is not just a reflection of the abundant tRNAs present in the cell. This selection of tRNAs in cells is also dependent on the presence of MA-HBR for some, but not all, of the select MA-bound tRNAs. Furthermore, the data suggest that the tRNA sequence and/or modification status could be a determinant for selection of tRNAs on MA.

Results:

Differential binding of tRNA species to MA in cells

It has been shown that MA and NC contribute equally to the amount of RNA bound to Gag (23). A PAR-CLIPSeq-based study determined that tRNA is the predominant RNA bound to MA in cells and that specific species of tRNAs are selected on MA (25). In order to be able to identify all tRNAs that bind to MA in cells and then specifically determine which of those tRNAs are lost due to membrane binding, we used two different Gag constructs. A Gag construct that was rendered incapable of binding membrane (1GA Gag) would allow us to sample all tRNAs that bind to MA in cells. A membrane binding-competent Gag (WT Gag) would allow us to detect those tRNAs that are bound to its cytosolic subpopulation while the identification of the tRNAs that are lost upon membrane binding of WT Gag can be extrapolated by comparison of the cytosolic WT Gag-bound RNA to the total tRNA population bound to 1GA Gag (Figure 3.2 A.).

We used the PAR-CLIPSeq (photoactivatable ribonucleoside crosslinking and immunoprecipitation followed by RNA sequencing) method to determine which tRNA species interact with MA in cells (24, 25, 31, 32) (Figure 3.2 B). Given that the NC domain also binds RNA and that we were interested in only the MA-bound tRNAs, we engineered the Gag constructs so as to allow us to quantify RNA that is bound to MA but not the NC domain (NC domain deletion mutant, delNC) (24). All the constructs were additionally tagged with GFP which was used as an epitope tag for immunoprecipitation.

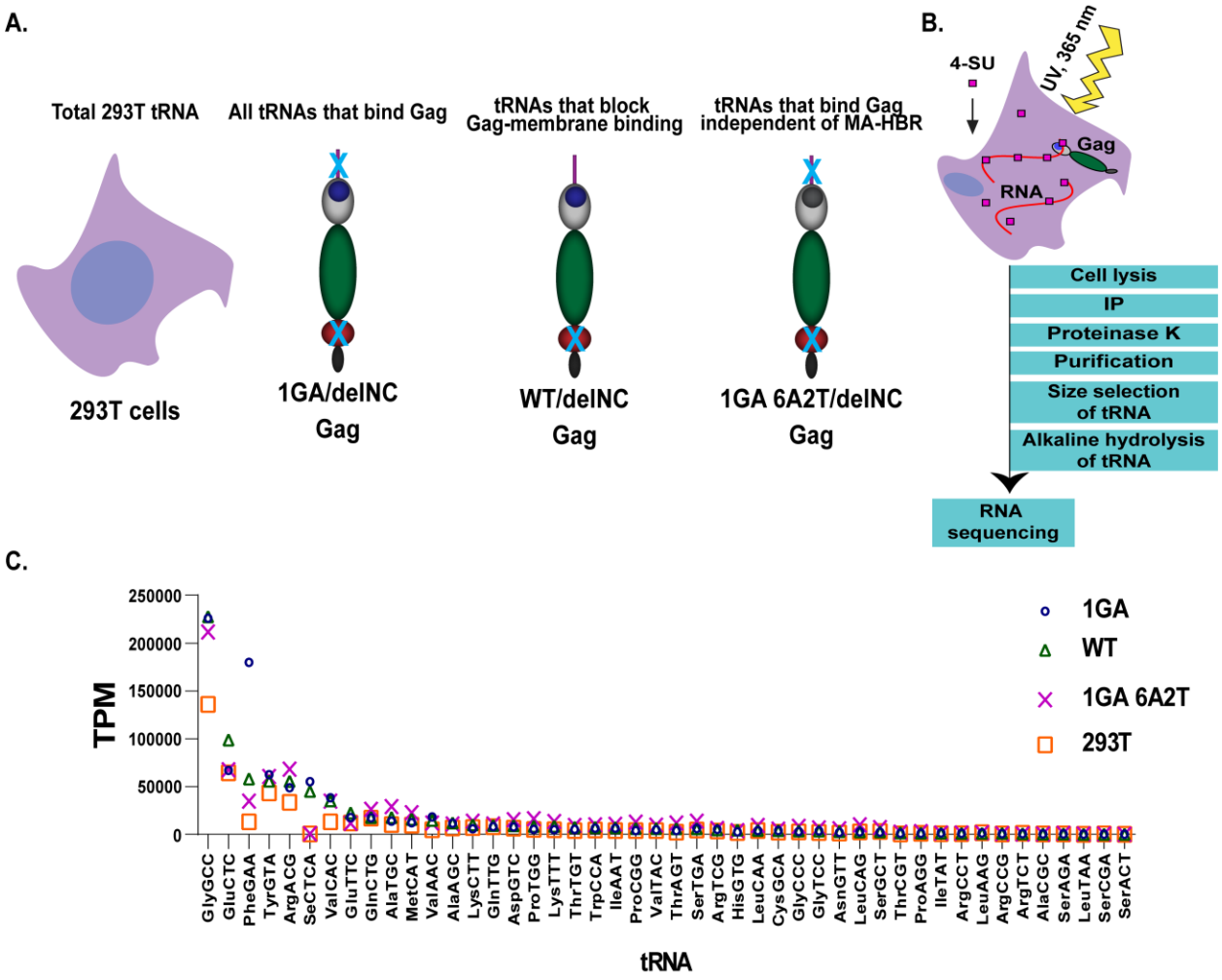

Figure 3.2. Select tRNAs show differential binding on Gag derivatives in cells. (A.) Schematic illustration of the comparisons made in this study. A cytomegalovirus (CMV) promoter-driven Gag-YFP construct lacking most of the NC domain (delNC) was used as the backbone for the Gag derivatives analyzed in this assay. To identify all the tRNAs bound by MA in cells, a cytosolic Gag derivative that lacks the myristoylation site (1GA) was used. To identify the tRNAs which potentially regulate Gag-membrane binding in cells, a Gag derivative capable of membrane binding (WT) was used. To determine whether the selection of tRNAs on MA was HBR-dependent, a mutant Gag with all MA-HBR basic residues switched to neutral Ala or Thr (1GA 6A2T) was used. Finally, to determine whether the selection of tRNAs on MA corresponded to their relative abundances in the host cell, the 293T tRNA population was determined. (B.) Schematic illustration of PAR-CLIPSeq method. The delNC/Gag-YFP constructs were expressed in 293T cells and crosslinked to 4-SU-containing RNA in the cells. Gag and Gag-bound RNA were recovered by immunoprecipitation (IP), Gag was digested using Proteinase K, and the Gag-bound RNA was recovered. tRNA-sized (70-95nt) RNAs were selected and partially hydrolyzed to generate short fragments (<50nt) and sequenced using 50nt single-end Illumina Miseq. Curated reference genome with artificial sequences accounting for reverse transcriptase-induced mismatches was used for alignment (32). Raw counts were normalized per length and sequencing depth to generate Transcripts per million (TPM) which is a measure of the relative abundance. (C.) Ranked order of abundance of tRNA isoacceptors (tRNAs that are charged with the same amino acid) bound to WT Gag. Relative abundances (TPM) of tRNA isoacceptors crosslinked to WT, 1GA, and 1GA 6A2T Gag derivatives, as well as in 293T cells is shown. To generate the total TPM for each tRNA isoacceptor, the TPMs for the individual isodecoders (tRNAs sharing the same anticodon sequence) and sequence variants were combined. n=1.

The delNC Gag-GFP constructs were transfected into 293T cells. The cells were subsequently cultured in a media containing a photoactivatable ribonucleoside analogue, 4-thiouridine (4-SU), which gets incorporated into nascent RNAs. The cells were irradiated with 365-nm UV light to crosslink the 4-SU-containing RNA to the RNA-binding proteins. The delNC Gag-GFP proteins were immunoprecipitated from the cell lysates using an anti-GFP Nanobody/ V_HH based immunoprecipitation (ChromoTek GFP-Trap®) for the immunoprecipitation (IP) of GFP-fused Gag proteins (Gag-GFP). GFP-Trap® has very high affinity (KD=1 pM) for GFP, thus allowing for the effective pulldown of Gag-GFP.

Proteinase K treatment was carried out to digest the Gag protein while leaving the Gag-bound RNA. Phenol chloroform extraction followed by ethanol precipitation was carried out to recover this RNA. The RNA was resolved on an agarose gel, the gel was stained with SYBR Gold and visualized with UV-light. tRNA-sized (~70-95 nt) RNA bands were cut out from the gel for each sample and the RNA was recovered from the gel fragments by diffusion through overnight agitation of gel fragments in buffer. Subsequently, the RNA was ethanol precipitated and then resuspended in nuclease-free water.

PAR-CLIP was then combined with HydrotRNASeq method (Figure 3.2 B.) to sequence the tRNAs bound to the Gag constructs (32). HydrotRNASeq involves the alkaline hydrolysis of tRNAs to generate a range of RNA fragments <~50 bases. The partially hydrolyzed tRNA fragments were then sequenced as per small RNA sequencing on Illumina Miseq. We also implemented the use of a modified RNA reference for alignment that has additional artificial sequences included. These artificial sequences (sequence variants) take into account the sequence mismatches due to misincorporation by the reverse transcriptase (RT) when it encounters tRNA modifications (32). The mismatches detected at sites of modification of tRNAs due to the RT are termed as RT-signatures (32). Inclusion of these sequence variants helps by increasing the mean read coverage over the tRNA length (32). We find that some of these sequence variants are actually observed in our samples. Following sequence alignment and counting of transcripts,

we used a normalized measure of raw counts, Transcripts per million (TPM) for our comparisons. The TPM is representative of the relative abundance of each tRNA species. tRNA isoacceptors are tRNAs that have different anticodons but are charged with the same amino acid while tRNA isodecoders are tRNA molecules that share the same anticodon but harbor sequence diversity outside of the anticodon (33, 34). Forty-seven different tRNA isoacceptors were identified in our study. The TPM of tRNA isodecoders as well as sequence variants for each tRNA isoacceptor were pooled to generate total TPM for each tRNA isoacceptor (Figure 3.2 C.). Based on this total TPM, several of the tRNAs previously identified as selected on MA (25) are also among the abundant tRNAs bound to WT Gag in our study, namely, GlyGCC, GluCTC, ValCAC, and GluTTC. Additionally, several tRNAs not previously identified as selected on MA (25) featured among the abundant tRNAs bound to WT Gag in our study, namely, SeCTCA, PheGAA, TyrGTA, ArgACG, and GlnCTG. A couple of the tRNAs previously reported as being selected on MA (25) were not among the abundant tRNAs on WT Gag in our study, namely, LysCTT and LysTTT. Of note, among the tRNAs newly identified in this study as being selected on MA, PheGAA was ~three-fold more abundant on 1GA Gag compared to WT Gag. SerACT, while not among the abundant tRNAs on Gag, exhibited an ~seven-fold increase in relative abundance on 1GA Gag relative to WT Gag. These data suggest that PheGAA and SerACT may be tRNAs that are lost when Gag binds to the PM, presumably through interaction of Gag with PM-specific PI(4,5)P2. SeCTCA (the tRNA for selenocysteine), though highly abundant on both 1GA Gag and WT Gag, does not show any differential enrichment between them, suggesting that SeCTCA is likely a tRNA that is resistant to removal by PI(4,5)P2 and thus, potentially retains Gag in the cytosol. While in vitro assays have suggested that ProTGG but not LysTTT inhibits Gag-membrane binding (26), we do not see a stark difference between LysTTT, LysCTT, ProTGG, ProCGG, and ProAGG in their ranked order of relative abundance on either WT Gag or 1GA Gag. The tRNAs that are not enriched on WT Gag are those that are removed upon Gag-PM binding. These tRNAs potentially regulate Gag-PM binding by preventing the promiscuous localization of Gag. Thus, by comparing membrane binding competent (WT) vs.

incompetent (1GA) Gag constructs, we were able to identify tRNAs with different selection profiles on Gag based on the potential of Gag to bind membrane, suggesting that select tRNAs that bind Gag could differentially regulate the membrane binding of Gag in cells.

Cellular abundance of tRNAs does not dictate the relative abundance of tRNAs on MA

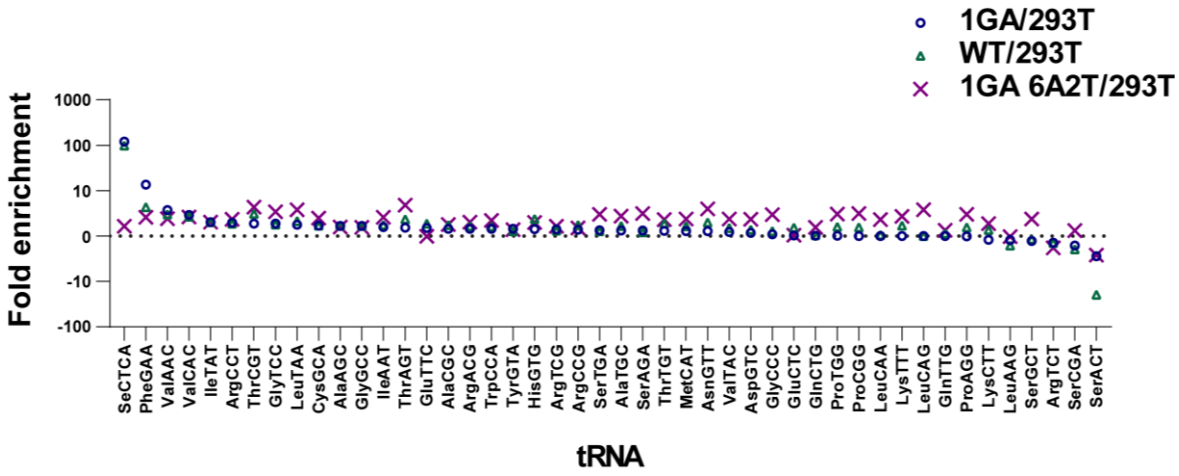

Figure 3.3. Selection of specific tRNAs on MA is not dictated by their relative abundances in cells. Graph displaying the fold enrichment of tRNAs on Gag derivatives relative to their abundance in 293T cells in descending order of enrichment. For each tRNA isoacceptor, the fold enrichment is calculated as the ratio of their relative abundance (TPM) when crosslinked to the Gag derivatives, WT, 1GA, and 1GA 6A2T, compared to their relative abundance (TPM) in the original 293T cell population. Calculations are based on TPM determined after PAR-CLIPSeq as described previously. n=1.

Of the pool of tRNA species in the cell, only specific tRNAs are selected on MA [(25) (this study)]. The reason for such specific selection could be based on the different sequence, different structure, or differences in other characteristics of the selected tRNAs. Yet another explanation could be that instead of a selection based on specific tRNA characteristics, the tRNA population captured on Gag is just a reflection of the tRNA population in the 293T cells. To determine if the relative abundances of cellular tRNAs dictate which tRNAs are selected on Gag, we determined the relative abundances of the tRNA population in 293T cells. We quantified the fold enrichment of each tRNA isoacceptor as a ratio of its relative abundance on WT Gag or Gag mutants to its relative abundance in the 293T cells (Figure 3.3). The

tRNAs showing enrichment relative to their cellular abundance were SeCTCA, PheGAA, ValAAC, ValCAC, and IleTAT on both WT MA as well as 1GA MA. ThrCGT, HisGTG, ThrAGT, LeuTAA, and AsnGTT were enriched relative to their cellular abundance on WT MA, and to a lesser extent on 1GA MA. Thus, the tRNAs selected on the Gag constructs were not just the highly abundant cellular tRNAs. These data suggest that specific tRNA characteristics, and not just their respective abundances in the cell, govern the selection of specific tRNAs on MA.

Enrichment of certain MA-bound tRNAs is dependent on MA-HBR

A previous PAR-CLIPSeq-based study had reported a progressive loss of tRNAs bound to Gag when the basic Lys residues in MA-HBR were switched with neutral Thr (K-to-T) (25). However, whether the selection of specific tRNAs on MA depended on the presence of the MA-HBR was not determined. We decided to address whether MA-HBR was involved in the selection of specific tRNAs on MA in cells.

For this purpose, we compared the relative abundances of tRNAs on 1GA Gag with that on 1GA 6A2T Gag (Figure 3.2 A. and C.). While the former allowed us to determine all the tRNAs bound to MA, the latter allowed us to capture those tRNAs which bind MA irrespective of MA-HBR. We found that the selection of SeCTCA on 1GA Gag was highly dependent on the presence of MA-HBR (>~seventy-three-fold enriched above 1GA 6A2T level). Another tRNA enriched on 1GA Gag, PheGAA, also showed an ~five-fold enrichment on 1GA Gag above 1GA 6A2T. Other enriched tRNAs, including those identified in the previous CLIPSeq study (25), either showed a small change in abundance (e.g., ValAAC and GluTTC) or did not display any fold change in abundance (e.g., GlyGCC, GluCTC, and ValCAC) between the two compared samples. These data suggest that the selection of SeCTCA and PheGAA on MA is in an MA-HBR dependent fashion. Perhaps the exposed basic residues outside of the MA-HBR, namely, Lys38, Arg42, Lys94 and Lys97, which were not mutated in the 1GA 6A2T mutant, may be involved in selection of the other selected tRNAs.

MA shows preference for some but not all tRNA isodecoders

Our data so far show that specific tRNAs bind MA despite having low relative abundance in the 293T cells suggesting that some selection process and, not just cellular abundance, regulates the binding of MA to preferred tRNAs. Our data further suggest that presence of MA-HBR is necessary for the selection of certain select tRNAs on MA. We wanted to investigate whether the preference of MA for the tRNAs was driven by any characteristics of the tRNAs. To this end, we examined the sequences of different tRNA isodecoders for each tRNA isoaccepter to determine if there is any difference in the sequences between the isodecoders that show enrichment relative to their cellular levels and those that do not.

We identified two tRNAs, PheGAA and AlaAGC, as showing differential enrichment on 1GA Gag relative to their cellular abundance among the various isodecoders in the 293T tRNA population (Figure 3.4). Out of the five isodecoders for PheGAA detected in our study, tRNAF13, tRNAF2, tRNAF5 and tRNAF1 showed five-fold or more enrichment relative to their cellular abundance, while the remaining isodecoder, tRNAF4, was not enriched (Figure 3.4 A.). When we compared the relative abundances (log10 TPM) of the individual PheGAA isodecoders in 293T cells and on 1GA Gag, we found that even though the relative abundance of tRNAF4 in cell lysates is similar to that of tRNAF13, tRNAF5, and tRNAF1, its relative abundance on 1GA Gag is ten-fold less (Figure 3.4 B.). Thus, the relative abundance of the isodecoder in the 293T cells is not a determinant of tRNA enrichment on MA. In a similar vein, only two, namely tRNAA2 and tRNAA3, out of the eight AlaAGC isodecoders detected in our study showed > five-fold enrichment on 1GA Gag relative to their cellular abundance in spite of tRNAA2 and tRNAA3 showing similar or lower relative abundance (log10 TPM) in 293T cells compared to the other AlaAGC isodecoders (Figure 3.4 C. and D.).

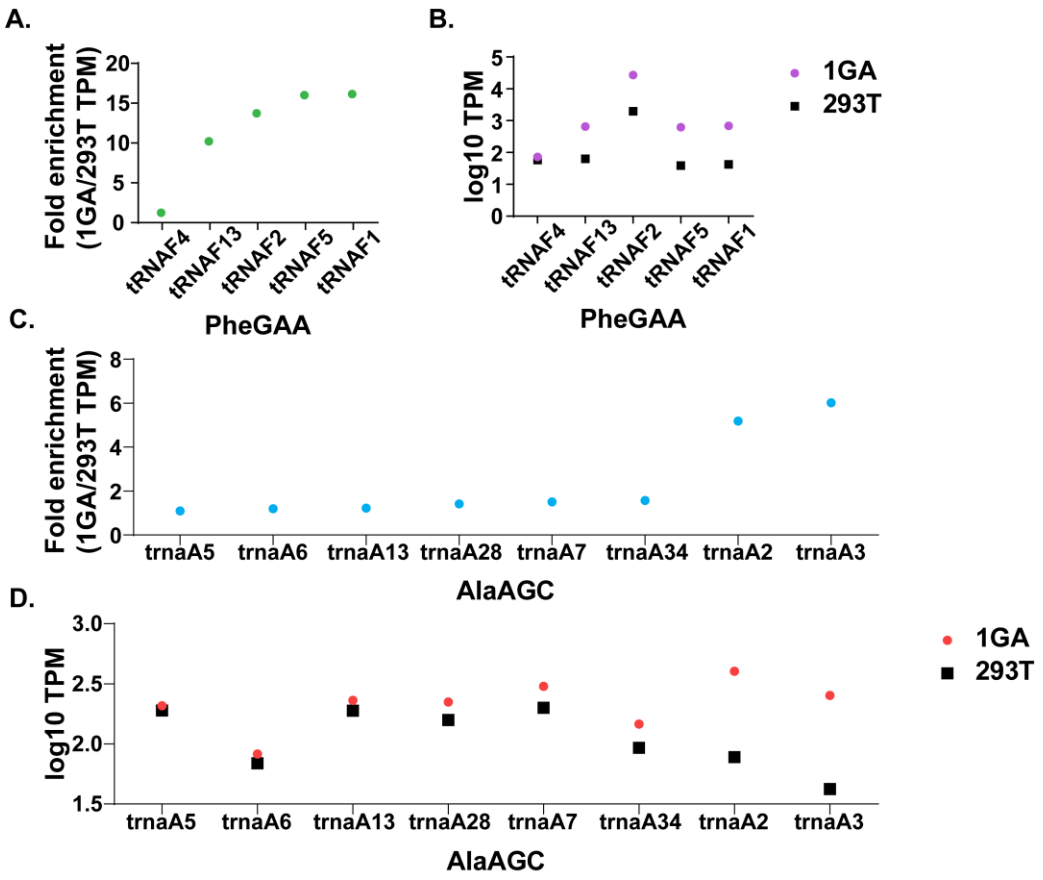

Figure 3.4. Not all tRNA isodecoders are equally enriched on MA. (A.) Graph displaying the fold enrichment of PheGAA isodecoders on 1GA Gag relative to their abundance in 293T cells. The fold enrichment is calculated as the ratio between the relative abundance (TPM) of each isodecoder crosslinked to 1GA Gag versus their starting relative abundance (TPM) in 293T cells. (B.) Graph displaying the log10 relative abundances (log10 TPM) of each of PheGAA isodecoders. To determine whether the original relative abundances in 293T cells affect the enrichment of the PheGAA isodecoders, we compared the relative abundances (TPM) of the isodecoders in the 293T cells versus those crosslinked to 1GA Gag. (C.) Graph displaying the fold enrichment of AlaAGC isodecoders on 1GA Gag relative to their abundance in 293T cells. The fold enrichment is calculated as above. (D.) Graph displaying the log10 relative abundances (log10 TPM) of each of AlaAGC isodecoders in the 293T cells versus those crosslinked to 1GA Gag. The relative abundances (TPM) were determined after PAR-CLIPSeq as described previously. n=1.

To understand what could be driving the difference in enrichment of the tRNA isodecoders, we compared their sequences to detect any sequence differences unique to either the enriched or the non-enriched groups. We found that tRNAF4, but not any of the other PheGAA isodecoders, harbored a different sequence in the acceptor stem region of the tRNA (Figure 3.5 A.). The sequence change is predicted to alter the secondary structure (based on minimum free energy) of tRNAF4 in the acceptor stem compared to the other isodecoders (35-37) (Figure 3.6 A.). Although such structural predictions are

not without uncertainty, we can speculate that the tRNA structure/structural stability is important for tRNA selection on MA and that disruption of the acceptor stem structure hinders the selection of tRNAF4 on MA compared to the PheGAA isodecoders with an intact acceptor stem structure.

Additionally, we found that the enriched isodecoders of AlaAGC, tRNAA2 and tRNAA3, shared common sequence with each other but not with the rest of the non-enriched isodecoders of AlaAGC (Figure 3.5 B.). These shared common regions between tRNAA2 and tRNAA3 were distributed throughout the tRNA sequence. Note that the tRNAA2 and tRNAA3 isodecoders showed differences in sequence with each other as well. However, the sequences in common between these two enriched isodecoders likely favor their selection compared to the rest of the isodecoders lacking these common sequences. While the predicted secondary structures (based on minimum free energy) of tRNAA2 and tRNAA3 are similar and appear to be canonical, the predicted secondary structures of the non-enriched tRNAs include either a lack of obvious D-arm, T-arm or V-loop (tRNAA5), an expanded V-loop (tRNAA6, tRNAA7, and tRNAA13) or an extended T-loop (tRNAA28 and tRNAA34) (35-37) (Figure 3.6 B.). Thus, we can speculate that the selection of the enriched AlaAGC isodecoders, tRNAA2 and tRNAA3, might involve the V-loop and/or the T-loop and the difference of these structures in the non-enriched AlaAGC isodecoders could explain why they were not enriched on MA. Overall, these data suggest that the tRNA isodecoder sequence and/or structure could influence the selection of specific tRNAs on MA.

A.

Isodecoder	Sequence
tRNAF4	GCCAAAATTGCTCAGTTGGGAGAGCGTTAGACTGAAGATCTAAAGGTCCCTGGTTCGATCCCGGGTTTCACCACCA
tRNAF13	GCCGAGATAGCTCAGTTGAGAGAGCGTTAGACTGAAGATCTAAAGGTCCCTGGTTCAATCCCGGGTTTCGGCACCA
tRNAF2	GCCGAAATAGCTCAGTTGGGAGAGCGTTAGACTGAAGATCTAAAGGTCCCTGGTTCGATCCCGGGTTTCGGCACCA
tRNAF5	GCCGAGATAGCTCAGTTGGGAGAGCGTTAGACTGAAGATCTAAAGGTCCCTGGTTCAATCCCGGGTTTCGGCACCA
tRNAF1	GCCGAAATAGCTCAGTTGGGAGAGCGTTAGACTGAAGATCTAAAGGTCCCTGGTTCAATCCCGGGTTTCGGCACCA

B.

Isodecoder	Sequence
tRNAA5	GGGGGTGTAGCTCAGTG-GTAGAGCGCGTGCTTCGCATGTACGAGGCCCCGGGTTCGACCCCCGGCTCCTCCACCA
tRNAA6	GGGGGTATAGCTCAGCG-GTAGAGCGCGTGCTTAGCATGCACGAGGTCCTGGGTTCAATCCCCAATACCTCCACCA
tRNAA13	GGGGGTGTAGCTCAGTG-GTAGAGCGCGTGCTTAGCATGCACGAGGCCCCGGGTTCAATCCCCGGCACCTCCACCA
tRNAA28	GGGGGTGTAGCTCAGTG-GTAGAGCGCGTGCTTAGCATGTACGAGGTCCCGGGTTCAATCCCCGGCACCTCCACCA
tRNAA7	GGGGATGTAGCTCAGTG-GTAGAGCGCATGCTTAGCATGCATGAGGTCCCGGGTTCGATCCCCAGCATCTCCACCA
tRNAA34	GGGGGTATAGCTCAGTG-GTAGAGCGCGTGCTTAGCATGCACGAGGTCCTGGGTTCGATCCCCAGTACCTCCACCA
tRNAA2	GGGGAATTAGCTCAAATGGTAGAGCGCTCGCTTAGCATGCGAGAGGTAGCGGGATCGATGCCCGCATTCTCCACCA
tRNAA3	GGGGGATTAGCTCAAATGGTAGAGCGCTCGCTTAGCATGCGAGAGGTAGCGGGATCGATGCCCGCATCCTCCACCA

Figure 3.5. Differences in sequence of MA-enriched vs MA-nonenriched tRNA isodecoders for PheGAA and AlaAGC. The isodecoders and their sequences have been arranged in ascending order of enrichment with respect to 293T levels (1GA Gag TPM/293T TPM) (A.) Comparison of sequences of PheGAA isodecoders. The regions of mismatch are highlighted in red. The sequences unique to tRNAF4, the only PheGAA isodecoder not enriched relative to its levels in 293T cells, are emphasized by underlining. (B.) Comparison of sequences of AlaAGC isodecoders. The regions of mismatch are highlighted in red. The sequences unique to tRNAA2 and tRNAA3, the highly enriched AlaAGC isodecoders relative to their levels in 293T cells, are emphasized by underlining. The relative abundances (TPM) were determined after PAR-CLIPSeq as described previously.

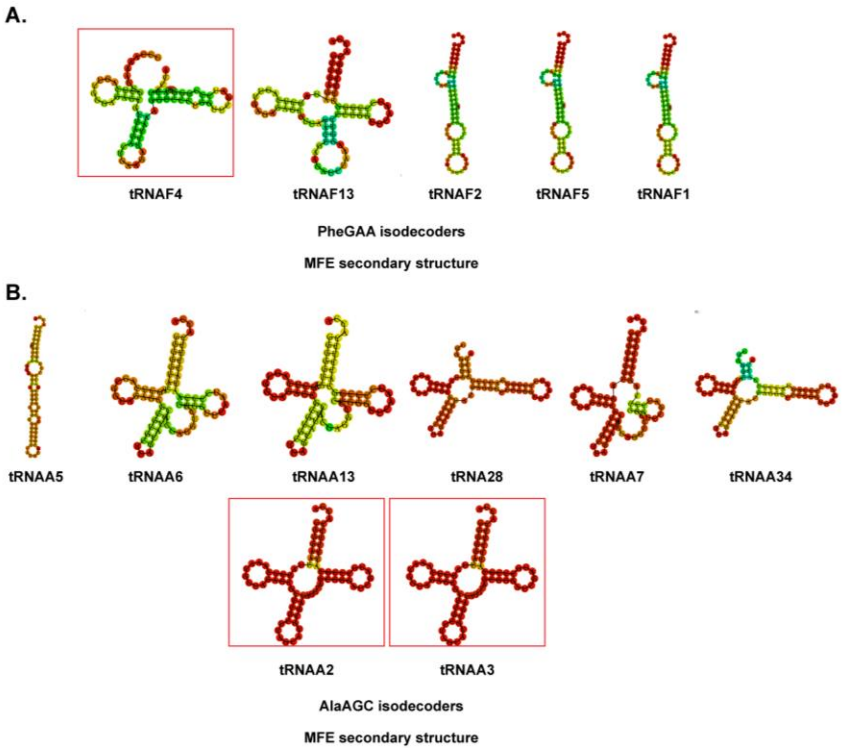

Figure 3.6. Predicted secondary structures of PheGAA and AlaAGC isodecoders. Depiction of the predicted minimum free energy (MFE) structures using RNAfold WebServer (35-37) with default parameters, showing a potential difference between the predicted MFE structures of enriched vs. nonenriched tRNAs on MA. (A.) Predicted MFE structure of PheGAA isodecoders. tRNAF13, tRNAF2, tRNAF5, and tRNAF1 are the enriched isodecoders while

tRNAF4 is the nonenriched isodecoder (highlighted in a red box). (B.) Predicted MFE structure of AlaAGC isodecoders. tRNAA5, tRNAA6, tRNAA13, tRNAA28, tRNAA7, and tRNAA34 are the nonenriched isodecoders while tRNAA2 and tRNAA3 are the enriched isodecoders (highlighted in a red box).

Potential role of tRNA modifications in determining the selection of tRNAs on MA

The reference set used for sequence alignment in this study included artificial tRNA sequences containing the RT-signatures which are the sequence mismatches at known sites of modifications due to RT. This unique reference set offered the unique opportunity to probe the effect of the tRNA modifications on the enrichment of a tRNA on MA relative to its cellular abundance. Given that tRNAs are highly modified and that the modifications have a bearing on multiple aspects of tRNA biology including structure (38-45), it is possible that site-specific modifications could be driving the differences in enrichment even between tRNA molecules sharing the same sequence.

We found that there was an apparent difference in enrichment between sequence variants of SeCTCA (Figure 3.7 A.). In humans, SeCTCA occurs as a single copy functional gene (TRNAU1) located on chromosome 19 (46, 47). The variant sequences harboring the observed modification-induced mismatches have both the mismatch positions and the nucleotide changes shown hyphenated following the gene name.

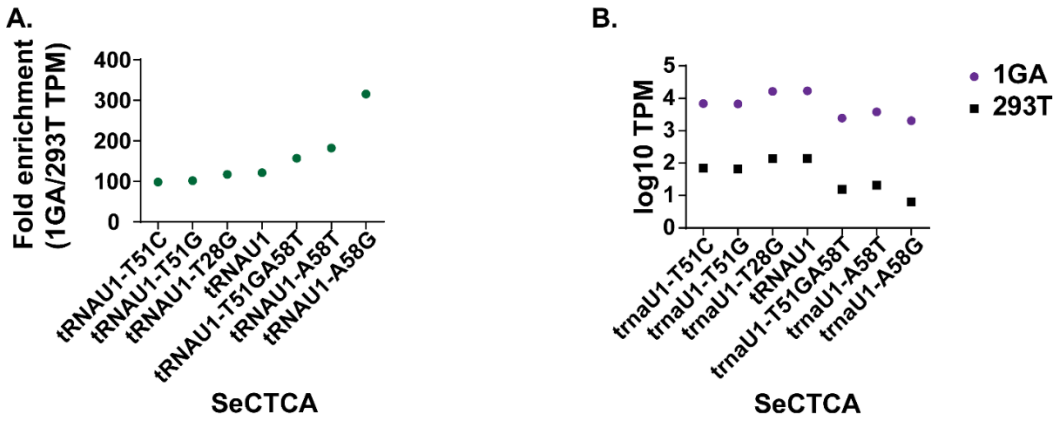

Figure 3.7. Potential role of tRNA modifications in determining the selection of tRNAs on MA. (A.) Graph displaying the fold enrichment of SeCTCA variants on 1GA Gag relative to their abundance in 293T cells. The fold enrichment is

calculated as the ratio between the relative abundance (TPM) of each variant crosslinked to 1GA Gag versus their starting relative abundance (TPM) in 293T cells. (B.) Graph displaying the log10 relative abundances (log10 TPM) of each of SeCTCA variants. To determine whether the starting relative abundances in 293T cells affect the enrichment of the tRNA SeCTCA variants, we compared the relative abundances (TPM) of the variants in the 293T cells versus those crosslinked to 1GA Gag. The relative abundances (TPM) were determined after PAR-CLIPSeq as described previously. n=1.

In case of SeCTCA, tRNAU1 is the sequence present in the original reference tRNA genes for the human genome (hg19). tRNAU1-T51C, tRNAU1-T51G, tRNAU1-T28G, tRNAU1-T51GA58T, tRNAU1-A58T, and tRNAU1-A58G represent sequence variants or artificial sequences that were introduced to create a modified reference set (32). The nucleotide changes in these sequence variants are caused by RT errors and represent tRNA modifications.

We find that SeCTCA is highly enriched (~>100-fold) across all the sequence variants (Figure 3.7 A.). However, the sequence tRNAU1-A58G bearing the A58G mismatch is ~3-fold more increased than tRNAU1 and ~2-fold more increased compared to the A58T variant, even though they show similar abundances in 293T cytosol (Figure 3.7 B.). The likely modification that induced the A58G as well as A58T mismatch in the T-loop is 1-methyladenosine (m1A) at position 58 (m1A58) (48-52). The RT-signatures can be different even for the same modification at the same site. It has been further shown that the +1 neighboring nucleotide 3' to the m1A modification can affect the RT-signature (53). The exact reason for the misincorporation of T in one case and G in another is not clear. We can speculate that what induced the different RT-signature likely also influenced the preference of MA for this specific SeCTCA variant (tRNAU1-A58G) compared to the tRNAU1-A58T (given that this difference in preference achieves significance in future experiments). One potential explanation for the different RT-signatures for the m1A58 may be undetected modifications of neighboring nucleotides around m1A58, that have not created any obvious RT-signatures themselves. These modifications in conjunction with m1A58 maybe potentially allowing for preferential selection of tRNAU1-A58G by MA. The other potential modifications

detected as T51C, T51G, T28G mismatches do not seem to affect the selection of SeCTCA on MA. Thus, some specific modifications of tRNA could potentially be favoring the selection of specific tRNA molecules.

Discussion

In a previous study, tRNA was shown to be the major RNA bound to HIV-1 MA in cells (25). That study along with others support the fact that tRNA is an important host cellular factor that regulates HIV-1 Gag-membrane binding (23, 25-29). Furthermore, specific tRNA isoacceptors were recognized as being selected on MA in cells (25). The same study reported that there was a decrease in Gag-bound tRNAs when Gag was membrane-bound compared to when Gag was cytosolic (4). This data suggested that the specific tRNAs that were identified were likely bound to cytosolic Gag. A previous study suggested that there is differential regulation of Gag-membrane binding by different tRNA species based on in vitro data (26). This gave rise to the idea that potentially there are two subsets of tRNAs in the cell; one group of tRNAs would prevent Gag from binding to nonspecific intracellular membranes but would be sensitive to removal by PI(4,5)P2 and permit Gag to bind PI(4,5)P2 at the PM, while another group of tRNAs would be resistant to removal by PI(4,5)P2 and would, therefore block the membrane binding of Gag to all membranes including the PM. Whether the specific tRNAs reported to be selected on MA in the previous CLIPSeq-based study were sensitive or resistant to removal by PI(4,5)P2 could not be determined in the previous study (25). Furthermore, it was not known whether the selection of the tRNAs on MA was solely due to those select tRNAs being the abundant cellular tRNAs or whether the selection of the specific tRNAs was based on the MA-HBR or specific tRNA characteristics.

In this study, we addressed these outstanding questions in a sequential manner. First, the sequencing of tRNA from 293T cells allowed us to catalog the tRNA repertoire in 293T cells as well as their relative abundances. Next, the use of a non-membrane binding Gag was designed to allow us to determine all the tRNA species that are bound to MA in the cytosol. Comparison of these Gag-bound tRNAs with the

total cellular tRNA population allowed us to gauge whether the tRNAs that were selected on MA were the highly abundant cellular tRNAs. If we found that the most abundant cellular tRNAs were bound to MA, it would imply that potentially there was no specific selection of the tRNAs based on tRNA sequence or structure. One caveat to this comparison is that the 293T cell tRNA population only captures the baseline tRNA population abundances in untransfected cells in this study. There is a potential that cell manipulation or stress, such as transfection, could induce the native tRNA population to change (54, 55). Previously, it has been reported based on microarray data that HIV-1 transfection changes the tRNA population in HEK293 cells in which the interferon-inducible human schlafen 11 (SLFN11) gene was knocked down, but not in the presence of SLFN11. In cells where SLFN11 was knocked down, HIV-1 transfection caused the upregulation of many tRNAs including SeCTCA but not PheGAA. Notably, SLFN11 was not detected in 293T cells even upon induction (56), suggesting that SLFN11-mediated regulation of tRNA population might not be applicable in 293T cells. Thus, even if SeCTCA is a rare tRNA in the untransfected 293T cells, SeCTCA may have been potentially upregulated in Gag/Rev-transfected 293T cells. Thus, potentially, the selection of SeCTCA, and other preferred tRNAs, could be contributed to their abundance in the transfected cells.

Previously, it was shown that the replacement of the basic residues of MA-HBR with neutral residues leads to a decrease in tRNAs bound to MA in cells (25). We compared the tRNA populations between 1GA Gag, in which the MA-HBR sequence and charge are preserved, and 1GA 6A2T Gag, in which the MA-HBR sequence and charge are disrupted. Through that comparison, we found that the enrichment of at least two tRNAs, SeCTCA and PheGAA, is dependent on MA-HBR, suggesting that the MA-HBR may form at least a part of the site of interaction between MA and the selected tRNAs. Interestingly, we have previously shown that just preserving the overall basic charge is not sufficient for WT-level RNA binding in cells (24). Thus, the identity of the basic residues, and not just the overall basic charge, could play a role in selection of tRNAs on MA, however; this remains to be determined. Of special interest is a previously studied MA-HBR mutant, 29/31KR Gag, which was shown to bind less RNA than WT Gag in cells and yet

lacked binding to any cellular membranes (24). We can speculate that the MA-HBR residues Lys29 and Lys31 are required for selecting specific tRNAs that allow Gag to bind to the PM, but not intracellular membranes, and that switching these residues to Arg results in the selection of tRNAs that are resistant to displacement by PI(4,5)P2 on 29/31KR MA. The membrane binding of 29/31KR was restored when the NC domain was replaced with a stronger dimerization leucine zipper (LZ) motif, and the 29/31KR GagLZ mutant bound to the PM specifically (24). Thus, comparison of the tRNA species bound to 29/31KR Gag versus 29/31KR GagLZ could help determine whether 29/31KR Gag, but not 29/31KR GagLZ, selects for the tRNAs that are resistant to removal by PI(4,5)P2.

In this study, we were also able to identify the potential characteristics of tRNA which could contribute to their enrichment on MA in cells. The sequence of tRNA isodecoders is a possible characteristic that influences the enrichment or exclusion of the isodecoders on MA in cells. The sequence changes we observed among the differentially enriched tRNA iodecoders were predicted to change the secondary structure of the isodecoders. Potentially, certain tRNA isodecoder structures favor selection on MA, while other structures fail to do so, but this remains to be confirmed. We also obtained some preliminary indications that tRNA modifications may play a role in preferential selection of tRNAs bearing the same sequence, based on the observation that a particular sequence variant of SeCTCA is apparently more enriched compared to the others. Based on the site of the mismatch, we inferred that the modification responsible for the particular enriched sequence variant was m1A58 modification in the T-loop, even though it is unclear why a sequence variant bearing a different RT-signature at the same site was not as enriched. Given the importance of m1A modification in structural stabilization of tRNA (39, 41-43), the m1A58 may be involved in stabilizing MA-tRNA interactions. This data also suggests that the T-loop either by itself or through stabilizing MA-interactions with other parts of the tRNA may be important for selection of SeCTCA by MA. Given that there is scarce data on the effect on tRNA modifications on viral replication (57), these preliminary findings are novel and potentially important.

In this study, we identified select tRNAs that potentially regulate Gag-membrane binding in cells. We profiled the tRNA population on WT Gag and compared this profile with that of the tRNA species bound to 1GA Gag. Our understanding, based on our working model, is that the WT Gag-bound tRNA population is a subset of total tRNA population as captured 1GA Gag; specifically the subset that retains Gag in the cytosol perpetually because they are resistant to removal by PI(4,5)P2. The tRNAs that would be bound to 1GA Gag but missing or less abundant on WT Gag would represent those tRNAs that are sensitive to removal by PI(4,5)P2 and that are lost when WT Gag binds the PM. PheGAA showed a decrease in relative abundance on WT Gag compared to 1GA Gag. This observation suggests that PheGAA is lost when WT Gag binds the PM. Thus, PheGAA is likely one of the tRNAs that blocks Gag binding to non-PI(4,5)P2 membranes but is displaced by PI(4,5)P2 at the PM, leading to specific localization of Gag to the PM (24). Another tRNA SeCTCA is unusual in being one of the most abundant tRNAs on Gag, highly enriched on Gag compared to its original population in 293T cells and also, being dependent on MA-HBR for its selection on Gag. We found that SeCTCA shows similar enrichment on WT Gag and 1GA Gag. These data suggest that SeCTCA may be a tRNA that is resistant to removal by PI(4,5)P2, forcing Gag to remain in the cytosol.

There are inherent challenges to sequencing tRNAs because they are highly structured and highly modified [93 different types of modifications in tRNA with typically 13-14 modifications per tRNA molecule (32, 39, 42, 58)]. The enzyme RT is needed to convert tRNA to cDNA in order to prepare the cDNA library. However, RT is blocked by the compact structure and heavy modifications of tRNA (32, 39, 42, 58). Commonly used RTs such as Superscript III, used in the previous CLIPSeq-based study (25), lose activity at the high temperature of 70°C at which the tRNA is unfolded to relieve the compact structure (20). Additionally, common tRNA modifications such as methylations could induce RT-stops or nucleotide misincorporation at the site of modification by the RT resulting in RT-signatures (32, 42, 58-60). Interestingly, different RTs have different rates of stopping or induction of RT-signatures (61). Truncated

sequences because of RT stops may be lost or misaligned leading to bias in data quantification. RT-induced mismatches can similarly lead to loss of alignment and a bias in quantification. Several recent papers have come up with compelling methods to ease tRNA sequencing, such as the use of thermostable RT (which is active up to 70°C) or using enzymes to remove modifications in vitro before sequencing (62-65). These methods have been shown to generate longer cDNAs from tRNAs (62-64). To reduce stalling of RT, we adopted the HydrotRNASeq method in which tRNAs are partially hydrolyzed to generate small RNA fragments (32, 66, 67). The rationale behind this method is that these tRNA fragments will have less structure due to their short length as well as have less modifications per tRNA fragment. The partial alkaline hydrolysis method results in more full-length tRNA coverage even compared to the previous methods of using thermostable RT or enzymes to remove modifications (32, 62, 63). In addition, we used a modified RNA reference set for alignment. Variant sequences incorporating RT-signatures at sites of modifications were included in this reference, the use of which was shown to improve the mean read coverage over the tRNA length (32).

The use of the modified RNA reference set (32) which accounted for the RT-induced mismatches allowed us to infer potentially modified transcripts and examine if the presence or absence of any modifications influenced the relative enrichment of any transcripts on 1GA Gag relative to its cellular abundance. However, there are several caveats that we must consider in the cautious interpretation of this modifications data. First, this sequencing-based method does not directly detect the tRNA modification profile, instead, it is an indirect extrapolation through the variant sequences that relies on the presence of RT-signatures induced by modifications at known sites. Not only can a single modification generate multiple RT-signatures, but it can also fail to generate any RT-signature (e.g., pseudouridine, inosine) in case the modifications do not disrupt the Watson-Crick base pairing during cDNA synthesis, or if the modification causes RT-arrest (61, 68). Thus, we can falsely assign significance to a modification when there is none as well as miss the contribution of a modification due to absence of the RT-signature.

Another potential concern is that the alkaline hydrolysis treatment that we perform may lead to the conversion of m1A to the RT-silent m6A (termed Dimroth rearrangement) (52, 68) which could cause the unintentional disappearance of the m1A signature in our study. Thus, what we observe as unmodified (e.g., tRNAU1 sequence), may in actuality be harboring the m1A58 modification, and thus, the data could be confounding. In addition, based on the site of modification, we can infer what the modification is, but the identity of the modification is only an extrapolation, and especially difficult to identify when there is a lack of information pertaining to modifications at a particular nucleotide in a particular tRNA, as well as when there are multiple potential modifications at the same site of the tRNA.

Another caveat to these data is that we have determined the Gag-bound tRNAs in NC-deleted constructs. In the previous CLIPSeq-based study, the deletion of the NC domain did not seem to alter the identities of tRNAs selected on MA in cells (25). However, in in vitro assays, yeast tRNA and ProTGG strongly suppressed Gag binding to non-PI(4,5)P2-containing membranes only in the context of NC (26).Thus, it is possible that the presence of NC changes the abundance of tRNAs on Gag. Thus, it would be necessary to see whether the presence of NC changes the tRNA specificity of MA.

SeCTCA and PheGAA (as well as GlnCTG, TyrGTA, and ArgACG) were not identified as preferentially bound on Gag in the previous CLIPSeq-based assay (25). In contrast, LysTTT and LysCTT were identified as being selected on MA over other tRNAs in the previous CLIPSeq study (25) but not ours. We surmise that differences in the constructs used, the tRNA sequencing strategies, the reference sets used for alignment, and data normalization may have accounted for the different results between the previous study and this current study.

Carlson et al. examined how the HIV-1 genome is selectively packaged by Gag in competition with cytosolic RNAs (28). Interestingly, they found that specifically 5’ untranslated region (5’UTR)-containing sequence significantly increased binding of Gag to PI(4,5)P2-containing liposomes compared to nonspecific RNAs, only in the presence of tRNA. This suggests that the tRNA bound to Gag may be allowing

for specific recognition and incorporation of viral RNA by Gag and furthermore, hints that the viral RNA potentially plays a role in overcoming tRNA mediated inhibition of Gag-membrane binding. In our current study, we have transfected the cells with only Gag- and Rev-encoding plasmids, instead of using a proviral plasmid. Thus, the contributions of viral RNA, as well as HIV-1 proteins other than Gag and Rev, to the selection or modulation of MA-tRNA interactions remain to be elucidated.

Currently, roles played by select tRNA species in the localization and binding of Gag (or other membrane-localizing protein) to the PM are not known. While this study is preliminary, it has some potentially interesting findings. Our data suggest that different tRNA species could be differentially regulating the membrane binding of Gag in cells. The data also suggest that the tRNAs selected on Gag are not the highly abundant cellular tRNAs and that the selection of tRNAs could potentially depend on particular tRNA characteristics such as sequence, structure and modifications. The MA-HBR could be forming the binding site for at least some tRNAs. The analyses of Gag interactions with tRNAs including particular tRNA characteristics could help guide the development of RNA aptamers with high binding affinity for Gag that renders them resistant to removal by PI(4,5)P2. Such RNA aptamers could lead to development of therapeutics that block the binding of Gag to the PM, and hence, block HIV-1 assembly.

Materials and Methods

Plasmids.

pCMVNLGagPolRRE Gag-YFP, which expresses HIV-1 GagNL4-3 fused to YFP in an HIV-1 Rev-dependent manner, was described in a previous report (24). pCMVNLGagPolRRE delNC/Gag-YFP (WT), 1GA pCMVNLGagPolRRE delNC/Gag-YFP and 1GA pCMVNLGagPolRRE 6A2T delNC/Gag-YFP were described previously (24).

pCMV-Rev was previously described (69) (kindly provided by S. Venkatesan, National Institutes of Health).

Cells and transfection.

293T cells were cultured as described previously (70). For PAR-CLIP experiments, 4×10^5 cells were plated into each well of six-well plates (Corning), cultured for 24 h, and transfected with plasmids encoding the indicated delNC/Gag-YFP derivatives using Lipofectamine 2000 (Invitrogen) according to the manufacturer's instructions.

PAR-CLIP assay

To recover the cellular RNA bound to transfected Gag, a PAR-CLIP assay was performed as described previously (47, 57), with some modifications. Briefly, in each well of a 6-well plate, 4×10^5 293T cells were cultured in Dulbecco's modified Eagle's medium (DMEM; Lonza) supplemented with 10% fetal bovine serum in the presence of the antibiotics penicillin and streptomycin. For each sample, 4.8 $X10^6$ cells were then transfected with either a plasmid encoding 1GA/delNC/Gag-YFP containing the indicated MA sequence. The cells were cultured for 24 h post-transfection before the addition of fresh medium containing 200 µM 4-thiouridine (4-SU; Sigma), a photo-crosslinkable ribonucleoside analogue. After 16 h, the cells were exposed to 365-nm UV light at 300 mJ/cm2 to cross-link RNA and RNA binding proteins. Cells were lysed with NP-40 lysis buffer (50 mM HEPES buffer [pH 7.5] containing 150 mM KCl, 2 mM EDTA, 0.5% [vol/vol] NP-40 substitute, and 0.5 mM dithiothreitol [DTT] and supplemented with a protease inhibitor cocktail). The Gag-RNA complex was immunoprecipitated by incubating the cell lysates with an anti-GFP nanobody coupled to magnetic agarose beads (ChromoTek GFP-Trap®) for 1 h on a rotating shaker at 4°C. Protease treatment was carried out with 2mg/ml Proteinase K (Sigma Aldrich) for 30 mins at 50°C to digest Gag (71, 72). After phenol chloroform extraction, ethanol precipitation, and elution in nuclease-free water, the RNA was run on an 8M Urea PAGE gel to resolve the RNA on basis of size. The RNA bands were visualized using UV light after staining the gel with SYBR Gold dye. tRNA-sized bands were cut out of the gel using a clean razor and the RNA was eluted from the gel by overnight incubation

in gel elution buffer (TE with 0.25% sodium dodecyl sulphate (SDS)). The RNA was ethanol precipitated and resuspended in nuclease-free water. tRNA was isolated from 293T cells using Trizol.

Alkaline hydrolysis of tRNA

An optimized protocol for partial alkaline hydrolysis of the tRNA-sized RNA was carried out (32, 66). The RNA was incubated with freshly prepared alkaline buffer (1mM EDTA, 50mM Na2CO3 and 50mM NaHCO3; pH 9.8, Sigma 75335) for 10 mins at 95°C. The alkaline hydrolysis reaction was stopped by ethanol precipitation of the RNA. The RNA was resuspended in nuclease-free water and submitted for next generation sequencing. During optimization step, the size of RNA fragments was checked by running on a 8M Urea PAGE gel and staining with SYBR Gold (described above) after treatment of RNA with different concentrations of alkali buffer, different times of treatment, and different temperatures.

Small RNA Sequencing

Library prep and next-generation sequencing were performed by Michigan Advanced Genomics Core. Library prep was done using Illumina TruSeq small RNA Library Prep Kit. Sequencing was done using single-end 50bp Illumina MiSeq.

Data analysis

The raw sequence data in fastq.gz format was acquired from the Michigan Advanced Genomics Core. The initial quality control, adapter trimming, and alignment was performed by the Bioinformatics Core of the University of Michigan Medical School's Biomedical Research Core Facilities. The quality of each sample was checked using FastQC (v0.11.7). Problematic reads were trimmed using Trim Galore (v0.6.4_dev), which is a wrapper for Cutadapt (v2.8) and FastQC (v0.11.7) with default parameters. The trimmed reads were further transformed using FASTX-Toolkit (v0.0.14) and customized script, then quantified using the scripts and reference shared by the Tuschl Lab (32). The sequence alignment was carried out using

Burrows-Wheeler Aligner (BWA, v0.7.17), allowing up to two mismatches. The raw counts were normalized by dividing by the length of the RNA, then dividing by the sum of all RNAs in the sample. The resultant number was further normalized by multiplying by 10^6 to generate Transcripts per million (TPM). Graphs were generated using GraphPad Prism and prepared for publication using Adobe Illustrator. All cartoons and tables were prepared using Microsoft powerpoint and Adobe illustrator.

Acknowledgements

We are grateful to our fellow lab members for their helpful discussions regarding this study. We acknowledge support from the University of Michigan Medical School's Biomedical Research Core Facilities, especially from Becky Tagett, and Drs. Christopher Krebs and Jingqun Ma. We are grateful to Dr. Pavel Morozov of Tuschl Lab, The Rockefeller University, for his help in sharing the scripts and reference set used for the data analysis. We would like to thank Drs. David Turner and Huanqing Zhang of the Turner Lab, University of Michigan, for sharing their crosslinker as well as for their advice during initial stages of this project. We would like to thank Drs. Sebla Kutluay and Karin Musier-Forsyth for helpful feedback regarding the PAR-CLIP assay.

References

1. Adamson CS, Freed EO. 2007. Human immunodeficiency virus type 1 assembly, release, and maturation. Adv Pharmacol 55:347-87.
2. Bieniasz PD. 2009. The cell biology of HIV-1 virion genesis. Cell Host Microbe 5:550-8.
3. Freed EO. 2015. HIV-1 assembly, release and maturation. Nat Rev Microbiol 13:484-96.
4. Swanstrom R, Wills J. 1997. Synthesis, Assembly, and Processing of Viral Proteins. *Retroviruses*:p 263 – 334.
5. Sundquist WI, Kräusslich HG. 2012. HIV-1 assembly, budding, and maturation. Cold Spring Harb Perspect Med 2:a006924.
6. Garnier L, Bowzard JB, Wills JW. 1998. Recent advances and remaining problems in HIV assembly. AIDS 12 Suppl A:S5-16.
7. Balasubramaniam M, Freed EO. 2011. New insights into HIV assembly and trafficking. Physiology (Bethesda) 26:236-51.
8. Jouvenet N, Neil SJ, Bess C, Johnson MC, Virgen CA, Simon SM, Bieniasz PD. 2006. Plasma membrane is the site of productive HIV-1 particle assembly. PLoS Biol 4:e435.
9. Finzi A, Orthwein A, Mercier J, Cohen EA. 2007. Productive human immunodeficiency virus type 1 assembly takes place at the plasma membrane. J Virol 81:7476-90.
10. Ono A, Ablan SD, Lockett SJ, Nagashima K, Freed EO. 2004. Phosphatidylinositol (4,5) bisphosphate regulates HIV-1 Gag targeting to the plasma membrane. Proc Natl Acad Sci U S A 101:14889-94.
11. Saad JS, Miller J, Tai J, Kim A, Ghanam RH, Summers MF. 2006. Structural basis for targeting HIV-1 Gag proteins to the plasma membrane for virus assembly. Proc Natl Acad Sci U S A 103:11364-9.
12. Shkriabai N, Datta SA, Zhao Z, Hess S, Rein A, Kvaratskhelia M. 2006. Interactions of HIV-1 Gag with assembly cofactors. Biochemistry 45:4077-83.
13. Chukkapalli V, Hogue IB, Boyko V, Hu WS, Ono A. 2008. Interaction between the human immunodeficiency virus type 1 Gag matrix domain and phosphatidylinositol-(4,5)-bisphosphate is essential for efficient gag membrane binding. J Virol 82:2405-17.
14. Chan R, Uchil PD, Jin J, Shui G, Ott DE, Mothes W, Wenk MR. 2008. Retroviruses human immunodeficiency virus and murine leukemia virus are enriched in phosphoinositides. J Virol 82:11228-38.
15. Alfadhli A, Barklis RL, Barklis E. 2009. HIV-1 matrix organizes as a hexamer of trimers on membranes containing phosphatidylinositol-(4,5)-bisphosphate. Virology 387:466-72.
16. Chukkapalli V, Oh SJ, Ono A. 2010. Opposing mechanisms involving RNA and lipids regulate HIV-1 Gag membrane binding through the highly basic region of the matrix domain. Proc Natl Acad Sci U S A 107:1600-5.
17. Anraku K, Fukuda R, Takamune N, Misumi S, Okamoto Y, Otsuka M, Fujita M. 2010. Highly sensitive analysis of the interaction between HIV-1 Gag and phosphoinositide derivatives based on surface plasmon resonance. Biochemistry 49:5109-16.
18. Inlora J, Chukkapalli V, Derse D, Ono A. 2011. Gag localization and virus-like particle release mediated by the matrix domain of human T-lymphotropic virus type 1 Gag are less dependent

on phosphatidylinositol-(4,5)-bisphosphate than those mediated by the matrix domain of HIV-1 Gag. J Virol 85:3802-10.
19. Chukkapalli V, Ono A. 2011. Molecular determinants that regulate plasma membrane association of HIV-1 Gag. J Mol Biol 410:512-24.
20. Inlora J, Collins DR, Trubin ME, Chung JY, Ono A. 2014. Membrane binding and subcellular localization of retroviral Gag proteins are differentially regulated by MA interactions with phosphatidylinositol-(4,5)-bisphosphate and RNA. MBio 5:e02202.
21. Alfadhli A, Still A, Barklis E. 2009. Analysis of human immunodeficiency virus type 1 matrix binding to membranes and nucleic acids. J Virol 83:12196-203.
22. Alfadhli A, McNett H, Tsagli S, Bächinger HP, Peyton DH, Barklis E. 2011. HIV-1 matrix protein binding to RNA. J Mol Biol 410:653-66.
23. Chukkapalli V, Inlora J, Todd GC, Ono A. 2013. Evidence in support of RNA-mediated inhibition of phosphatidylserine-dependent HIV-1 Gag membrane binding in cells. J Virol 87:7155-9.
24. Thornhill D, Olety B, Ono A. 2019. Relationships between MA-RNA Binding in Cells and Suppression of HIV-1 Gag Mislocalization to Intracellular Membranes. J Virol 93.
25. Kutluay SB, Zang T, Blanco-Melo D, Powell C, Jannain D, Errando M, Bieniasz PD. 2014. Global changes in the RNA binding specificity of HIV-1 gag regulate virion genesis. Cell 159:1096-1109.
26. Todd GC, Duchon A, Inlora J, Olson ED, Musier-Forsyth K, Ono A. 2017. Inhibition of HIV-1 Gag-membrane interactions by specific RNAs. RNA 23:395-405.
27. Dick RA, Kamynina E, Vogt VM. 2013. Effect of multimerization on membrane association of Rous sarcoma virus and HIV-1 matrix domain proteins. J Virol 87:13598-608.
28. Carlson LA, Bai Y, Keane SC, Doudna JA, Hurley JH. 2016. Reconstitution of selective HIV-1 RNA packaging in vitro by membrane-bound Gag assemblies. Elife 5.
29. Gaines CR, Tkacik E, Rivera-Oven A, Somani P, Achimovich A, Alabi T, Zhu A, Getachew N, Yang AL, McDonough M, Hawkins T, Spadaro Z, Summers MF. 2018. HIV-1 Matrix Protein Interactions with tRNA: Implications for Membrane Targeting. J Mol Biol 430:2113-2127.
30. Freed EO, Orenstein JM, Buckler-White AJ, Martin MA. 1994. Single amino acid changes in the human immunodeficiency virus type 1 matrix protein block virus particle production. J Virol 68:5311-20.
31. Hafner M, Landthaler M, Burger L, Khorshid M, Hausser J, Berninger P, Rothballer A, Ascano M, Jungkamp AC, Munschauer M, Ulrich A, Wardle GS, Dewell S, Zavolan M, Tuschl T. 2010. PAR-CliP--a method to identify transcriptome-wide the binding sites of RNA binding proteins. J Vis Exp.
32. Gogakos T, Brown M, Garzia A, Meyer C, Hafner M, Tuschl T. 2017. Characterizing Expression and Processing of Precursor and Mature Human tRNAs by Hydro-tRNAseq and PAR-CLIP. Cell Rep 20:1463-1475.
33. Chan PP, Lowe TM. 2009. GtRNAdb: a database of transfer RNA genes detected in genomic sequence. Nucleic Acids Res 37:D93-7.
34. Chan PP, Lowe TM. 2016. GtRNAdb 2.0: an expanded database of transfer RNA genes identified in complete and draft genomes. Nucleic Acids Res 44:D184-9.
35. Lowe TM, Chan PP. 2016. tRNAscan-SE On-line: integrating search and context for analysis of transfer RNA genes. Nucleic Acids Res 44:W54-7.
36. Lorenz R, Bernhart SH, Höner Zu Siederdissen C, Tafer H, Flamm C, Stadler PF, Hofacker IL. 2011. ViennaRNA Package 2.0. Algorithms Mol Biol 6:26.
37. Gruber AR, Lorenz R, Bernhart SH, Neuböck R, Hofacker IL. 2008. The Vienna RNA websuite. Nucleic Acids Res 36:W70-4.
38. Koh CS, Sarin LP. 2018. Transfer RNA modification and infection - Implications for pathogenicity and host responses. Biochim Biophys Acta Gene Regul Mech 1861:419-432.

39. Lorenz C, Lünse CE, Mörl M. 2017. tRNA Modifications: Impact on Structure and Thermal Adaptation. Biomolecules 7.
40. El Yacoubi B, Bailly M, de Crécy-Lagard V. 2012. Biosynthesis and function of posttranscriptional modifications of transfer RNAs. Annu Rev Genet 46:69-95.
41. Schimmel P. 2018. The emerging complexity of the tRNA world: mammalian tRNAs beyond protein synthesis. Nat Rev Mol Cell Biol 19:45-58.
42. Pan T. 2018. Modifications and functional genomics of human transfer RNA. Cell Res 28:395-404.
43. Väre VY, Eruysal ER, Narendran A, Sarachan KL, Agris PF. 2017. Chemical and Conformational Diversity of Modified Nucleosides Affects tRNA Structure and Function. Biomolecules 7.
44. Pereira M, Francisco S, Varanda AS, Santos M, Santos MAS, Soares AR. 2018. Impact of tRNA Modifications and tRNA-Modifying Enzymes on Proteostasis and Human Disease. Int J Mol Sci 19.
45. Huber SM, Leonardi A, Dedon PC, Begley TJ. 2019. The Versatile Roles of the tRNA Epitranscriptome during Cellular Responses to Toxic Exposures and Environmental Stress. Toxics 7.
46. Labunskyy VM, Hatfield DL, Gladyshev VN. 2014. Selenoproteins: molecular pathways and physiological roles. Physiol Rev 94:739-77.
47. Santesmasses D, Mariotti M, Guigó R. 2017. Computational identification of the selenocysteine tRNA (tRNASec) in genomes. PLoS Comput Biol 13:e1005383.
48. Boccaletto P, Machnicka MA, Purta E, Piatkowski P, Baginski B, Wirecki TK, de Crécy-Lagard V, Ross R, Limbach PA, Kotter A, Helm M, Bujnicki JM. 2018. MODOMICS: a database of RNA modification pathways. 2017 update. Nucleic Acids Res 46:D303-D307.
49. Itoh Y, Chiba S, Sekine S, Yokoyama S. 2009. Crystal structure of human selenocysteine tRNA. Nucleic Acids Res 37:6259-68.
50. de Crécy-Lagard V, Boccaletto P, Mangleburg CG, Sharma P, Lowe TM, Leidel SA, Bujnicki JM. 2019. Matching tRNA modifications in humans to their known and predicted enzymes. Nucleic Acids Res 47:2143-2159.
51. Limbach PA, Paulines MJ. 2017. Going global: the new era of mapping modifications in RNA. Wiley Interdiscip Rev RNA 8.
52. Zhang C, Jia G. 2018. Reversible RNA Modification N. Genomics Proteomics Bioinformatics 16:155-161.
53. Hauenschild R, Tserovski L, Schmid K, Thüring K, Winz ML, Sharma S, Entian KD, Wacheul L, Lafontaine DL, Anderson J, Alfonzo J, Hildebrandt A, Jäschke A, Motorin Y, Helm M. 2015. The reverse transcription signature of N-1-methyladenosine in RNA-Seq is sequence dependent. Nucleic Acids Res 43:9950-64.
54. Torrent M, Chalancon G, de Groot NS, Wuster A, Madan Babu M. 2018. Cells alter their tRNA abundance to selectively regulate protein synthesis during stress conditions. Sci Signal 11.
55. Schwenzer H, Jühling F, Chu A, Pallett LJ, Baumert TF, Maini M, Fassati A. 2019. Oxidative Stress Triggers Selective tRNA Retrograde Transport in Human Cells during the Integrated Stress Response. Cell Rep 26:3416-3428.e5.
56. Li M, Kao E, Gao X, Sandig H, Limmer K, Pavon-Eternod M, Jones TE, Landry S, Pan T, Weitzman MD, David M. 2012. Codon-usage-based inhibition of HIV protein synthesis by human schlafen 11. Nature 491:125-8.
57. Nunes A, Ribeiro DR, Marques M, Santos MAS, Ribeiro D, Soares AR. 2020. Emerging Roles of tRNAs in RNA Virus Infections. Trends Biochem Sci.
58. Clark WC, Evans ME, Dominissini D, Zheng G, Pan T. 2016. tRNA base methylation identification and quantification via high-throughput sequencing. RNA 22:1771-1784.

59. Ryvkin P, Leung YY, Silverman IM, Childress M, Valladares O, Dragomir I, Gregory BD, Wang LS. 2013. HAMR: high-throughput annotation of modified ribonucleotides. RNA 19:1684-92.
60. Ebhardt HA, Tsang HH, Dai DC, Liu Y, Bostan B, Fahlman RP. 2009. Meta-analysis of small RNA-sequencing errors reveals ubiquitous post-transcriptional RNA modifications. Nucleic Acids Res 37:2461-70.
61. Werner S, Schmidt L, Marchand V, Kemmer T, Falschlunger C, Sednev MV, Bec G, Ennifar E, Höbartner C, Micura R, Motorin Y, Hildebrandt A, Helm M. 2020. Machine learning of reverse transcription signatures of variegated polymerases allows mapping and discrimination of methylated purines in limited transcriptomes. Nucleic Acids Res 48:3734-3746.
62. Cozen AE, Quartley E, Holmes AD, Hrabeta-Robinson E, Phizicky EM, Lowe TM. 2015. ARM-seq: AlkB-facilitated RNA methylation sequencing reveals a complex landscape of modified tRNA fragments. Nat Methods 12:879-84.
63. Zheng G, Qin Y, Clark WC, Dai Q, Yi C, He C, Lambowitz AM, Pan T. 2015. Efficient and quantitative high-throughput tRNA sequencing. Nat Methods 12:835-837.
64. Dai Q, Zheng G, Schwartz MH, Clark WC, Pan T. 2017. Selective Enzymatic Demethylation of N(2) ,N(2) -Dimethylguanosine in RNA and Its Application in High-Throughput tRNA Sequencing. Angew Chem Int Ed Engl 56:5017-5020.
65. Wilusz JE. 2015. Removing roadblocks to deep sequencing of modified RNAs. Nat Methods 12:821-2.
66. Marchand V, Pichot F, Thüring K, Ayadi L, Freund I, Dalpke A, Helm M, Motorin Y. 2017. Next-Generation Sequencing-Based RiboMethSeq Protocol for Analysis of tRNA 2'-O-Methylation. Biomolecules 7.
67. Arimbasseri AG, Blewett NH, Iben JR, Lamichhane TN, Cherkasova V, Hafner M, Maraia RJ. 2015. RNA Polymerase III Output Is Functionally Linked to tRNA Dimethyl-G26 Modification. PLoS Genet 11:e1005671.
68. Motorin Y, Helm M. 2019. Methods for RNA Modification Mapping Using Deep Sequencing: Established and New Emerging Technologies. Genes (Basel) 10.
69. Hogue IB, Grover JR, Soheilian F, Nagashima K, Ono A. 2011. Gag induces the coalescence of clustered lipid rafts and tetraspanin-enriched microdomains at HIV-1 assembly sites on the plasma membrane. J Virol 85:9749-66.
70. Inlora J, Chukkapalli V, Bedi S, Ono A. 2016. Molecular Determinants Directing HIV-1 Gag Assembly to Virus-Containing Compartments in Primary Macrophages. J Virol 90:8509-19.
71. Cottrell KA, Djuranovic S. 2016. Urb-RIP - An Adaptable and Efficient Approach for Immunoprecipitation of RNAs and Associated RNAs/Proteins. PLoS One 11:e0167877.
72. Garzia A, Meyer C, Morozov P, Sajek M, Tuschl T. 2017. Optimization of PAR-CLIP for transcriptome-wide identification of binding sites of RNA-binding proteins. Methods 118-119:24-40.

Chapter 4

Discussion

The plasma membrane (PM)-specific localization of HIV-1 Gag is an essential early step in infectious progeny generation. While it is well established that the interaction between the matrix highly basic region (MA-HBR) of Gag and the PM-enriched lipid PI(4,5)P2 is critical for Gag localization to the PM, there is limited evidence supporting the role of RNA in this process. Specifically, whether MA-RNA binding in cells promotes the specific localization of Gag to the PM, and not to intracellular membranes, was not known in the context of HIV-1 Gag. The focus of my study was therefore MA-RNA interactions in cells and their effect on the membrane binding of Gag in cells. The strategy I employed for this purpose is the crosslinking of cellular RNAs to various Gag constructs and then further quantification or sequencing of the Gag-bound RNAs.

In **chapter 2**, I established that a correlation exists between MA-RNA binding in cells and the PM-specific localization of Gag, providing the much-needed cell-based evidence supporting the role of MA-RNA binding in the PM-specific localization of Gag. In **chapter 3**, I focused on MA-tRNA interactions in cells. I investigated both the determinants of MA-tRNA interactions in cells as well as their potential effects on Gag-membrane binding in cells. While these data are preliminary and need to be approached cautiously, it suggests that multiple determinants, including the MA-HBR, the tRNA sequence and structure, and potentially even the tRNA post-transcriptional modifications, promote MA interactions with specific tRNAs in cells. Furthermore, I identified two tRNAs of interest, SeCTCA and PheGAA, which may be modulating Gag-membrane binding in cells. In this chapter, I will discuss the findings from **chapters 2 and 3** as well as the prospective future directions of this work.

Summary of data

(i) Correlation between MA-RNA binding in cells and suppression of Gag binding to intracellular membranes: Our working model of Gag membrane binding is that MA-RNA binding blocks the binding of Gag to intracellular membranes containing acidic lipids such as phosphatidylserine (PS), thereby ensuring the specific recruitment of Gag to the PM due to the interactions of MA with the PM-enriched lipid, PI(4,5)P2. Individual portions of this model were supported by mainly in vitro studies; the competition between RNA and lipids was supported by in vitro studies (1, 2); the contribution of MA in Gag-RNA binding in cells has been established (3, 4); and further, the RNA bound to MA in cells has been shown to inhibit the membrane binding of Gag (3, 4). However, the final piece of the puzzle, whether RNA binding to MA prevented the mislocalization of Gag to intracellular membranes, was not supported directly in the context of HIV-1 Gag. In **chapter 2**, I presented data revealing a strong correlation between MA-RNA binding in cells and prevention of Gag mislocalization (5). I used a mutagenesis-based approach creating a panel of MA-HBR mutants in which Lys25/Lys26 and Lys29/Lys31 were switched from Lys to Arg (25/26KR and 29/31KR) or from Lys to Thr (25/26KT and 29/31KT). While the KR substitutions preserve the overall basic charge of the MA-HBR, the KT mutants reduce the overall basic charge. Using a cell-based PAR-CLIP assay, I determined that both the KT mutants failed to bind RNA via MA efficiently in cells unlike the KR mutants. When I examined the subcellular localization of these mutants, I observed that the KT mutants displayed substantial mislocalization to intracellular membranes while the KR mutants did not exhibit such mislocalization. The 25/26KR mutant was exclusively localized to the PM, which implicated the total MA-HBR positive charge and/or MA-bound RNA in guiding Gag specifically to the PM. Interestingly, the 29/31KR mutant showed predominantly cytosolic distribution, binding to neither the PM nor intracellular membranes. The high positive charge preserved in 29/31KR MA was unable to mediate PM localization despite previous data showing that highly cationic proteins tend to associate specifically with the PM (6). The complete block in membrane binding of 29/31KR was likely due to the

RNA bound through its MA-HBR. When the membrane binding of 29/31KR was enhanced through augmented Gag multimerization, 29/31KR showed increased binding to the PM while binding to intracellular membranes remained blocked. Overall, through these comparisons, I provided cell-based data supporting a model in which MA binding by RNA inhibits the mislocalization of Gag in cells, and in conjunction with PI(4,5)P2, ensures the specific localization of Gag to the PM.

(ii) Role of specific MA-HBR residues in MA-RNA binding in cells: A previous study from our lab suggested that the preservation of the overall MA-HBR basic charge, and not the exact MA-HBR sequence, was sufficient for RNA binding ability of Gag as a Gag mutant with all the MA-HBR residues switched (K→R and R→K) was still sensitive to the RNA-mediated block of Gag binding to PS-containing liposomes (7). However, this had not been tested in cells, nor was the contribution of specific HBR residues tested in this context. In cells, the substitution of MA-HBR residues with neutral threonine had led to a decrease in tRNA populations bound to Gag relative to the total RNA populations bound to Gag (4). However, whether the basic charge or MA-HBR sequence affected the RNA binding ability of MA in cells remained to be determined. In **chapter 2**, I find that, consistent with previous data, disrupting the MA-HBR basic patch by pairwise K→T mutations reduces the RNA bound to Gag to background levels of a Gag mutant in which every basic residue of the MA-HBR is switched to neutral amino acids. Furthermore, I determined that while Lys25/Lys26 could be switched to Arg and still maintain efficient RNA binding by Gag, the presence of Lys at residues Lys29/Lys31 was indispensable for WT-level RNA binding. Thus, the sequence of MA-HBR, and not just overall basic charge, is a determinant of MA-RNA binding in cells. While I compared the amount of RNA-binding to Gag mutants in cells in **chapter 2**, whether the specific MA-HBR residues select for specific RNA species remains to be determined.

(iii) Role of specific MA-HBR residues in Gag-membrane binding: In **chapter 2,** I determined that the 25/26KR mutant showed increased hydrophobic interactions compared to WT Gag, binding neutral PC-liposomes efficiently in a myristate-dependent manner. Thus, Lys25/Lys26 may be involved in the

modulation of myristate exposure, which is consistent with previous data from our lab (1). However, the mechanism by which Lys 25/26 affects myristate exposure remains to be determined. The 25/26KR mutant also showed enhanced virus-like particle release compared to WT Gag, likely due to the increased myristate-mediated hydrophobic interactions. Thus, presence of Arg at residues 25/26 could confer a fitness advantage to the virus. However, the Lys 25/26 residues are highly conserved across various clades of HIV-1 (8). The reason for such a strong conservation of Lys at these residues is not clear, and whether the 25/26KR mutation negatively affects other aspects of the HIV-1 life cycle remains to be tested.

The 29/31KR mutant showed a drastic loss of binding to all cellular membranes and had severely attenuated virus-like particle (VLP) release. The residue Lys31 is also highly conserved, but not Lys29, (8) and I have found that 31KR Gag mutant fully recapitulates the phenotype of 29/31KR Gag mutant in cells. Whether the serial passage of 29/31KR or 31KR mutant in T cells results in the emergence of revertants is of interest, given that Lys31 is also shown to be important as an MA-PI(4,5)P2 interface (1, 5, 9). The mutated residue/s could revert back, which would predict some success for small molecule inhibitors targeting MA-PI(4,5)P2 to prevent HIV-1 assembly and spread. Alternatively, there could be the rise of compensatory mutants, which may reveal some information regarding how MA balances RNA- and PI(4,5)P2-binding to mediate membrane binding. For example, a compensatory mutation could arise that forms an substitute interface for MA-PI(4,5)P2 interaction. Another possibility is a compensatory mutation that could induce MA to lose contact with inhibitory tRNAs. Based on my work presented in **chapter 3** that shows the MA-HBR-dependent selection of an inhibitory tRNA (SeCTCA), I would surmise that the possible compensatory mutation in MA, which would block tRNA binding, could involve the disruption of the MA-HBR. In addition, myristate exposure has been shown to modulate MA-tRNA binding (10), therefore a compensatory mutation which triggers an increase in myristate exposure of Gag can also arise.

(iv) Potential determinants of MA-tRNA interaction in cells: A previous CLIPSeq-based study showed that the MA-bound RNA in cells is tRNA (4). Additionally, tRNA has also been shown to regulate Gag-membrane

binding (3, 4, 10-13). Notably, the CLIPSeq-based study also reported that specific cellular tRNA species were selectively bound to MA compared to other tRNA species. However, there was a reduction in Gag-bound tRNAs when Gag is membrane-bound compared to when Gag is cytosolic (4). Thus, the tRNAs that were identified were likely bound to cytosolic Gag. An in vitro study suggested that there is differential regulation of Gag-membrane binding by different tRNA species (11). This lead to an attractive hypothesis that there are potentially two subsets of tRNA in the cell; one group of tRNAs would be sensitive to removal by PI(4,5)P2 and allow Gag to bind PI(4,5)P2 at the PM, while another group would prevent MA-PI(4,5)P2 interaction and prevent Gag from binding to the PM. Whether the tRNAs reported to be selected on MA in the previous CLIPSeq-based study belonged to a subset of tRNAs that are sensitive or resistant to removal by PI(4,5)P2 could not be determined in the previous study (4).

In **chapter 3**, I compared the total tRNA bound to a non-membrane binding Gag (1GA Gag) with total tRNA bound to a membrane binding-competent Gag (WT Gag) in 293T cells. Similar to the previous study (4), the tRNAs enriched on WT Gag likely represent the tRNAs bound to the cytosolic fraction of WT Gag. I further catalogued the starting tRNA population in 293T cells as well as the tRNAs bound to a Gag mutant in which all the MA-HBR basic residues have been switched to neutral residues. Using this strategy of comparison, I was able to determine that indeed there may be different subsets of tRNAs; one subset is bound to both 1GA Gag and WT Gag, suggesting that this tRNA inhibits Gag-membrane binding and is thus impervious to the effect of PI(4,5)P2, while one subset is found on 1GA Gag but lost on WT Gag, suggesting that this tRNA permits Gag-membrane binding and is thus, susceptible to PI(4,5)P2-mediated removal (Fig 4.1). There is a possibility that the two subsets of tRNAs only appear to respond differently to PI(4,5)P2 as a consequence of the limiting amount of PI(4,5)P2 in the PM, and without that limitation, all tRNAs would be removed. In vitro assays will allow us to address this caveat.

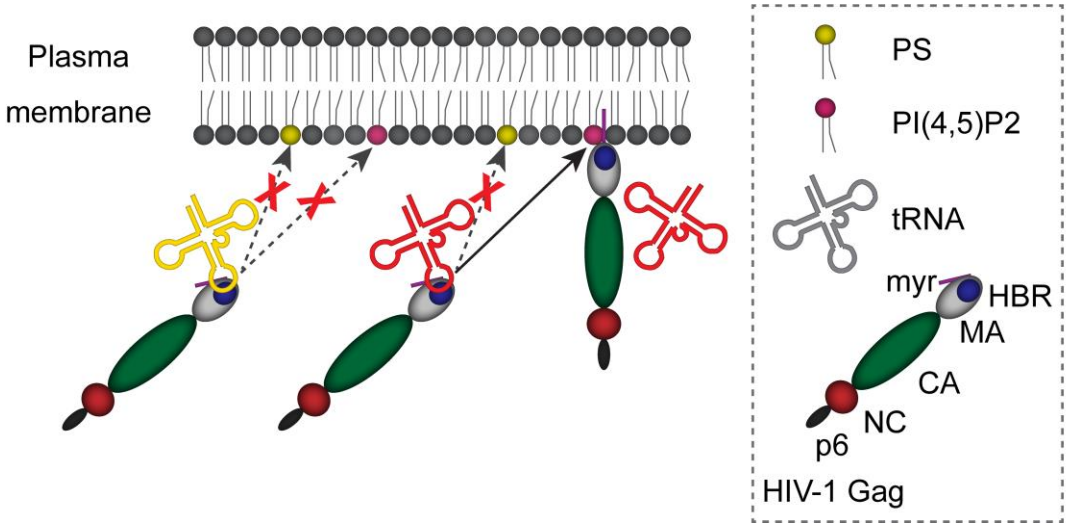

Fig 4.1. Model of PI(4,5)P2-dependent membrane binding of Gag as dictated by the differential regulation by two subsets of tRNAs. The tRNA subset represented by the red tRNA blocks Gag binding to PS-containing membranes but allows binding to PI(4,5)P2-containing PM. The tRNA subset represented by the yellow tRNA is resistant to removal by PI(4,5)P2 and blocks Gag-membrane binding to all membranes, including those containing PI(4,5)P2.

Notably, I was further able to identify two tRNAs, SeCTCA and PheGAA, which may be involved in the regulation of Gag-membrane binding. These two tRNAs have not been previously implicated in the context of Gag-membrane binding and could thus hold a wealth of new information on HIV-1 assembly and even other aspects of HIV-1 life cycle [see **(v)** below]. In addition, the data in **chapter 3** support that factors other than the original abundances of tRNA species in cells could determine the selection of specific tRNAs on MA. I determined that the presence of MA-HBR plays a role in the selection of some, but not all, tRNAs. For example, the selection of GlyGCC, one of the abundant tRNA species identified in both my study as well as the previous CLIPSeq-based study (4), was not dependent on the presence of MA-HBR while the selection of both SeCTCA and PheGAA was MA-HBR-dependent. My work further suggests that the sequence/structure of tRNAs may be an additional determinant for enrichment on MA. Among a pool of isodecoders of PheGAA and AlaAGC, only some select isodecoders displayed an enrichment on MA relative to their starting levels in 293T cells. Preliminary data also suggests that presence or absence of post-transcriptional modifications may form the basis for further discrimination

by MA as the potentially modified transcripts of SeCTCA may be enriched compared to unmodified transcripts relative to their original abundances in cells.

(v) Predicted effects of enriched tRNA on Gag-membrane binding: In **chapter 3,** I identified two tRNAs of interest, SeCTCA and PheGAA, based on their differential binding to the Gag constructs described above. SeCTCA was enriched on both 1GA Gag and WT Gag and did not figure among the tRNAs abundant in 293T cells. This suggested that SeCTCA was selected by MA even though it was among the relatively low abundance tRNAs in the untransfected 293T cells. As mentioned in **chapter 1**, tRNAs are differentially expressed in different tissues and cells (14). tRNAs are transcribed by RNA Polymerase III (RNAPIII). Most tRNAs have type 2 promoter which comprises two internal promoter elements (A and B boxes), however, SeCTCA has type 3 promoter with extensive upstream control regions (a TATA box, a proximal sequence element and a distal sequence element) along with the B box (15-17). In canonical tRNAs, TFIIIC recognizes and binds A and B boxes and recruits TFIIIB, which recruits RNAPIII. For SeCTCA, the transcription factors are SNAPc and a variant of TFIIIB, in which one the subunits of TFIIIB, Brf1, is replaced with another subunit, Brf2. Brf2 is a critical factor for the oxidative stress response of SeCTCA (17). As mentioned before, we could attribute the differential expression of various tRNAs in the different tissues to the variation in the sequence of the promoter regions (18-20).

The relative abundance of SeCTCA on 1GA 6A2T Gag was decreased compared to its relative abundance on 1GA Gag. This suggested that the selection of SeCTCA on MA was dependent on the presence of MA-HBR. Furthermore, due to similar enrichment of SeCTCA on both 1GA MA and WT MA, we can infer that it may be a tRNA that is relatively resistant to removal from MA by PI(4,5)P2. Whether SeCTCA can block Gag membrane binding to the PM remains to be tested. Second tRNA of interest is PheGAA, which was specifically enriched only on 1GA MA. PheGAA on 1GA MA also appears to be enriched compared to its relative abundance in 1GA 6A2T MA, suggesting that PheGAA is also selected in an MA-

HBR-dependent manner. Moreover, given that PheGAA was not enriched on WT MA, one can infer that it may be a tRNA species that can be removed from MA by PI(4,5)P2 and thus allow Gag to bind PM.

Overall, the preliminary PAR-CLIPSeq based data suggests that in cells, MA is bound to select tRNAs, and that upon binding of Gag to the PM, some tRNAs are selectively lost. The physiological significance of this selective binding and selective loss is that potentially, some MA-bound tRNAs in cells may be sensitive to removal by PI(4,5)P2, while other MA-bound tRNAs may be resistant to removal by PI(4,5)P2. This finding advances the model through providing cell-based support for the differential regulation of PI(4,5)P2-dependent membrane binding of Gag by different tRNA species (See Fig 4.1 for the new model).

Implications and Future Directions

In this section, I will discuss implications of the work presented here and future directions.

1**. Near future directions:** The covid-19-related lockdown and shutdown of labs compelled me to base **chapter 3** of my thesis on only one set of experiments. First and foremost, the findings detailed in that chapter need to be confirmed by biological replicates of the PAR-CLIPSeq experiment. Northern blot-based confirmation of the tRNAs of interest can be used as additional supporting data. We will also address a drawback in our current experiments, which is the lack of additional controls of mock-transfected, and non-crosslinked/Gag transfected 293T cells. As detailed before in **chapter 3**, the tRNA population could potentially be altered upon various cellular stresses including transfection of Gag (21, 22). There is a possibility that upon cell manipulation/stress, such as transfection, the native tRNA population changes (21-23). If the control experiments show that there is an upregulation of the tRNAs that we have identified as being selected on MA, then I would infer that the MA is simply binding the abundant cellular tRNAs. This would suggest that potentially there is no specific selection of these tRNAs by MA. On the other hand, if these control conditions show that there is no change in the tRNA landscape,

then such findings would suggest that potentially MA is selecting for specific tRNAs, perhaps based on certain tRNA characteristics. Not only the abundance of tRNA species but their post-transcriptional modifications may change upon cellular stress and translational status (24-31). If the control experiments show that instead of an upregulation of the tRNA species, there is an increase/or alteration of the modification status, and we observe that these modified tRNAs are the ones we find selected on MA, then it would suggest that potentially the modifications are not playing any role in the selection process, and are selected just on the basis of cellular abundance. On the other hand, if the control conditions do not induce any change in modification status, then the role of modifications in selection of specific tRNAs on MA is better supported. In vitro based binding assays can be used for confirmation.

2. Do SeCTCA and PheGAA impact binding of Gag to model membranes? To test our prediction that SeCTCA blocks the membrane binding of Gag irrespective of the presence of PI(4,5)P2 in the membrane, we can use in vitro addback assays (see Discussion section in **chapter 3**). In brief, in vitro transcribed and translated Gag will be treated with RNase and then incubated with PC+PS liposomes with or without PI(4,5)P2 in the presence of in vitro transcribed SeCTCA. If our prediction is true, we would expect SeCTCA to inhibit Gag from binding liposomes irrespective of the presence of PI(4,5)P2, suggesting that even PI(4,5)P2 is unable to overcome the block imposed by SeCTCA. We can extend this experiment to determine potential regions of SeCTCA, which may be mediating its binding to MA. SeCTCA possesses a truly unique structure compared to the canonical tRNAs (Fig 4.2).

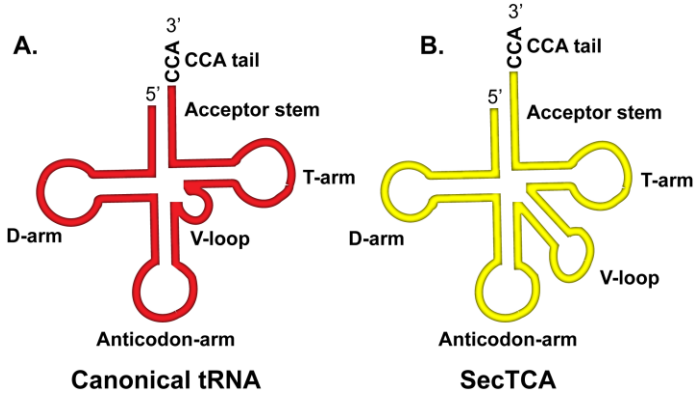

Fig 4.2. Cartoon comparing the canonical tRNA secondary structure with that of SeCTCA. (A.) Schematic illustration of the generic tRNA cloverleaf secondary structure. The acceptor stem bearing the 3' CCA tail, the D-arm, the T-arm, the V-loop and the anticodon arm are depicted. (B.) Schematic illustration of the non-canonical SeCTCA structure. SeCTCA has an extended V-loop, an extended acceptor stem, shorter D-loop and longer D-stem, and shorter T-stem compared to the canonical tRNA structure.

SeCTCA is a type II tRNA, with extended V-loop region (15, 16). Other type II tRNAs in eukaryotes are tRNASer and tRNALeu. SeCTCA contains the longest V-loop (16 nt folded in a stemloop) of the three, making it the longest tRNA (90nt) (15, 32). I speculate that the extended SeCTCA V-loop may be influencing the binding of SeCTCA to MA by virtue of increased charge due to increased RNA length and therefore tighter affinity for Gag compared to PI(4,5)P2. As RNA binding apparently modulates myristate exposure (1), the potentially tighter binding of the V-loop could additionally interfere with myristate exposure and inhibit Gag-membrane binding through that mechanism. Whether or not SeCTCA's V-loop negatively impacts Gag-membrane binding can be tested by using mutant SeCTCA with either the V-loop deleted or substituted with the V-loop from other type II tRNAs in the addback assays as mentioned above and seeing if such a mutant SeCTCA retains the ability to suppress Gag-PI(4,5)P2 binding. Of interest, I have identified another type II tRNA, SerACT, as being enriched on 1GA Gag relative to WT Gag, suggesting that this tRNA, similar to PheGAA, may be one of the tRNAs that are lost from Gag upon Gag-membrane binding (Fig 4.1). The V-loop of SerACT may be a potential candidate for replacing the V-loop of SeCTCA with (and vice versa) to see if the length of the V-loop has any impact on the sensitivity of tRNAs to removal by PI(4,5)P2 in addback assays. SeCTCA further has a unique D-arm compared to canonical tRNAs. The loop is smaller (4nt) and the stem is longer (6bp) than for other tRNAs (loop 6nt, stem 4bp). In addition, there are further divergences from the canonical tRNAs with a longer acceptor stem (9 bp vs 7 bp) and a shorter T stem (4 bp vs 5 bp) compared to canonical tRNAs (32-34). As described above, deletion or substitution of SeCTCA D-arm or T-arm could help determine the impact, if any, of these SeCTCA regions on Gag-PI(4,5)P2 interactions using the addback assays.

In a similar vein, we will also test whether PheGAA and SerACT are susceptible to removal from MA by PI(4,5)P2 using the addback assays. If our prediction is true, then these tRNAs would inhibit binding of Gag to PC+PS liposomes but fail to inhibit the binding of Gag to the PI(4,5)P2-containing liposomes.

3. Do SeCTCA and PheGAA impact Gag membrane binding in cells? In order to validate the functional importance of the enriched SeCTCA, overexpression or depletion of SeCTCA in cells can be carried out to reveal if SeCTCA plays a role in HIV-1 life cycle. Transfection of cells with plasmid expressing TRNAU1 has been shown to increase levels of SeCTCA in cells (15). Supplementation of the cell growth media with selenocysteine (SeC) has also been shown to increase the levels of SeCTCA by ~20% (15, 35). Although this is a modest increase, we can try to optimize the amount of SeC added to the media and correlate it with the increase in cellular SeCTCA, which we can detect and compare using northern blotting. Given that there is only one gene for SeCTCA (TRNAU1), we can suppress SeCTCA production by just targeting the single TRNAU1 gene. The complete knockout of SeCTCA in mice proved to be lethal (36), thus it is may potentially have deleterious effects in human cell lines as well. A recent paper used the clustered regularly interspaced short palindromic repeats (CRISPR) genome editing in order to target TRNAU1 (15). CRISPR consists of bacterial derived nuclease CRISPR-associated protein 9 (Cas9) along with a single-guide RNA (sgRNA) which is complementary to the gene of interest. Guided to the target gene by sgRNA, Cas9 induces a double-stranded DNA break which upon repair, alters the target gene with insertion or deletion of several nucleotides. The sgRNA employed in the study was designed to bind the acceptor stem at the 3' end. Nucleotide insertion or deletion at the target region could potentially disrupt the B box or the termination site and interfere with SeCTCA transcription. Use of this CRISPR-Cas9 strategy lead to a decrease in SeCTCA levels by ~50% in HEK293 cells (15). Additionally, the post-transcriptional modifications at the adjoining T-arm could be disrupted due to the preference of the modification enzymes for particular structure of the T-arm (15, 37), which could potentially also reduce the binding of SeCTCA to Gag (see **chapter 3**).

The levels of SeCTCA in cells upon overexpression or reduction can be determined by northern blot or RT-qPCR. Ultimately, we can test whether conditions inducing overexpression or reduction of SeCTCA in cells affect localization of Gag to the PM as well as Gag VLP release. As per the preliminary data presented in **chapter 3,** we would predict that overexpression of SeCTCA would increase the cytosolic distribution of Gag and inhibit VLP release, while reduction of SeCTCA will enhance PM localization of Gag and increase the VLP release. In the background of SeCTCA depletion, rescue experiment with overexpression of TRNAU1 led to the restoration of SeCTCA expression and the recovery of WT-level selenoprotein expression in the cells (15). Overexpression of a modified TRNAU1 gene in which the site of modification has been eliminated (38) can also be additionally used to determine the role of specific SeCTCA modifications on MA-SeCTCA interaction. Thus, overexpression of WT SeCTCA will potentially inhibit localization of Gag to the PM, while overexpression of mutant SeCTCA lacking site of modification may have less inhibitory effects on Gag localization [see **(5)** below]. This strategy of overexpressing TRNAU1 and a mutant version can be utilized to also test the importance of the V-loop on Gag-SeCTCA binding and the role of V-loop in the potential inhibition of Gag by SeCTCA. Of course, the magnitude of the effect the manipulation of a single tRNA species level in the cell will have on Gag assembly and release remains to be seen.

As detailed in **chapter 1** and mentioned in **chapter 2**, the expression of 5ptase IV depletes PI(4,5)P2 from the PM (39) and causes the loss of Gag-PM binding **(5, 40-47)**. To test the prediction that Gag membrane binding potentially removes PheGAA, we could sequence tRNAs bound to Gag co-expressed with either full-length 5ptase IV (FL 5ptase IV) or a catalytically inactive version (Δ1 5ptase IV). In case of FL 5ptase IV-expressing cells, PheGAA would be similarly enriched on both 1GA Gag and WT Gag, as both will be present in the cytosolic fraction and there will be no PI(4,5)P2 at the PM to remove PheGAA. In contrast, in the case of Δ1 5ptase IV-expressing cells, PheGAA will be enriched on 1GA Gag

compared to WT Gag (similar to what we observed in the experiments carried out in the absence of 5ptase IV expression as described in **chapter 3**).

A slightly less straightforward approach can be adopted to determine if SeCTCA is a tRNA that is not removed upon membrane binding. In **chapter 2**, a strong dimerizing motif LZ was utilized to enhance the membrane binding of Gag through augmented multimerization as tested for PM-localizing WT Gag, mislocalized 29/31KT Gag, and the cytosolic 29/31KR Gag mutant. Introduction of the LZ motif seemed to tip the balance between Gag-RNA and Gag-PI(4,5)P2 binding in the favor of PI(4,5)P2 and lead to the PI(4,5)P2-dependent PM-specific localization of 29/31KRGagLZ, but did not change the localization of the other two Gag derivatives.

One possible reason for the inability of the 29/31KR mutant to bind any membranes as observed in **chapter 2** may be because this mutant binds tRNAs that are resistant to removal by PI(4,5)P2. As we are predicting SeCTCA to be one such tRNA, we can determine if SeCTCA is enriched on 29/31KR Gag but not 29/31KRGagLZ. It would also be interesting to identify tRNAs which show differential enrichment on WT Gag vs 29/31KR Gag and what characteristics of those tRNAs could explain the differences in membrane binding phenotype between WT Gag and 29/31KR Gag. WT GagLZ shows less hazy cytosolic signal compared to WT Gag (unpublished observation), suggesting an enhanced binding to the PM compared to WT Gag. Thus, tRNAs which block the binding of Gag to the PM, may not be able to do the same for GagLZ. The enrichment of SeCTCA on WT Gag could therefore be potentially higher than on GagLZ and SeCTCA could bind with higher affinity to Gag than GagLZ. Such experiments would improve our understanding of the importance of MA-HBR sequence in tRNA selection as well as inform the development of RNA aptamers as antiviral therapy [see **(11)** below].

Additionally, in vitro studies indicate that the presence of NC enhances the binding of tRNA on MA (11). Therefore, it may be useful to also determine whether the presence of the NC domain changes the selection of specific tRNAs on MA or alters the MA-tRNA site of interaction [see **(7)** below].

4. Alternative roles of SeCTCA in HIV-1 life cycle? Selenocysteine (SeC) is famous as the 21st amino acid. It is an analogue of cysteine (Cys) in which selenium is substituted in the place of the sulphur of Cys. Proteins that incorporate at least one SeC are known as selenoproteins. SeC is introduced in selenoproteins by SeCTCA in response to the opal suppressor (UGA) codon in a process dependent on a cis-acting SeC Insertion Sequence (SECIS) element found in the 3' untranslated region of all eukaryotic selenoprotein mRNAs. Even though there are only 25 selenoproteins in humans, these proteins are indispensable for life being involved in oxidoreductase functions (16, 32, 33). Reactive oxygen species (ROS) such as hydrogen peroxide (H2O2) and superoxide anion ($O2^-$) are known to be generated during various viral infections, including HIV and HTLV. HIV infection is marked by pronounced oxidative stress; there is a reduction in antioxidants including gluthathione peroxidase and an increase in ROS production (48, 49). Glutathione peroxidase (GPx1) is the most abundant selenoprotein in mammals as well as a key antioxidant enzyme. Gpx1 protects cells from H2O2-mediated oxidative damage by catalyzing glutathione (GSH)-dependent reduction of H2O2 to water (16). The increased ROS production during HIV infection could be a consequence of the host inflammatory process and/or may be induced by the virus. Several viral proteins have been implicated in the increased generation of ROS including the viral protein Tat (49). A previous study reported a decrease in major selenoproteins including GPx1 in HIV-1 infected and Tat-treated T cells, suggesting that HIV-1 may be regulating the levels of selenoproteins (50). Furthermore, ROS were found to stimulate HIV replication with in vitro data suggesting that oxidative stress activates nuclear transcription factor (NF-kB), which is necessary for HIV replication (48, 49). Given that SeCTCA is highly enriched on Gag (both 1GA and WT MA), it is very tempting for me to speculate that Gag may be sequestering SeCTCA and inhibiting the production of selenoproteins to gain a replication advantage.

Alternatively, SeCTCA may be a cellular defense mechanism in response to HIV-1 infection, with the cell upregulating SeCTCA or changing SeCTCA modifications, to bind Gag and suppress Gag-membrane binding, thereby reducing the formation of virus particles. A microarray-based analysis found an upregulation of multiple tRNA species, including SeCTCA, upon HIV-1 transfection in SLFN11-knockdown cells, but not in the presence of SLFN11 (23). It is conceivable that HIV-1 could be altering tRNA composition in cells lacking SLFN11 such as 293T cells [the cell type used in the current study (**chapter 3**)]. In addition, SeCTCA was shown to be affected specifically by cellular stress triggered by treatment of cells with H2O2 with the cleavage and retrograde transport of SeCTCA into the nucleus (22). A previous CLIP-Seq-based assay did not identify SeCTCA as one of the MA enriched tRNAs (4). One experimental difference between the previous study (4) and this current study is that we carried out the experiments with the expression of only the Gag and Rev proteins, while they used proviral clones. Thus, I can speculate that increased ROS production triggered by HIV-1 Tat (or other HIV-1 proteins) could either mislocalize or alter SeCTCA such that it is unable to bind Gag. Alternatively, HIV-1-triggered increased ROS could redirect SeCTCA pools to the generation of more selenoproteins, and thus, SeCTCA would not be available to bind and suppress Gag-membrane binding. In any case, it would be interesting to determine the tRNA population in 293T cells and whether SeCTCA is enriched on MA in the context of the proviral clone. Apart from regulation of Gag-membrane binding, we can also determine whether manipulating SeCTCA levels (see **(3)** above) and, consequently selenoprotein levels in cells, impacts HIV-1 replication.

5. Potential importance of tRNA modifications in HIV-1 life cycle: Modifications of tRNAs may potentially be involved in several steps of HIV life cycle.

i. Modification induced structural stability of tRNA could affect MA-tRNA binding: As described before in **chapter 1**, posttranscriptional modification of tRNA is a dynamic process that can be affected by many cellular conditions including oxidative stress (24-31). In addition, tRNA modifications modulate tRNA stability (28, 29, 51-55) and could therefore affect its interaction with MA in the cells. Indeed, preliminary

data presented in **chapter 3** suggests that tRNA modifications could be a determinant for selection of specific tRNAs, such as SeCTCA, on MA.

ii. tRNA modifications could affect HIV-1 translation: Certain tRNA anticodon arm modifications can also affect the translational efficiency of tRNAs through modulating codon recognition, blocking of programmed ribosomal frameshifting (PRF), and stabilizing codon-anticodon interaction. Position 34 (wobble position) and/or 37 (located 3' of the anticodon) are commonly modified in most tRNAs. A-ending codons are enriched in HIV-1 genome unlike in the human genome (31, 56, 57). Anticodon modification has been proposed to affect the translation of proteins of some viruses (31), it may be a possibility for HIV-1 as well.

A unique wybutosine (yW) modification at position 37 (yW37) has been reported exclusively for PheGAA (which I have also identified as a tRNA of interest for Gag membrane binding in **chapter 3**). yW37 stabilizes the anticodon loop and prevents -1 PRF (26, 29). As described previously in **chapter 1**, HIV-1 employs -1 PRF for translation of the Gag-Pol fusion protein, which is critical for HIV-1 replication. The slippery site encodes Phe (UUU) and Leu (UUA) in the 0 frame and two Phe (UUU) in the -1 frame (58-60). Thus, whether PheGAA (which decodes UUU) has yw37 modification could potentially affect HIV-1 -1PRF. Whether or not any modifications subject to modulation by HIV-1 infection additionally alter the Gag:Gag-Pol ratio would also be important.

iii. tRNA modifications could affect RT fidelity: Previously, the m1A58 in tRNALys3 (HIV-1 RT primer) was shown to have an important role in HIV-1 replication (see **chapter 1**) (61). N6-threonylcarbamoyladenosine (t6A) and 2-methylthio-N6-threonylcarbamoyladenosine (ms2t6A) modifications at position 37 (t6A37 and ms2t6A37) of tRNALys3 have been suggested to promote tRNA binding to the ribosome and prevent frameshifting (29, 62). Interestingly, the bulky ms2t6A37 hypermodification is also a strong stop for RT (~stopped 98% of the time) while the m1A58 is not as

effective as a stop signal (61, 62). In fact HIV-1 RT can copy as far as ms2t6A37 of the Lys3 (61). Thus, particular tRNA modifications could be affecting the RT fidelity.

Overall, the modification status of tRNAs may be of great biological significance in HIV-1 life cycle. It would be therefore interesting to determine not just the relative abundances of tRNAs but also their modification status during HIV-1 infection. Previously, HIV-1 transfection has been shown to alter the total cellular RNA modifications but the modification status for individual RNA species was not determined (63). The approach I applied in **chapter 3** was the inference of tRNA modifications based on enrichment of RT-signatures (sequence variants) in the transcripts. I was able to determine whether the presence of certain modifications is associated with the selection of the transcripts on MA. This same protocol can be used as a high throughput method to determine modification status of all tRNAs in the cells in case of HIV-1 infection.

However, as detailed in **chapter 3**, the determination of tRNA modifications via sequencing is an indirect method. A caveat of this method is the possibility of false positives and false negatives (see **chapter 3**). Therefore, the direct method of liquid chromatography–tandem mass spectrometry (LC-MS/MS) can be adopted to confirm/determine the modification status of specific tRNAs of interest detected in our studies, and further used to get a complete picture of the modification status of such important tRNAs (31, 64).

6. How does PI(4,5)P2 outcompete the negative regulation of tRNA during Gag-membrane binding? As per our working model, MA-PI(4,5)P2 interactions lead to the removal of susceptible tRNA from MA and consequently remove the membrane binding block imposed by tRNA.

The relative binding affinities of MA to tRNAs and PI(4,5)P2 could dictate the susceptibility or resistance of the tRNA to removal by PI(4,5)P2. There could be multiple factors that affect the MA-tRNA and MA-PI(4,5)P2 binding affinities.

i. Potential factors affecting the binding affinity of MA to tRNA: The affinity of myristoylated MA to tRNA is weakened under conditions that force myristate exposure relative to when the myristoyl moiety is sequestered (10). Thus, factors that promote the exposure of myristate, such as multimerization of Gag (65) driven by dimerizing domains (CA and NC) downstream of MA, can diminish the affinity of MA to tRNA. In contrast, Mg^{2+} ions have a stabilizing effect on tRNA structure (30) and have been shown to promote MA-tRNA binding (10). Posttranscriptional modifications of tRNA are also important determinants of tRNA stability (28, 29, 51-55). The preliminary data presented in **chapter 3** suggests that tRNA modifications may influence selection of certain tRNAs on MA. Thus, the dynamic tRNA modifications could potentially enhance the binding affinity of MA to tRNA. Finally, the differences in tRNA sequence and length could contribute to the MA-tRNA affinity, perhaps through influencing the tRNA structure. Overall, a combination between these various factors will determine the affinity of MA to different tRNAs and influence the susceptibility or resistance of these tRNAs to PI(4,5)P2-mediated removal.

ii. Potential factors affecting the binding affinity of MA to PI(4,5)P2: The affinity of MA to PI(4,5)P2 can be augmented by the inclusion of PS or cholesterol in the PI(4,5)P2-containing membranes (66), artificial trimerization of MA (67), and presence of myristoyl moiety on MA (66). Consistent with these data, multimerization of Gag, which has been shown to promote myristate exposure (65), also increases the membrane binding of MA (5, 12). Therefore, multiple factors can enhance the affinity of MA to PI(4,5)P2 including presence of other lipids, myristoyl exposure, and the multimerization status of Gag and thus, influence the sensitivity of tRNAs to PI(4,5)P2-mediated removal from MA.

Till date, there has been no side-by-side comparison of MA binding affinity to tRNA or membranes using the same method and the same experimental set-up. A side-by-side comparison may be important, since differences in experimental conditions such as the effect of ions on tRNA or PI(4,5)P2 (**see chapters 1 and 3**) can affect the binding affinity values. Further, given the potential role of CA and NC in modulating

the affinity of MA to tRNA and PI(4,5)P2, it would be important to test how the presence of such domains affects both MA-tRNA and MA-PI(4,5)P2 interactions. As the binding affinities will be determined with in vitro transcribed tRNAs, it could also be possible to generate the tRNAs using modified nucleotides which will allow us to determine the impact of tRNA modification on MA-tRNA binding affinity.

A possible method to carry out a side-by-side comparison can be through nanodiscs (ND), which have been recently used to determine the affinity of MA and artificially trimerized MA to PI(4,5)P2-containing nanodiscs (67). An ND is a phospholipid bilayer circled and stabilized by a belt made of two molecules of a membrane scaffold protein (MSP). Affinity of MA bound to specific tRNAs can be determined on PC+PS NDs with and without PI(4,5)P2 using Surface Plasmon Resonance (SPR) (68, 69). Constructs with MA downstream dimerizing domains, CA and NC, could help promote myristate exposure (65); however, these could also potentially cause the irreversible nanodisc aggregations. In addition, as mentioned before ions including Mg^{2+} ions stabilize tRNA structure and have been shown to promote MA-tRNA binding (10). However, these can cause PI(4,5)P2-containing NDs to aggregate (70). Thus, the side-by-side comparison of MA binding affinity to tRNA as well as PI(4,5)P2 under same experimental conditions may prove to be technically challenging.

7. Sites of interactions between tRNA and MA: The determination of binding sites between MA and the select tRNAs can reveal the mechanism of tRNA selection by MA. In addition, it can also inform the generation of RNA aptamers against MA. One way of determining the sites of MA-tRNA binding is to utilize in vitro binding assays using tRNAs with deleted or substituted arms in the addback assay which would inform which tRNA arm may be involved in the MA-tRNA interactions [see **(2)** above]. However, the identity of the site of interaction is inferred by the magnitude of the effect of mutations on Gag-membrane binding, and not directly determined. For a direct approach, one can determine the binding affinity of MA (with and without downstream multimerizing domains) to mutant tRNAs to determine if mutation of a particular site disrupts MA-tRNA interactions. One disadvantage of both these assays is that they use in

vitro transcribed tRNAs that lack modifications, given that modifications could influence MA-tRNA binding [see **(5)** above and **chapter 3**]. Additionally, we cannot be sure if tRNA mutants fold properly.

An in-silico method of determining sites of interaction between tRNA and MA can be through molecular docking calculations of solved structures of tRNA on MA in multiple positions and determining the most energetically favorable position (71). These can be followed by Molecular Dynamic (MD) simulation to confirm the binding interfaces (72). One advantage of MD simulation can be the simulation of stabilizing modifications in the tRNA molecules, which can potentially allow us to also determine more physiologic interactions similar to what is observed in cells or determine the impact of modifications on MA-tRNA interactions. Furthermore, MD simulations could potentially be used to probe MA, tRNAs and PI(4,5)P2 interactions together in the same system [see **(6)** above]. However, MD simulation studies are not without challenges (73, 74). One important challenge is the availability of an accurate experimental structure of the molecules to be ensembled. For example, while a crystal structure for human SeCTCA exists (PDB 3A3A), there is not a solved structure that I could find for human PheGAA. Additionally, while the idea of testing MA, tRNA and PI(4,5)P2-containing membrane is attractive, there is a lack of a solved structure of MA bound to PI(4,5)P2-containing membrane. Such a structure could indeed be generated using cryo-EM with MA (with and without CA and NC) and PI(4,5)P2-NDs; however, the process of generating such a structure can be a challenge in itself [see **(6)** above]. Thus, the feasibility of the simulation studies is contingent on the availability of experimental structures (73, 74). In addition, there is a requirement of specialized computing hardware and considerable time for the simulation experiments. Finally, the simulation results will need to be validated with follow-up experiments, and thus, the design of the simulation experiments will be influenced by the feasibility of such experiments.

PAR-CLIPSeq can also be used to determine sites of MA-tRNA interaction by analyzing the increased thymidine-to-cytidine (T→C) mismatches that are the signature of sites of crosslinking between 4-SU containing RNA and the protein of interest (75). When the RT encounters the crosslinked nucleotide,

it misincorporates a guanosine into the cDNA, which is converted to cytidine post-PCR amplification. This specific nucleotide change at the site of crosslinking may be due to altered base pairing preferences or residual oligopeptide after proteolysis at the crosslinked nucleotide (75, 76). The fractions of sequence reads with T→C changes were reportedly increased from background 10-20% (non-UV-irradiated) to 50-80% upon crosslinking (75, 76). While these rates of conversion are variable, comparison with rates of T→C conversion in non-crosslinked samples can serve as a negative control. One advantage of such a method is that it is high throughput and we will get an idea of the sites of crosslinking for multiple MA-tRNA pairs. Additionally, the site of binding detected by such a cell-based assay would be most representative of the physiological site of interaction as captured in cells under physiological ion conditions, the contribution of tRNA modifications to the binding, and even, the presence of potential binding partners. There can be potential challenges to the identification of binding sites between MA-tRNA based on PAR-CLIPSeq and the T→C signature. First, the generation of the T→C signature will be dependent on the efficiency of 4-SU incorporation in the tRNA, the efficiency of the UV crosslinking, the efficiency of proteinase K treatment to remove the protein, and even the RT used for generating the cDNA (75-78). Next, the actual site of interaction on the tRNA may not have any uridines or potential sites for 4-SU incorporation. To address this potential problem, another photoactivatable ribonucleoside analogue, 6-thioguanosine (6SG), that generates characteristic G→A signatures at the sites of crosslinking (75) can be used in side-by-side experiments. Another potential scenario can be the inaccurate determination of a potential MA-tRNA binding site that arises when a 4-SU/6SG containing region of tRNA, which is not part of the MA-tRNA interface, gets crosslinked to MA owing to the fluctuation of molecules. However, we can potentially reach a consensus for sites of MA-tRNA interactions by examining multiple sequences and predicted sites of crosslinking.

8. Follow up experiments in physiologically relevant T cells: While the experiments described in **chapters 2 and 3** were conducted in HeLa cells and 293T cells, it would be important to gauge the relevance of these findings in the native host T cells.

As described previously, the localization phenotype of Gag and Gag mutants is likely dependent on the tRNAs that are bound to MA in the cells as well as the PI(4,5)P2 present in the PM. It has been previously shown that even in T cells, Gag localization and release are PI(4,5)P2-dependent (43). However, the decrease in release of VLP on FL 5ptase IV co-expression was smaller than what is observed in HeLa cells (43). The tRNA expression is also shown to be different in different cells and tissues (18, 19). Therefore, there is a possibility that due to potential differences in T cell and HeLa cell PI(4,5)P2 and tRNA population, the localization of the 25/26KR Gag and 29/31KR Gag mutants will be different in T cells than in HeLa cells. Thus, it would be important to repeat the subcellular localization and VLP release experiments in T cells like we have done in HeLa cell in **chapter 2**. If the phenotypes are confirmed, then we can follow up with more experiments to look at the structure function relationship of the mutants in T cells or T cell-derived indicator cell lines.

As described previously, the 29/31KR Gag mutant exhibited a loss of all membrane binding and was distributed mainly in the cytosol, likely due to an imbalance between tRNA- and PI(4,5)P2-binding of Gag. In order to determine the structure-function relationship of the Lys29/Lys31 residues in $CD4^{+}$T cell lines, we can utilize the T-lymphoblastic lymphoma-derived indicator cell line, Sup-GGR (Gaussia GFP Reporter). Sup-GGR expresses the HIV-1 receptor CD4, and the co-receptors CCR5 and CXCR4. Sup-GGR also expresses humanized Renilla GFP (hrGFP) and Gaussia luciferase (GLuc) upon HIV infection in a Tat/Rev-dependent manner (79). The GLuc is secreted into the cell supernatant which can be harvested for reporter readout. The GFP-expression can be used for visualization of the infected cells and also, quantification of infected cells by flow cytometry (79). An advantage of this cell line is the ability to test at multiple timepoints without having to lyse the cells.

We can transfect or electroporate T cells with the HIV-1 molecular clone pNL4-3 WT or pNL4-3-derived 29/31KR mutant (7, 9). The T cells can then be co-plated with the indicator cell line, Sup-GGR (79). If revertants or compensatory mutations arise in case of the 29/31KR that allow for this mutant Gag to bind the PM, form and release infectious virus particles, we will be able to visually detect the infected GFP-expressing indicator cells. We can measure the luciferase activity as a read out for Tat/Rev-activity and prepare DNA from the sorted GFP-positive cells at the peak of replication. Additionally, we can test the levels of viral CA protein (p24) released in the media by p24 ELISA. Sequencing of the viral genomes will allow us to detect the compensatory mutations (43, 79). The findings will be validated using in vitro and cell-based assays looking at the subcellular localization, VLP release, infectivity, and liposome binding of the revertants.

As detailed above in the summary section, 25/26KR Gag exhibited increased VLP release compared to WT Gag, suggesting that this mutant could have a fitness advantage over WT Gag. Notably, Lys, and not Arg, is highly conserved at MA-HBR residues 25 and 26 across various clades of HIV-1 (8). As a first step to determining whether the 25/26KR mutation has detrimental effects on other aspects of HIV-1 life cycle, we can determine the Env incorporation as well as the infectivity of 293T-derived viruses bearing WT vs 25/26KR Gag. Env incorporation can be determined as described previously (9, 80). Infectivity of this 25/26KR mutant can also be determined using an indicator cell line such as Sup-GGR or TZM-Bl (79, 81, 82).

In **chapter 3**, I used PAR-CLIPSeq assay in 293T cells to determine tRNA binding partners of MA that potentially regulate Gag-membrane binding. How about in T cells? Are the tRNA species enriched on MA in 293T cells representative of the MA-binding population in the physiologically relevant T cells? Ideally, we would carry out PAR-CLIPSeq analysis using T cells infected with VSV-G pseudotyped HIV-1 with the different Gag derivatives. One consideration is that 293T cells have high expression of Gag which is necessary for PAR-CLIP assay. Such high Gag expression may not be possible in T cells or would require

an inordinately large starting T cell population. Given this practical concern, we could use T cell derived tRNA for crosslinking experiments using in vitro transcribed Gag-GFP derivatives. T cells would be cultured in media containing 4-SU so that the 4-SU is incorporated into nascent RNA in the cells. The in vitro transcribed Gag-GFP would be treated with RNase to remove any RNA bound to Gag. The RNase-treated Gag would be incubated with T cell lysates (containing the 4-SU-containing RNA) and then, subjected to UV crosslinking. As described in **chapter 3**, the Gag-GFP would be incubated with GFP-Trap magnetic agarose beads to capture Gag and Gag-bound RNA following which rest of the PAR-CLIPSeq protocol can be carried out as usual. While this experimental process will doubtless require some optimization, it would be a potential way to test whether the tRNAs of interest that regulate Gag membrane binding in 293T cells also regulate Gag-membrane binding in T cells.

9. Does tRNA also serve as a chaperone for the PM-specific localization of cellular proteins?

Previously it was suggested that electrostatic interactions between strongly cationic proteins, such as K-Ras, and the strong negative charge-carrying PM were responsible for the specific PM-localization of such proteins (6). I have shown in **chapter 2** that merely possessing a large basic patch is not sufficient for binding to the PM. It is a possibility that the interaction between the large basic patch and cellular membranes is generally regulated by cellular RNAs. In case of HIV-1 Gag, MA-HBR-bound tRNAs regulate the specific localization of Gag to the PM (see **chapters 2 and 3**). Whether or not tRNA also plays a role in regulating membrane binding of cellular proteins, which localize specifically to select cellular compartments, would be interesting to determine. Thus, we are interested in determining whether tRNAs could be a universal regulator of protein-membrane interaction in cells.

Using a machine-learning method, a study identified 37 mammalian proteins that potentially bind tRNAs based on that protein's binding potential for tRNA structure. Nine of the 37 proteins were also validated experimentally (83). These potential tRNA-binding proteins could be good candidates for initial

membrane binding experiments. These include membrane binding protein Sar1, a small GTP binding protein that is involved in Coat Protein Complex II (COPII)-mediated membrane trafficking of other proteins (83). Interestingly, Sar1 (Sar1b) was also identified as a PI(4,5)P2-interacting protein in a mass spectroscopy-based detection of cytosolic proteins captured on phosphatidylinositol phosphate-conjugated beads or liposomes (84).

In an effort to identify cellular proteins whose membrane binding may be regulated by cellular RNA and PI(4,5)P2, a previous graduate student in the lab carried out a proteomics screen. This preliminary study was designed to identify proteins present in HeLa cell cytosol that successfully bound PC+PS liposomes only upon RNase treatment, suggesting these proteins are under negative regulation by RNA. Samples also include cellular proteins that show efficient binding to PI(4,5)P2-containing liposomes, suggesting that these proteins show PI(4,5)P2-dependent membrane binding. In order to capture those cellular proteins who may already be bound at the PM through efficient PI(4,5)P2 interaction, proteins were also collected from the cytosol of FL 5ptase IV-expressing HeLa cells (while the other samples were collected from Δ1 5ptase IV-expressing HeLa cells). FL 5ptase IV expression would deplete PI(4,5)P2 from the PM which would force the PI(4,5)P2-interacting cellular proteins to remain in the cytosol. Thus, proteins that show an increase in PC+PS binding upon RNase treatment bind PI(4,5)P2 liposomes efficiently (either with or without FL 5ptase IV binding) can be candidates to pursue. Upon mining the data from this screen, I found Sar1a to be a protein that shows increased binding to PC+PS liposomes upon RNase treatment. While Sar1a was not enriched on PI(4,5)P2-liposomes in case of Δ1 5ptase IV-expressing cells, it was enriched in case of FL 5ptase IV expressing cells. Additionally, while Sar1 is not myristoylated (unlike Gag), it interacts with membranes using basic residues (85). Thus, Sar1 [Sar1A and Sar1B proteins are 90% identical (86)] could be a potentially interesting candidate to examine for PI(4,5)P2 and tRNA mediated regulation, although it is not known whether Sar1 interacts with the PM and for what function. Additionally, minor populations of PI(4,5)P2 are present in intracellular compartments including ER and

Golgi complex (87), and perhaps, tRNA regulates the interaction of Sar1 with the PI(4,5)P2 contained in these compartments or prevents localization of Sar1 to certain other cellular compartments. In any case, data mining from the 2 studies (83, 84) and 1 preliminary experiment mentioned above could reveal other cellular proteins potentially under the opposing regulation by tRNA and PI(4,5)P2 in mediating localization to a specific membrane compartment. After identification of candidate proteins, initials tests probing the potential role of cell-derived tRNA in regulating the binding of the candidate proteins to PC+PS liposomes with and without PI(4,5)P2 can be carried out.

11. Implications of the current findings in the development of RNA aptamers:

RNA aptamers are short, single-stranded RNA that bind their target molecule with high affinity and specificity (88). In **chapter 2**, I described the 29/31KR mutant, which shows a complete loss of membrane binding in cells presumably due to MA-RNA binding that is stronger than the MA-PI(4,5)P2 interaction. This serves as a proof-of-concept for the feasibility of using RNA aptamers as an antiretroviral therapy. The preliminary data presented in **chapter 3** suggests that potentially in cells there may be two different populations of tRNAs. Those that are susceptible to removal by PI(4,5)P2 (e.g., PheGAA) and those that are resistant (e.g., SeCTCA). Studying the differences between such tRNAs could better inform the design of an aptamer that can bind Gag strongly and prevent Gag-membrane binding thereby blocking HIV-1 assembly. Several of the experiments I have proposed can yield data that define the properties of potentially effective RNA aptamers. An effective aptamer would be one that binds MA with an affinity stronger than that of MA to PI(4,5)P2, and thereby, prevents HIV-1 assembly. Determining the binding affinities of MA to tRNAs which are predicted to inhibit Gag membrane binding, such as SeCTCA, can form the basis for the design of an effective aptamer. Of course, as mentioned above, it will be important to consider the contribution of oligomerizing domains downstream of MA in the overall binding affinity of Gag to tRNA vs. PI(4,5)P2-membranes. Comparing the different tRNA structures/structural elements that potentially either favor or inhibit selection by MA can additionally help determine if a specific RNA

structure is preferred for binding. Furthermore, determining sites of interaction between MA and tRNA can reveal structural preference of MA, for example, the V-loop of SeCTCA could be favored strongly by MA. In addition, my data suggest that presence or absence of modifications may affect the MA-tRNA binding. The enzymes that modify RNA could show preference for a particular sequence and structural motif (37). In future, apart from structure, perhaps inclusion of certain sequence motifs that can favor aptamer modification in cells or synthesis of the aptamers using modified nucleotides (89) may further help stabilize MA-aptamer interaction. The impact of the candidate aptamers, designed with the above-mentioned properties, on Gag assembly in cells can be determined by transfecting the candidate aptamers along with Gag into cells. The successful aptamer would block Gag membrane binding and retain Gag in the cytosol, preventing Gag assembly at the PM. The addback assay can be further used to validate that the mechanism of the successful aptamer candidates in preventing Gag assembly at the PM is the blocking of Gag binding to PI(4,5)P2-containing membranes.

Conclusion

The specific localization of HIV-1 Gag to the PM is an essential early step in the production of infectious progeny. MA-bound RNA in cells plays an important role in the specific localization of HIV-1 Gag to the PM. Gag that fails to bind RNA through MA is mislocalized to nonspecific intracellular membranes, while Gag that binds RNA efficiently through MA does not show any such mislocalization. The charge as well as the sequence of the MA-HBR of HIV-1 Gag seems important for efficient binding of RNA in cells. Overall, MA-bound RNA prevents the promiscuous localization of Gag in cells, and along with PI(4,5)P2, helps in the specific recruitment of Gag to the PM. Whether RNA serves as a chaperone for membrane-binding proteins in the cell remains to be determined.

The preliminary PAR-CLIPSeq based data suggest that in cells, MA is bound to select tRNAs and that upon binding of Gag to the PM, some tRNAs are selectively lost. This suggests that some MA-bound

tRNAs in cells may be sensitive to removal by PI(4,5)P2, while others may be resistant to removal by PI(4,5)P2. How PI(4,5)P2 outcompetes the negative regulation of tRNA during Gag-membrane binding remains to be elucidated. The tRNAs that are lost upon PM binding potentially prevent the binding of Gag to intracellular membranes containing PS, allowing Gag to specifically localize to the PM, where the tRNAs are displaced by PI(4,5)P2 allowing Gag to bind to the PM. The function of the tRNAs that potentially restrict Gag binding to even PI(4,5)P2-containing membranes is more of an enigma. The study of specific MA-tRNA interactions can provide insight into hitherto unexplored roles of tRNAs in the HIV-1 life cycle. Additionally, study of tRNAs resistant to removal by PI(4,5)P2 could help inform the design and development of RNA aptamers targeted against HIV-1 assembly.

References

1. Chukkapalli V, Oh SJ, Ono A. 2010. Opposing mechanisms involving RNA and lipids regulate HIV-1 Gag membrane binding through the highly basic region of the matrix domain. Proc Natl Acad Sci U S A 107:1600-5.
2. Alfadhli A, Still A, Barklis E. 2009. Analysis of human immunodeficiency virus type 1 matrix binding to membranes and nucleic acids. J Virol 83:12196-203.
3. Chukkapalli V, Inlora J, Todd GC, Ono A. 2013. Evidence in support of RNA-mediated inhibition of phosphatidylserine-dependent HIV-1 Gag membrane binding in cells. J Virol 87:7155-9.
4. Kutluay SB, Zang T, Blanco-Melo D, Powell C, Jannain D, Errando M, Bieniasz PD. 2014. Global changes in the RNA binding specificity of HIV-1 gag regulate virion genesis. Cell 159:1096-1109.
5. Thornhill D, Olety B, Ono A. 2019. Relationships between MA-RNA Binding in Cells and Suppression of HIV-1 Gag Mislocalization to Intracellular Membranes. J Virol 93.
6. Yeung T, Gilbert GE, Shi J, Silvius J, Kapus A, Grinstein S. 2008. Membrane phosphatidylserine regulates surface charge and protein localization. Science 319:210-3.
7. Llewellyn GN, Grover JR, Olety B, Ono A. 2013. HIV-1 Gag associates with specific uropod-directed microdomains in a manner dependent on its MA highly basic region. J Virol 87:6441-54.
8. **HIV Sequence Compendium 2018** Foley B LT, Apetrei C, Hahn B, Mizrachi I, Mullins J, Rambaut A, Wolinsky S, and Korber B, Eds. Published by Theoretical Biology and Biophysics Group, Los Alamos National Laboratory, NM, LA-UR 18-25673. **HIV Sequence Compendium 2018**.
9. Mercredi PY, Bucca N, Loeliger B, Gaines CR, Mehta M, Bhargava P, Tedbury PR, Charlier L, Floquet N, Muriaux D, Favard C, Sanders CR, Freed EO, Marchant J, Summers MF. 2016. Structural and Molecular Determinants of Membrane Binding by the HIV-1 Matrix Protein. J Mol Biol 428:1637-55.
10. Gaines CR, Tkacik E, Rivera-Oven A, Somani P, Achimovich A, Alabi T, Zhu A, Getachew N, Yang AL, McDonough M, Hawkins T, Spadaro Z, Summers MF. 2018. HIV-1 Matrix Protein Interactions with tRNA: Implications for Membrane Targeting. J Mol Biol 430:2113-2127.
11. Todd GC, Duchon A, Inlora J, Olson ED, Musier-Forsyth K, Ono A. 2017. Inhibition of HIV-1 Gag-membrane interactions by specific RNAs. RNA 23:395-405.
12. Dick RA, Kamynina E, Vogt VM. 2013. Effect of multimerization on membrane association of Rous sarcoma virus and HIV-1 matrix domain proteins. J Virol 87:13598-608.
13. Carlson LA, Bai Y, Keane SC, Doudna JA, Hurley JH. 2016. Reconstitution of selective HIV-1 RNA packaging in vitro by membrane-bound Gag assemblies. Elife 5.
14. Dittmar KA, Goodenbour JM, Pan T. 2006. Tissue-specific differences in human transfer RNA expression. PLoS Genet 2:e221.
15. Vindry C, Guillin O, Mangeot PE, Ohlmann T, Chavatte L. 2019. A Versatile Strategy to Reduce UGA-Selenocysteine Recoding Efficiency of the Ribosome Using CRISPR-Cas9-Viral-Like-Particles Targeting Selenocysteine-tRNA. Cells 8.
16. Labunskyy VM, Hatfield DL, Gladyshev VN. 2014. Selenoproteins: molecular pathways and physiological roles. Physiol Rev 94:739-77.
17. Arimbasseri AG, Maraia RJ. 2016. RNA Polymerase III Advances: Structural and tRNA Functional Views. Trends Biochem Sci 41:546-559.

18. Paule MR, White RJ. 2000. Survey and summary: transcription by RNA polymerases I and III. Nucleic Acids Res 28:1283-98.
19. Geiduschek EP, Kassavetis GA. 2001. The RNA polymerase III transcription apparatus. J Mol Biol 310:1-26.
20. Goodenbour JM, Pan T. 2006. Diversity of tRNA genes in eukaryotes. Nucleic Acids Res 34:6137-46.
21. Torrent M, Chalancon G, de Groot NS, Wuster A, Madan Babu M. 2018. Cells alter their tRNA abundance to selectively regulate protein synthesis during stress conditions. Sci Signal 11.
22. Schwenzer H, Jühling F, Chu A, Pallett LJ, Baumert TF, Maini M, Fassati A. 2019. Oxidative Stress Triggers Selective tRNA Retrograde Transport in Human Cells during the Integrated Stress Response. Cell Rep 26:3416-3428.e5.
23. Li M, Kao E, Gao X, Sandig H, Limmer K, Pavon-Eternod M, Jones TE, Landry S, Pan T, Weitzman MD, David M. 2012. Codon-usage-based inhibition of HIV protein synthesis by human schlafen 11. Nature 491:125-8.
24. Alings F, Sarin LP, Fufezan C, Drexler HC, Leidel SA. 2015. An evolutionary approach uncovers a diverse response of tRNA 2-thiolation to elevated temperatures in yeast. RNA 21:202-12.
25. Chionh YH, McBee M, Babu IR, Hia F, Lin W, Zhao W, Cao J, Dziergowska A, Malkiewicz A, Begley TJ, Alonso S, Dedon PC. 2016. tRNA-mediated codon-biased translation in mycobacterial hypoxic persistence. Nat Commun 7:13302.
26. Roundtree IA, Evans ME, Pan T, He C. 2017. Dynamic RNA Modifications in Gene Expression Regulation. Cell 169:1187-1200.
27. Arimbasseri AG, Blewett NH, Iben JR, Lamichhane TN, Cherkasova V, Hafner M, Maraia RJ. 2015. RNA Polymerase III Output Is Functionally Linked to tRNA Dimethyl-G26 Modification. PLoS Genet 11:e1005671.
28. Pan T. 2018. Modifications and functional genomics of human transfer RNA. Cell Res 28:395-404.
29. Koh CS, Sarin LP. 2018. Transfer RNA modification and infection - Implications for pathogenicity and host responses. Biochim Biophys Acta Gene Regul Mech 1861:419-432.
30. Hori H. 2019. Regulatory Factors for tRNA Modifications in Extreme- Thermophilic Bacterium. Front Genet 10:204.
31. Chan C, Pham P, Dedon PC, Begley TJ. 2018. Lifestyle modifications: coordinating the tRNA epitranscriptome with codon bias to adapt translation during stress responses. Genome Biol 19:228.
32. Santesmasses D, Mariotti M, Guigó R. 2017. Computational identification of the selenocysteine tRNA (tRNASec) in genomes. PLoS Comput Biol 13:e1005383.
33. Itoh Y, Chiba S, Sekine S, Yokoyama S. 2009. Crystal structure of human selenocysteine tRNA. Nucleic Acids Res 37:6259-68.
34. Ganichkin OM, Anedchenko EA, Wahl MC. 2011. Crystal structure analysis reveals functional flexibility in the selenocysteine-specific tRNA from mouse. PLoS One 6:e20032.
35. Hatfield D, Lee BJ, Hampton L, Diamond AM. 1991. Selenium induces changes in the selenocysteine tRNA[Ser]Sec population in mammalian cells. Nucleic Acids Res 19:939-43.
36. Carlson BA, Yoo MH, Tsuji PA, Gladyshev VN, Hatfield DL. 2009. Mouse models targeting selenocysteine tRNA expression for elucidating the role of selenoproteins in health and development. Molecules 14:3509-27.
37. Safra M, Sas-Chen A, Nir R, Winkler R, Nachshon A, Bar-Yaacov D, Erlacher M, Rossmanith W, Stern-Ginossar N, Schwartz S. 2017. The m1A landscape on cytosolic and mitochondrial mRNA at single-base resolution. Nature 551:251-255.

38. Warner GJ, Berry MJ, Moustafa ME, Carlson BA, Hatfield DL, Faust JR. 2000. Inhibition of selenoprotein synthesis by selenocysteine tRNA[Ser]Sec lacking isopentenyladenosine. J Biol Chem 275:28110-9.
39. Kisseleva MV, Wilson MP, Majerus PW. 2000. The isolation and characterization of a cDNA encoding phospholipid-specific inositol polyphosphate 5-phosphatase. J Biol Chem 275:20110-6.
40. Ono A, Ablan SD, Lockett SJ, Nagashima K, Freed EO. 2004. Phosphatidylinositol (4,5) bisphosphate regulates HIV-1 Gag targeting to the plasma membrane. Proc Natl Acad Sci U S A 101:14889-94.
41. Chukkapalli V, Hogue IB, Boyko V, Hu WS, Ono A. 2008. Interaction between the human immunodeficiency virus type 1 Gag matrix domain and phosphatidylinositol-(4,5)-bisphosphate is essential for efficient gag membrane binding. J Virol 82:2405-17.
42. Chan R, Uchil PD, Jin J, Shui G, Ott DE, Mothes W, Wenk MR. 2008. Retroviruses human immunodeficiency virus and murine leukemia virus are enriched in phosphoinositides. J Virol 82:11228-38.
43. Monde K, Chukkapalli V, Ono A. 2011. Assembly and replication of HIV-1 in T cells with low levels of phosphatidylinositol-(4,5)-bisphosphate. J Virol 85:3584-95.
44. Inlora J, Collins DR, Trubin ME, Chung JY, Ono A. 2014. Membrane binding and subcellular localization of retroviral Gag proteins are differentially regulated by MA interactions with phosphatidylinositol-(4,5)-bisphosphate and RNA. MBio 5:e02202.
45. Inlora J, Chukkapalli V, Derse D, Ono A. 2011. Gag localization and virus-like particle release mediated by the matrix domain of human T-lymphotropic virus type 1 Gag are less dependent on phosphatidylinositol-(4,5)-bisphosphate than those mediated by the matrix domain of HIV-1 Gag. J Virol 85:3802-10.
46. Mücksch F, Laketa V, Müller B, Schultz C, Kräusslich HG. 2017. Synchronized HIV assembly by tunable PIP. Elife 6.
47. Chan J, Dick RA, Vogt VM. 2011. Rous Sarcoma Virus Gag Has No Specific Requirement for Phosphatidylinositol-(4,5)-Bisphosphate for Plasma Membrane Association In Vivo or for Liposome Interaction In Vitro.
48. Guillin OM, Vindry C, Ohlmann T, Chavatte L. 2019. Selenium, Selenoproteins and Viral Infection. Nutrients 11.
49. Ivanov AV, Valuev-Elliston VT, Ivanova ON, Kochetkov SN, Starodubova ES, Bartosch B, Isaguliants MG. 2016. Oxidative Stress during HIV Infection: Mechanisms and Consequences. Oxid Med Cell Longev 2016:8910396.
50. Gladyshev VN, Stadtman TC, Hatfield DL, Jeang KT. 1999. Levels of major selenoproteins in T cells decrease during HIV infection and low molecular mass selenium compounds increase. Proc Natl Acad Sci U S A 96:835-9.
51. Lorenz C, Lünse CE, Mörl M. 2017. tRNA Modifications: Impact on Structure and Thermal Adaptation. Biomolecules 7.
52. El Yacoubi B, Bailly M, de Crécy-Lagard V. 2012. Biosynthesis and function of posttranscriptional modifications of transfer RNAs. Annu Rev Genet 46:69-95.
53. Schimmel P. 2018. The emerging complexity of the tRNA world: mammalian tRNAs beyond protein synthesis. Nat Rev Mol Cell Biol 19:45-58.
54. Väre VY, Eruysal ER, Narendran A, Sarachan KL, Agris PF. 2017. Chemical and Conformational Diversity of Modified Nucleosides Affects tRNA Structure and Function. Biomolecules 7.
55. Pereira M, Francisco S, Varanda AS, Santos M, Santos MAS, Soares AR. 2018. Impact of tRNA Modifications and tRNA-Modifying Enzymes on Proteostasis and Human Disease. Int J Mol Sci 19.

56. van Weringh A, Ragonnet-Cronin M, Pranckeviciene E, Pavon-Eternod M, Kleiman L, Xia X. 2011. HIV-1 modulates the tRNA pool to improve translation efficiency. Mol Biol Evol 28:1827-34.
57. Berkhout B, Grigoriev A, Bakker M, Lukashov VV. 2002. Codon and amino acid usage in retroviral genomes is consistent with virus-specific nucleotide pressure. AIDS Res Hum Retroviruses 18:133-41.
58. Korniy N, Goyal A, Hoffmann M, Samatova E, Peske F, Pöhlmann S, Rodnina MV. 2019. Modulation of HIV-1 Gag/Gag-Pol frameshifting by tRNA abundance. Nucleic Acids Res 47:5210-5222.
59. Jacks T, Power MD, Masiarz FR, Luciw PA, Barr PJ, Varmus HE. 1988. Characterization of ribosomal frameshifting in HIV-1 gag-pol expression. Nature 331:280-3.
60. Parkin NT, Chamorro M, Varmus HE. 1992. Human immunodeficiency virus type 1 gag-pol frameshifting is dependent on downstream mRNA secondary structure: demonstration by expression in vivo. J Virol 66:5147-51.
61. Auxilien S, Keith G, Le Grice SF, Darlix JL. 1999. Role of post-transcriptional modifications of primer tRNALys,3 in the fidelity and efficacy of plus strand DNA transfer during HIV-1 reverse transcription. J Biol Chem 274:4412-20.
62. Clark WC, Evans ME, Dominissini D, Zheng G, Pan T. 2016. tRNA base methylation identification and quantification via high-throughput sequencing. RNA 22:1771-1784.
63. McIntyre W, Netzband R, Bonenfant G, Biegel JM, Miller C, Fuchs G, Henderson E, Arra M, Canki M, Fabris D, Pager CT. 2018. Positive-sense RNA viruses reveal the complexity and dynamics of the cellular and viral epitranscriptomes during infection. Nucleic Acids Res 46:5776-5791.
64. Jora M, Lobue PA, Ross RL, Williams B, Addepalli B. 2019. Detection of ribonucleoside modifications by liquid chromatography coupled with mass spectrometry. Biochim Biophys Acta Gene Regul Mech 1862:280-290.
65. Tang C, Loeliger E, Luncsford P, Kinde I, Beckett D, Summers MF. 2004. Entropic switch regulates myristate exposure in the HIV-1 matrix protein. Proc Natl Acad Sci U S A 101:517-22.
66. Barros M, Heinrich F, Datta SAK, Rein A, Karageorgos I, Nanda H, Lösche M. 2016. Membrane Binding of HIV-1 Matrix Protein: Dependence on Bilayer Composition and Protein Lipidation. J Virol 90:4544-4555.
67. Murphy RE, Samal AB, Vlach J, Mas V, Prevelige PE, Saad JS. 2019. Structural and biophysical characterizations of HIV-1 matrix trimer binding to lipid nanodiscs shed light on virus assembly. J Biol Chem 294:18600-18612.
68. Trahey M, Li MJ, Kwon H, Woodahl EL, McClary WD, Atkins WM. 2015. Applications of Lipid Nanodiscs for the Study of Membrane Proteins by Surface Plasmon Resonance. Curr Protoc Protein Sci 81:29.13.1-29.13.16.
69. Rouck JE, Krapf JE, Roy J, Huff HC, Das A. 2017. Recent advances in nanodisc technology for membrane protein studies (2012-2017). FEBS Lett 591:2057-2088.
70. Her C, Filoti DI, McLean MA, Sligar SG, Alexander Ross JB, Steele H, Laue TM. 2016. The Charge Properties of Phospholipid Nanodiscs. Biophys J 111:989-98.
71. Meng XY, Zhang HX, Mezei M, Cui M. 2011. Molecular docking: a powerful approach for structure-based drug discovery. Curr Comput Aided Drug Des 7:146-57.
72. Santos LHS, Ferreira RS, Caffarena ER. 2019. Integrating Molecular Docking and Molecular Dynamics Simulations. Methods Mol Biol 2053:13-34.
73. Hollingsworth SA, Dror RO. 2018. Molecular Dynamics Simulation for All. Neuron 99:1129-1143.
74. Hospital A, Goñi JR, Orozco M, Gelpí JL. 2015. Molecular dynamics simulations: advances and applications. Adv Appl Bioinform Chem 8:37-47.
75. Hafner M, Landthaler M, Burger L, Khorshid M, Hausser J, Berninger P, Rothballer A, Ascano M, Jungkamp AC, Munschauer M, Ulrich A, Wardle GS, Dewell S, Zavolan M, Tuschl T. 2010. PAR-

CliP--a method to identify transcriptome-wide the binding sites of RNA binding proteins. J Vis Exp.
76. Ascano M, Hafner M, Cekan P, Gerstberger S, Tuschl T. 2012. Identification of RNA-protein interaction networks using PAR-CLIP. Wiley Interdiscip Rev RNA 3:159-77.
77. Rädle B, Rutkowski AJ, Ruzsics Z, Friedel CC, Koszinowski UH, Dölken L. 2013. Metabolic Labeling of Newly Transcribed RNA for High Resolution Gene Expression Profiling of RNA Synthesis, Processing and Decay in Cell Culture, J Vis Exp.
78. Muthmann N, Hartstock K, Rentmeister A. 2020. Chemo-enzymatic treatment of RNA to facilitate analyses. Wiley Interdiscip Rev RNA 11:e1561.
79. Salasc F, Gludish DW, Jarvis I, Boliar S, Wills MR, Russell DG, Lever AML, Mok HP. 2019. A novel, sensitive dual-indicator cell line for detection and quantification of inducible, replication-competent latent HIV-1 from reservoir cells. Sci Rep 9:19325.
80. Tedbury PR, Ablan SD, Freed EO. 2013. Global rescue of defects in HIV-1 envelope glycoprotein incorporation: implications for matrix structure. PLoS Pathog 9:e1003739.
81. Derdeyn CA, Decker JM, Sfakianos JN, Wu X, O'Brien WA, Ratner L, Kappes JC, Shaw GM, Hunter E. 2000. Sensitivity of human immunodeficiency virus type 1 to the fusion inhibitor T-20 is modulated by coreceptor specificity defined by the V3 loop of gp120. J Virol 74:8358-67.
82. Wei X, Decker JM, Liu H, Zhang Z, Arani RB, Kilby JM, Saag MS, Wu X, Shaw GM, Kappes JC. 2002. Emergence of resistant human immunodeficiency virus type 1 in patients receiving fusion inhibitor (T-20) monotherapy. Antimicrob Agents Chemother 46:1896-905.
83. Parisien M, Wang X, Perdrizet G, Lamphear C, Fierke CA, Maheshwari KC, Wilde MJ, Sosnick TR, Pan T. 2013. Discovering RNA-protein interactome by using chemical context profiling of the RNA-protein interface. Cell Rep 3:1703-13.
84. Catimel B, Schieber C, Condron M, Patsiouras H, Connolly L, Catimel J, Nice EC, Burgess AW, Holmes AB. 2008. The PI(3,5)P2 and PI(4,5)P2 interactomes. J Proteome Res 7:5295-313.
85. Bi X, Corpina RA, Goldberg J. 2002. Structure of the Sec23/24-Sar1 pre-budding complex of the COPII vesicle coat. Nature 419:271-7.
86. Georges A, Bonneau J, Bonnefont-Rousselot D, Champigneulle J, Rabès JP, Abifadel M, Aparicio T, Guenedet JC, Bruckert E, Boileau C, Morali A, Varret M, Aggerbeck LP, Samson-Bouma ME. 2011. Molecular analysis and intestinal expression of SAR1 genes and proteins in Anderson's disease (Chylomicron retention disease). Orphanet J Rare Dis 6:1.
87. Tan X, Thapa N, Choi S, Anderson RA. 2015. Emerging roles of PtdIns(4,5)P2--beyond the plasma membrane. J Cell Sci 128:4047-56.
88. Catuogno S, Esposito CL, Ungaro P, de Franciscis V. 2018. Nucleic Acid Aptamers Targeting Epigenetic Regulators: An Innovative Therapeutic Option. Pharmaceuticals (Basel) 11.
89. Svensen N, Jaffrey SR. 2016. Fluorescent RNA Aptamers as a Tool to Study RNA-Modifying Enzymes. Cell Chem Biol 23:415-25.